MICROCHANNEL ENABLED REFORMING OF GLYCEROL TO HYDROGEN OVER NI-BASED CATALYSTS

by

Sinan Koç

B.S., Chemical Engineering, Boğaziçi University, 2012

Submitted to the Institute for Graduate Studies in
Science and Engineering in partial fulfillment of
the requirements for the degree of
Master of Science

Graduate Program in Chemical Engineering
Boğaziçi University

2015

ACKNOWLEDGEMENTS

First of all, I would like to express my special appreciation and thanks to my supervisor Assoc. Prof. Ahmet Kerim Avcı for his guidance, encouragements and wise advices helping me during my MS thesis. His advice on both research as well as on my academic career have been priceless. Without his endless help, this study would have been a lot harder for me. I am very grateful to have the opportunity to work with him in the design, construction, development and each stage of my experimental study.

I would like to acknowledge my thesis committee members, Prof. Ramazan Yıldırım and Asst. Prof. Alper Uzun for devoting their valuable time to read and comment on my thesis. Their comments and suggestions are very valuable for me.

I am very happy to be with Merve Koç who has always been with me. Words cannot express how grateful I am to my wife for all of the things that she has made on my behalf. She has an endless patience and support in the moment when there was no one to answer my difficulties. Additionally, I present my deepest appreciations towards my family members. They are always in my heart with a great love.

My special thanks go to H. Onur Kavaklı for his guidance and helps during my thesis work. He always gives answers to my endless questions. He has been a tremendous mentor to me. I am also very happy to have Can Ekici as co-worker. His share in this work cannot be underestimated. I am also grateful to be the teaching assistant of ChE 433 – Design of Chemical Processing Units course with Melek Selcen Başar and Özgür Yaşar Çağlar. I also present my special thanks to my best friend Utku Deniz. He is always with me event at my marriage as my groomsman. Their supports while I am writing my thesis are unforgettable.

I want to present my special appreciation towards Bilgi Dedeoğlu for his contribution during the construction of my experimental set up. Melike Gürbüz, Başak Ünen, Yakup Bal and Murat Düzgünoğlu were also very helpful during my study. Thanks to Bilge Gedik Uluocak for her kind attitude and great help in SEM and EDX analyses conducted at Boğaziçi University Research and Development Center.

I would also like to thank Elif Erdinç, Aybüke Leba, Aysun İpek Paksoy, İrem Şen, Emre Demirel, Doğa Demirhan, Barış Burnak, Elif Can, Elif Gençtürk, Serhat Erşahin, Kerem Aksakal, Ali Uzun, Merve Eropak, Manouchehr Nadjafi, and Burcu Karagöz and all my friends. Special thanks to all CATREL team members.

This thesis is devoted to my family. They have made preparing this thesis possible. Their prayer for me was what sustained me thus far.

Finally, financial support provided by TÜBİTAK 1003 – Project No: 113M962 is acknowledged.

ABSTRACT

MICROCHANNEL ENABLED REFORMING OF GLYCEROL TO HYDROGEN OVER NI-BASED CATALYSTS

The aim of this study is to investigate glycerol steam reforming (GSR) and oxidative glycerol steam reforming (OGSR) over Ni-based catalysts in a microchannel reactor. The parametric study to investigate effects of reaction temperature, molar steam-to-carbon ratio in the feed (S/C), total flow rate and microchannel reactor configuration (packed and coated) on glycerol conversion and product distributions in GSR are investigated in the context of a parametric plan. Moreover, OGSR reactions are performed to study the effects of temperature and molar carbon-to-oxygen ratio at the inlet (C/O) on glycerol conversion and product distributions. 5 wt.% Ni/Al_2O_3 and 10 wt.% Ni/Al_2O_3 catalysts with 3-μm particle size (used in coated microchannel configuration) and 60-80 mesh (250 – 177 μm) size of 5 wt.% Ni/Al_2O_3 catalyst is prepared using incipient-to-wetness impregnation method. Blank tests show that the microchannel reactor components do not remain inert during the reactions. It is observed that glycerol conversion increases with temperature. Thermal decomposition of glycerol leads to production of methane, ethane and ethylene, and coke. S/C ratio affects the products distribution via the water gas shift reaction. Higher S/C ratios result in higher H_2 selectivity which is defined as the moles of H_2 produce per moles of glycerol converted. However, sintering of the Ni particles has a negative impact on glycerol conversion. Decreasing the total flow rate leads to an exponential increase in glycerol conversion because of increase in residence time. Coated microchannel configuration shows higher conversions and H_2 selectivities than those observed in the packed microchannel configuration. OGSR experiments are found to give glycerol conversions significantly higher than those observed in GSR. Higher O_2 content in the feed improves conversions, but decrease H_2 yields and selectivity. Coke formation over catalyst surface in GSR and OGSR is inevitable. SEM and EDX analysis of catalysts are carried out to provide insight into the dispersion of active metal and carbon formation over catalyst surface at different values of temperature and S/C ratio.

ÖZET

NİKEL BAZLI KATALİZÖRLER ÜZERİNDE GLİSEROL REFORMLANMASININ MİKROKANAL REAKTÖRLERDE İNCELENMESİ

Bu çalışmanın amacı Ni bazlı katalizör üzerinde gliserol buhar reformlama (GBR) ve oksijenli gliserol buhar reformalama (OGBR) deneylerini bir mikrokanal içinde incelemektir. Sıcaklık, buhar-karbon molar oranı, toplam akış hızı ve reaktör konfigürasyonlarının (doldurulmuş ve kaplanmış), gliserol dönüşümü ve ürün dağılımı üzerindeki etkisini incelemek için, bir plan dahilinde parametrik çalışma yapılmıştır. Ek olarak, sıcaklık ve girişteki karbon-oksijen molar oranının gliserol dönüşümü ve ürün dağılımı üzerindeki etkisini çalışmak için OGBR reaksiyonları gerçekleştirilmiştir. 3-µm büyüklüğünde tanecik yapıdaki, ağırlıkça %5 Ni/Al_2O_3 ve %10 Ni/Al_2O_3 katalizörleri (kaplamalı mikrokanal konfigürasyonu için) ve 250-177 µm büyüklüğünde tanecik yapıdaki, ağırlıkça %5 Ni/Al_2O_3 katalizörü ardışık emdirme tekniği kullanılarak hazırlanmıştır. Boş deneyler, mikrokanal reaktör parçalarının deneylerde etkisiz olarak kalmadığını göstermiştir. Sıcaklık artıkça gliserol dönüşümünün arttığı görülmüştür. Gliserolün termal dağılımı metan, etan ve etilen, ve karbon üretimine yol açmıştır. Buhar-karbon oranı ürün dağılımını su-gaz değişim reaksiyonuna bağlı olarak değiştirmiştir. Yüksek buhar-karbon oranı, dönüştürülen gliserol başına üretilen H_2 molü olarak tanıtılan, yüksek H_2 seçiciliğine sebep olmuştur. Fakat, Ni parçacıklarının toplaşması gliserol dönüşümü üzerine olumsuz etki etmiştir. Akış hızını düşürmek, kalma zamanını arttırdığı için, gliserol dönüşümünün üstel artmasını sağlamıştır. Kaplamalı mikrokanal konfigürasyonu, doldurmalı mikrokanal konfigürasyonuna göre daha yüksek dönüşümler ve H_2 seçiciliği göstermiştir. OGBR reaksiyonlarının GBR reaksiyonlarına göre daha yüksek dönüşüm vermiştir. Girişteki yüksek O_2, yüksek dönüşümlere ve düşük H_2 üretimi ve seçiciliğine sebebiyet vermiştir. OGBR ve GBR reaksiyonları için katalizör yüzeyinde karbon oluşumu kaçınılmazdır. Aktif metal dağılımını ve farklı sıcaklıklar ve su-karbon oranlarında katalizör üzerinde oluşan karbonu incelemek için SEM ve EDX analizleri yapılmıştır.

TABLE OF CONTENTS

LIST OF FIGURES

LIST OF TABLES

LIST OF SYMBOLS

D	Diameter of the housing (mm)
$D_{particle}$	Diameter of catalyst particle (mm)
D_{tube}	Tube inner diameter (mm)
H	Height of the microchannel (mm)
L	Length of the housing (mm)
L_{tube}	Tube length packed with catalyst (mm)
T	Temperature (°C)
W	Width of the microchannel (mm)
υ_i	Flow rate of the species i (Nml min^{-1})
$X_{glycerol}$	Glycerol conversion
ΔH	Enthalpy of reaction (kJ/mol)

LIST OF ACRONYMS/ABBREVIATIONS

BET	Brunauer-Emmett-Teller
BSE	Backscattering Electron
C/O	Carbon-to-Oxygen Ratio
EDX	Energy Dispersive X-ray Analysis
GC	Gas Chromatography
GSR	Glycerol Steam Reforming
HPLC	High Pressure Liquid Chromatography
ID	Inside Diameter
MFC	Mass Flow Controller
OD	Outer Diameter
OGSR	Oxidative Glycerol Steam Reforming
PID	Proportional Integral Derivative
S/C	Steam-to-Carbon Ratio
SEM	Scanning Electron Microscopy
SR	Steam Reforming
TCD	Thermal Conductivity Detector
WGS	Water Gas Shift
W/F	Catalyst Weight to Feed Flow Rate Ratio

1. INTRODUCTION

Crude oil is an important property for the energy generation in order to sustain our daily life. However, fossil fuels have limited reserves on earth and because of growing population, these reserves are diminishing. Additionally, consumption of fossil fuels increases the amount of pollutants such as CO_2 in the atmosphere. As a result, people are investigating alternative energy sources which are cheaper, and cause less pollution than the conventional ones. Biofuel, such as biodiesel, is an example of alternative energy source for conventional fossil fuels because they are renewable and carbon neutral (Dieuzeide *et al.*, 2013; Adhikari *et al.*, 2008). Biodiesel is produced by the transesterification of vegetable oils with alcohols producing esters as the main product (biodiesel) and glycerol as a by-product (Thessen *et al.*, 2013).

$$C_3H_5(OOC)_3(R_n)_3 + 3R'OH \leftrightarrow 3R_nCOOR' + C_3H_5(OH)_3 \quad (1.1)$$

Glycerides Alcohols Esters Glycerol

Because of higher prices of crude oil and increasing demand for environmentally acceptable fuels, biodiesel has become a very good candidate for replacing petroleum diesel. On the other hand, biodiesel is not consumed extensively because of its comparable price with that of conventional diesel fuel. Avasthi et al. (2013) are investigated the comparison of the prices between the biodiesel and conventional diesel fuel. A similar comparison that additionally includes natural gas is provided in Figure 1.1 in which graphical representation of prices of diesel, biodiesel (B20, (B2/B5), (B99/B100)) and natural gas are given.

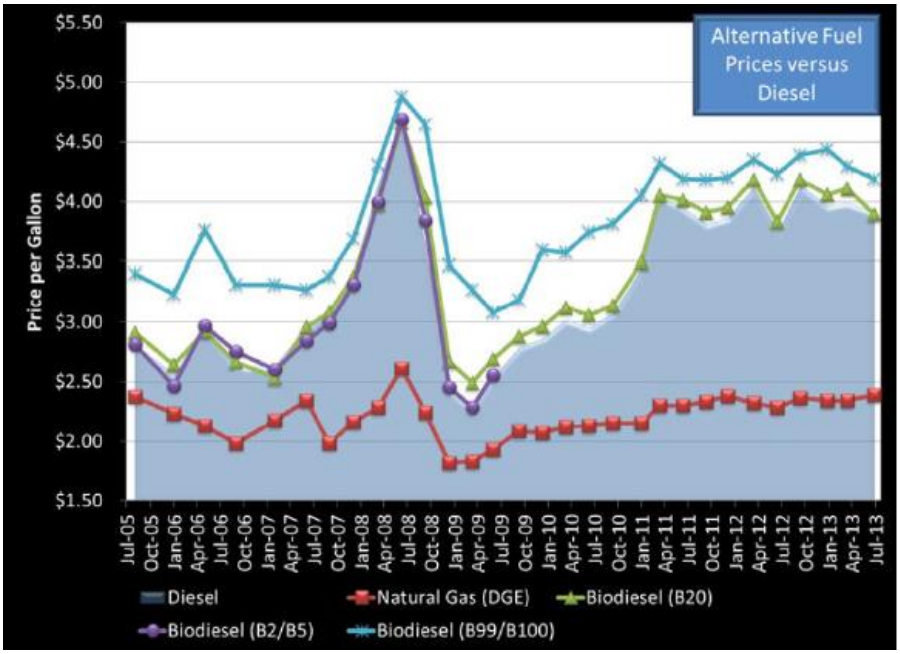

Figure 1.1. Graphical Comparison between the Prices of Diesel, Biodiesel (B20, (B2/B5), (B99/B100)) and Natural gas in USA (adopted from Clean Cities Alternative Fuel Price Report, US Department of Energy, 2013).

The main by product in the transesterification reactions is glycerol. About 10 wt.% of glycerol can be produced during biodiesel production (Dou *et al.*, 2013). For instance, in 1 kg of product mixture, 900 g will be biodiesel and about 100 g will be glycerol. Glycerol is the simplest trihydric alcohol and is a very useful chemical that is involved in various applications (Lin, 2013).

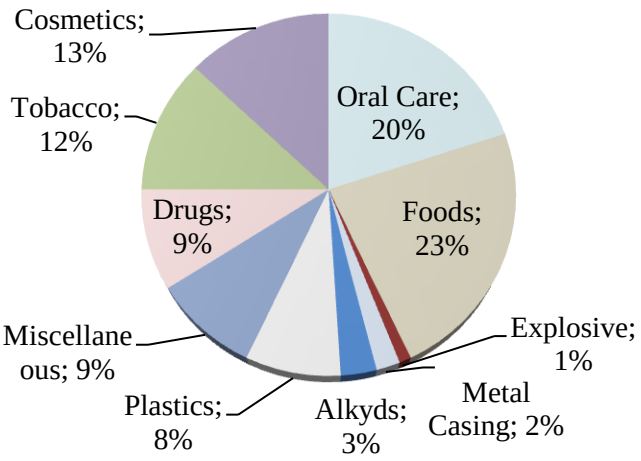

Figure 1.2. Areas of use of Glycerol (Lin, 2013).

The rise in biodiesel production is expected to lead an increase in glycerol production. It is predicted that there will be 3 megatones of glycerol production by 2020, whereas the amount of glycerol consumption in commercial applications will be less than 500 kilotons (Lin, 2013). As a result, a huge surplus of glycerol is expected to occur, and new ways should be investigated for the valorization of glycerol. Hydrogen or syngas production is one of the promising ways of utilizing glycerol. Hydrogen is key substance which is heavily used in ammonia production, petroleum industry, and to power fuel cell systems (Avasthi *et al.*, 2013). Nowadays, 95 % of the produced hydrogen comes from nonrenewable resources based on fossil fuels such as natural gas and naphtha (Avasthi *et al.*, 2013; Manfro *et al.*, 2013).

Glycerol steam reforming (Reaction 1.2) is an important process for the utilization of glycerol to produce hydrogen. The main products of steam reforming are H_2 and CO_2, CO and CH_4, with the last two molecules appearing generally at low concentrations. The overall reaction of steam reforming of glycerol can be given as follows (Manfro *et al.*, 2013):

$$C_3H_8O_3+3H_2O\leftrightarrow 3CO_2+7H_2 \qquad \Delta H(298\ K) = 346.4\ kJ/mol \qquad (1.2)$$

Based on the reaction equation, 7 mole of H_2 can be produced theoretically per one mole of glycerol fed into the system. CO formation, catalyst deactivation by both carbon deposition and sintering at high temperatures, and high energy consumption are stated as the major concerns in glycerol steam reforming (Vaidya and Rodrigues, 2009).

Another way of converting glycerol to hydrogen is partial oxidation (Reaction 1.3). Because of the exothermic nature of partial oxidation, rapid startups and high reaction rates are observed. With a proper insulation, the reaction does not require external heat input. Compared with steam reforming, coke formation is negligible and this leads to less catalyst deactivation allowing long-term operation. The overall reaction of glycerol partial oxidation can be given as follows (Lin, 2013):

$$C_3H_8O_3+\frac{3}{2}O_2\leftrightarrow 3CO_2+4H_2 \qquad \Delta H(298\ K) = -598\ kJ/mol \qquad (1.3)$$

Steam can also be fed to the system under partial oxidation conditions in order to improve hydrogen yield. This route, described in Reaction 1.4, is defined as autothermal or oxidative steam reforming. The overall reaction equation for glycerol autothermal reforming can be expressed as follows (Lin, 2013):

$$C_3H_8O_3+3/4O_2+3/2H_2O\leftrightarrow 3CO_2+\frac{11}{2}H_2 \qquad \Delta H(298K) = -240\ kJ/mol \qquad (1.4)$$

Nickel, cobalt and noble metals such as Rh, Pt and Ru supported over alumina, ceria and zirconia are investigated as catalysts for glycerol steam reforming (Lin, 2013). Majority of the related studies, mentioned in Section 2, are aimed to understand either the effect of metal or the support or their interaction on glycerol conversion and on product distribution. These studies are carried out by using catalysts in particulate form within packed-bed reactor geometry. The effect of the reactor configuration on glycerol steam reforming is not studied in the literature. It is shown that microchannel enabled reactions deliver reactant conversions higher than those obtained in packed bed reactors, and microchannel units provide better utilization of the catalyst by increasing the heat and mass transfer rates (Karakaya *et al.*, 2012). The focal point of this study is to investigate Ni-catalyzed reforming of glycerol to hydrogen in a microchannel reactor configuration in the context of a parametric study.

This study includes the design and construction of an experimental set-up suitable to conduct experiments for non-oxidative and oxidative steam reforming of glycerol in a catalytic microchannel reactor, and involves the investigation of the effect of active metal loading, temperature, feed composition (S/C and C/O ratios), total flow rate and reactor configuration (coated or packed microchannel) on glycerol conversion and on product distribution. Moreover, the changes in surface structure of catalyst after and before the reaction tests are analyzed by SEM and EDX characterization.

This work is composed of five chapters. In Chapter 2, a literature survey about the experimental studies of glycerol steam reforming over nickel based catalysts is given. A

detailed explanation of experimental set-up, methods and procedures for catalyst preparation and catalytic activity tests are presented in Chapter 3. Results of the catalytic activity tests are given and discussed in Chapter 4. Chapter 5 includes major conclusions from the parametric study and recommendations for the future studies.

2. LITERATURE SURVEY

2.1. Microchannel Reactors

There are various types of reactors used in the industry, and among these, the packed reactors have been frequently used reactor type for the catalytic reactions for decades. Most of lab-scale studies are performed in packed bed reactor; however, the scaling up these reactors for a mass production is still a challenge. The most difficult parts of scaling up a packed bed reactor are the addition of mass and heat transfer resistances in mass production. On the other hand, new technological advancements provide new reactor types such as microchannel reactors which have a potential to overcome some of the disadvantages of packed bed reactors.

Microchannel reactors have provided an introduction for new reaction procedures in chemistry, pharmaceutical industry, and molecular biology. Microchannel reactors compose of parallel and identical channels having diameters between 10 to several hundred micrometers. The volume reduction compared to an industrial packed bed reactor may be up to ca. 90% (Ehrfeld *et al.*, 2001). These miniaturized reaction systems offers many technical advantages for a large number of applications (Löwe *et al*., 2002). One of the technical advantages of microchannel reactors over macroscopic reactors can be stated as effective heat management by facilitating isothermal operation or enabling the coupling of endothermic and exothermic reactions. In addition to that, one of the unique characteristic of the microchannel reactor is having very small dimensions, and this provides safe operation while producing highly reactive and hazardous products (Commenge *et al.*, 2004). Due to smaller reactor volumes, the hold-up of the reactor is decreased which brings about increased process safety. Another outcome of smaller hold-up is that shorter residence time, which improves the selectivity of the desired products (Ehrfeld *et al.*, 2001; Hasabe *et al.*, 2004). Moreover, the scaling up the production form lab scale to industrial scale is much easier in microchannel reactors.

Microchannel structures as intensified systems provide good mass transports, less transport resistance and improved flow patterns. The residence time distribution of microchannel reactors is well defined based on improved flow patterns. Flow pattern of a microchannel is fully developed laminar flow. Because of the flow type, the Sherwood number, which is mass transfer coefficient multiplied by hydraulic diameter and divided by the diffusion coefficient, reaches a constant value showing that as the hydraulic diameter gets smaller the mass transfer coefficient gets larger. High mass transfer coefficient leads to decrease in mass transfer resistances (Fichtner *et al.*, 2001).

Another important feature of a microchannel reactor is having high surface to volume ratios. In conventional reactors, surface to volume ratio changes between 100 m^2/m^3 and 1000 m^2/m^3 whereas these numbers increase to 10,000 - 50,000 m^2/m^3 surface to volume ratio values for a microchannel reactor (Ehrfeld *et al.*, 2001). High surface area and heat transfer coefficients prevent the formation of hotspots especially for rapid exothermic reactions. Preventing the hotspot increases the life time of the catalyst, keeps the product distribution unchanged and directly decreases the operational costs in the production. (Hessel and Kolp, 2004; Kiwi-Minsker and Renken, 2005).

Fabrication of microchannel reactors can be performed using variety of substrates such as stainless steel, aluminum alloys, copper, silicon, polymers, ceramic and glass, silver, titanium and so on. Material of construction of a microchannel reactor is chosen in order to meet desired conditions for operations. For adiabatic conditions, the materials with low thermal conductivity and high durability are preferable. Fabrication techniques are determined depending on the substrate selected. In general, material of construction must have a good thermal and pressure resistance (Ehrfeld *et al.*, 2001; Watts and Wiles, 2006).

Gas phase glycerol steam reforming has not been investigated over microchannel reactors. It is shown that these reactors serve better utilization of the catalyst via good heat transfer properties and higher reactant conversion as well as higher product selectivity for methane steam reforming (Karakaya *et al.*, 2012). Effective usage and results of microchannel reactor for methane steam reforming makes it preferable to investigate for the gas phase reforming of the glycerol.

2.2. Glycerol Reforming for Hydrogen Production

Steam reforming is the most common method to utilize hydrocarbons for syngas production which is a mixture of H_2 and CO. Syngas is an important mixture to be used in various industrial processes such as Fischer-Tropsch synthesis and methanol production (Chiodo *et al*., 2010). Steam reforming of glycerol consists of two main steps. The first step is the pyrolysis of glycerol, and the second step is the water gas shift. In general, glycerol steam reforming is given as combination of these two reactions. The pyrolysis reaction is given as Reaction 2.1 and this reaction is an endothermic reaction with standard enthalpy of the reaction given as 251 kJ mol^{-1}.

$$C_3H_8O_3 \leftrightarrow 3CO + 4H_2 \qquad \Delta H(298\ K) = 251\ kJ/mol \tag{2.1}$$

Pyrolysis reaction produces CO and H_2, and produced CO reacts with water to produce H_2 and CO_2. Name of this process is called as water gas shift reaction and reaction equation is given as Reaction 2.2. Water gas shift reaction is an exothermic reaction having a standard enthalpy of reaction as -41 kJ mol^{-1}.

$$CO + H_2O \leftrightarrow CO_2 + H_2 \qquad \Delta H(298\ K) = -41\ kJ/mol \tag{2.2}$$

As it is stated before, glycerol steam reforming reactions are the combinations of Reaction 2.1 and Reaction 2.2. Combination of Reactions 2.1 and Reaction 2.2, gives the overall glycerol steam reforming reaction. General form of glycerol steam reforming reaction is given as Reaction 2.3. Lin (2013) is defined a parameter "x" in the general steam reforming reaction which indicates the degree of water gas shift reaction involved. The range of this parameter is defined in an interval of 0 to 3. The syngas can be obtained when this parameter is not equal to 3 (Lin, 2013). The maximum hydrogen yield is obtained when the x is equal to 3. This situation indicates that all produced CO from the pyrolysis is consumed in water gas shift.

$$C_3H_8O_3 + xH_2O \leftrightarrow (3-x)CO + xCO_2 + (4+x)H_2 \tag{2.3}$$

Glycerol is a large molecule and the reaction mechanism of glycerol reforming does not only contain the steam reforming reaction but also there are some side reactions, especially reactions responsible for coke formation. Lists of this possible reversible side reaction are given as (Slinn *et al.,* 2008):

$$C + H_2O \leftrightarrow CO + H_2 \quad (2.4)$$

$$C + 2H_2 \leftrightarrow CH_4 \quad (2.5)$$

$$CO + 3H_2 \leftrightarrow CH_4 + H_2O \quad (2.6)$$

$$CO_2 + 4H_2 \leftrightarrow CH_4 + 2H_2O \quad (2.7)$$

$$C + CO_2 \leftrightarrow 2CO \quad (2.8)$$

Pyrolysis reactions are highly endothermic reactions and need for external heat input. If the heat input is large enough to create steep thermal gradients, the formation of non-equilibrium products is inevitable (Rennard *et al.,* 2009). The dehydration and dehydrogenation of glycerol are two major routes for production of non-equilibrium products at high temperatures. At high temperatures, glycerol may decompose into non equilibrium products, most commonly through dehydration and dehydrogenation routes. Dehydration produces hydroxyacetone and 3-hydroxypropanal, the latter being the precursor of acrolein (Lin, 2013):

$$C_3H_8O_3 \leftrightarrow C_3H_6O_2 + H_2O \quad (2.9)$$

$$C_3H_6O_2 \leftrightarrow C_3H_4O + H_2O \quad (2.10)$$

Dehydrogenation generates glyceraldehydes and dihydroxyacetone (Lin, 2013):

$$C_3H_8O_3 \leftrightarrow C_3H_6O_3 + H_2 \quad (2.11)$$

2.2.1. Ni-based Catalysts for Glycerol Steam Reforming

Czernic *et al.* (2002) used crude glycerol to produce hydrogen. Crude glycerol was a very viscous liquid and partially miscible with water. They reported its elemental composition as 54.7% carbon, 9.9% hydrogen and 35.5% oxygen and this shows that the liquid was a mixture of glycerin (55%) with methyl esters of fatty acids (45%). Fluidized bed reactor was used for steam reforming of this solution. The reactor contained 150-200 g of commercial Ni-based catalyst with particle size of 300-500 μm. Steam reforming reactions were carried out at the temperature of 1073 K and 1123 K. They showed that the yield of hydrogen decreased from the initial value of 95% to 77 % after 12 hours on stream. An optimal hydrogen selectivity value of 95% is expected if a water-gas shift reactor followed the reformer (Czernik *et al.*, 2002; Lin, 2013).

Adhikari and coworkers (2008) made experimental test for glycerol steam reforming over Ni/CeO_2, Ni/MgO and Ni/TiO_2 catalysts. The catalysts were prepared using the incipient to wetness procedure with nickel nitrate hexahydrate ($Ni(NO_3)_2.6H_2O$). The surface areas of the catalysts were 67.0 m^2/g, 64.9 m^2/g and 50.2 m^2/g for Ni/CeO_2, Ni/TiO_2, and Ni/MgO, respectively. The experiments were performed in a tubular furnace which could be heated up to 1373 K. Glycerol water solution was injected to the system using HPLC pump. The products were first sent to the crushed ice and water to cool down. The unreacted water, glycerol, and other liquids were eliminated from gaseous products. The gas products were analyzed by using gas chromatographs. Among the catalysts tested, Ni/CeO_2 was found to be best performing one; this catalyst results in 74.7% hydrogen selectivity at water to glycerol molar ratio of 12:1, temperature of 873 K, and feed flow rate of 0.5 ml/min. At these conditions, Ni supported by MgO showed 38.6% hydrogen yield, and Ni supported by TiO_2 revealed hydrogen yield of 28.3%.

Dou *et al.* (2013) conducted an experiment using Ni-Mg-Al based catalysts to make use of glycerol to produce more valuable product hydrogen. The reactor type was fixed bed that was operated under atmospheric pressure in the 723-923 K range. The Ni-Mg-Al based catalysts were prepared by the co-precipitation method with rising pH method. Active metals in the catalyst were in oxide forms and catalysts with different compositions had the surface areas ranging between 99-127 m^2/g. They concluded that the glycerol

conversion increased with temperature. At low temperature, carbon formation was a serious problem in glycerol steam reforming. Optimum catalyst composition was reported as 24.1 wt% NiO, 26.1 wt% MgO, and Al_2O_3 of 49.8 wt% which gave 78.5 % hydrogen selectivity and 88% glycerol conversion at 923 K. The authors also tested the effects of temperature, steam-to-carbon ratio, glycerol inlet concentration and the flow rate of the carrier gas on glycerol steam reforming with the optimum catalyst composition. Water-glycerol mixture was introduced into the system using syringe infusion pump. 1 g of catalyst was used in each experiment (Dou *et al.*, 2013). Space velocity was reported as $1.5x10^3$ ml/(g cat.h) (Lin, 2013). Dou and his coworkers observed that CO concentration increased with increase in the temperature because of the increased activity of the reverse water gas shift reaction. Hydrogen concentration increased with increase of steam-to-carbon ratio from 3 to 4.5, and then it started to decrease from 4.5 to 7.5 of steam-to-carbon ratios (Dou *et al.*, 2013).

Sorption-enhanced reaction processes have been examined in glycerol steam reforming. CO_2 is captured selectively in reaction medium by a proper sorbent (e.g., $(CaMg)(CO_3)_2$), dolomite) which increased hydrogen yield (Lin, 2013). Wang et al. (2010) conducted an experimental test to study the effect of CaO as a CO_2 sorbent in glycerol steam reforming. The catalyst used in the experiments was Ni/ZrO_2. A quartz fixed bed reactor was used in catalytic performance tests with 0.2 ml of catalyst with or without of 0.4 ml of CaO. The products from the reactor were passed through a condenser to separate condensable products from the non-condensable ones. Non-condensable products were analyzed by a gas chromatograph equipped with a TCD detector. Without CaO, maximum hydrogen concentration of 67% could be obtained at 925 K with water-to-glycerol ratio of 9 based on thermodynamic analysis; however, in the experiments maximum hydrogen concentration was measured as 64%. With the presence of CaO, 95% hydrogen purity could be attained below 925 K with water-to-glycerol ratios of 6 and 9 based on thermodynamic analysis (Wang *et al.*, 2010). He *et al.* (2009) used Co-Ni catalyst for glycerol steam reforming reactions with or without dolomite, which is a CO_2 sorbent. Steam-to-glycerol ratio changed in a range of 3-9 and temperatures were varied between 723-823 K. All reactions were performed in a tubular fixed bed reactor. In the experiments, 99% of hydrogen yield and purity was observed with a steam-to-glycerol ratio of 9 (He *et al.*, 2010).

There is an extensive research on different catalysts and their performance on glycerol steam reforming. Suzuki *et al.* (2005) searched Group 8-10 metals as the active metals such as Ru, Rh, Ni, Ir, Co, Pt, Pd, and Fe on the support as Y_2O_3, ZrO_2, CeO_2, La_2O_3, SiO_2, MgO, and Al_2O_3. These catalysts were prepared by a conventional impregnation method. The activities of the catalysts were measured with a fixed bed, flow type reactor made of stainless steel, operating at atmospheric pressure. An aqueous solution of glycerol was fed by a micropump for high performance liquid chromatography (HPLC). In order to preheat the solution, alumina balls were placed above a catalyst bed. Glycerol reforming reactions were conducted at a temperature range of 723-823 K, a steam-to-carbon molar ratio of 3.3, and the contact time of glycerol was taken as 13.4 gcat h/mol on 100 mg of catalyst in each run (Suzuki *et al.*, 2005). Among the catalyst being prepared Ru (3 wt%) supported on Y_2O_3 was the best catalyst that gave more than 80% H_2 yield with a CO selectivity of approximately 20% in 24 h (Lin, 2013). The order of the activity of the metals were found as Ru ≈ Rh > Ni > Ir > Co > Pt >Pd > Fe. Ru supported by Y_2O_3 and ZrO_2 showed high glycerol conversion compared to Ru supported by MgO and Al_2O_3 (Suzuki *et al.*, 2005).

Zhang *et al.* (2007) studied glycerol steam reforming on ceria-supported Ir, Co, and Ni catalysts, and discovered that Ir/CeO_2 showed the best performance with 100% glycerol conversion and more than 85% H_2 selectivity at 623 K. This was explained by the interaction between the active metal and the support material and the redox chemistry of ceria. A similar performance was also discovered on ceria-promoted Pt/Al_2O_3 (Montini *et al.*, 2010). Zhang *et al.* (2007) used a continuous flow fixed bed quartz micro-reactor operating under atmospheric pressure within the temperature range of 523-873 K. In each experiment, 0.2 g of catalyst was used. Feeding gas composition was reported as 2 vol% glycerol, 18 vol% water, and 80 vol% of He. The gas hourly space velocity was 11,000 ml/gcat.h. The effluent gas from the reactor was analyzed by a gas chromatograph.

Experimental tests in this study are performed over Ni-based catalysts which include Al_2O_3 as support material. In glycerol steam reforming, acidic and basic properties of the support materials affect the catalyst morphology, reactivity and its stability. Pompeo and his coworkers (2010) investigated the effect of the acidity of the support materials at

temperatures lower than 723 K. They used Pt supported on α-Al_2O_3, γ-Al_2O_3, ZrO_2, SiO_2 modified with Ce and Zr. A fixed-bed quartz reactor operated isothermally at atmospheric pressure was used in each experiment. The aqueous solution of glycerol (10 wt%) was injected to the reaction medium by a HPLC pump with a feed flow rate of 0.1 ml/min. The evaporator was a 6 mm diameter quartz tube filled with quartz pellets heated by an electric furnace. The space time was between 0.2-6 min with different catalyst weights from 0.035 to 0.1 g. The analysis of the gaseous products was made by using a Shimadzu GC-8A gas chromatography equipped with a column HayeSep DB 110-120 and a TCD detector. They concluded that the acidic supports tend to dehydrate glycerol leading a fast deactivation of the catalysts by the coke formation. However, SiO_2 was a neutral support and promoted the dehydration reactions and cleavage of carbon to carbon bonds. The catalyst made by Pt supported by SiO_2 catalyst resulted in stable operation for 40 hours. Additionally, basic support materials did not guarantee a better performance compared to acidic supports. Suzuki *et al.* (2005) used Ru supported on MgO (basic support) and observed a poor glycerol conversion (Suzuki *et al.*, 2005). Soares *et al.* (2006) used Pt supported on Al_2O_3, ZrO_2, CeO_2/ZrO_2, and MgO/ZrO_2 catalysts and they concluded that Pt on Al_2O_3 showed better stability than a strong basic support (MgO/ZrO_2). A possible explanation is that reduction of oxide support can facilitate the synthesis of unsaturated hydrocarbons (e.g. ethylene) for carbonaceous deposits on Pt. Similar catalytic behaviors were observed on Ni-based catalysts (Lin, 2013). Chiodo *et al.* (2010) made a comparison between Ni supported on both MgO and Al_2O_3 and observed nearly same amount of coke formation on catalysts. Therefore, supports are frequently modified with promoters such as CeO_2, La_2O_3, and ZrO_2. Decorating these promoters on Ni/Al_2O_3 not only reduces support's acidity, but also promotes H_2 production and maintains catalyst's durability. This is attributed to their redox natures (Lin, 2013).

Nichele and his friends (2012) studied on the effect of support materials for the glycerol steam reforming reactions. They had used Ni-based catalysts with supports TiO_2, SBA-15 and ZrO_2. They concluded that strong interaction between the active metal and support ensured stability, activity and selectivity of the catalyst in glycerol steam reforming reactions. Negligible activity was observed for Ni/TiO_2 catalyst due to the low strength of intermolecular forces to keep nickel in the reduced state. Moreover, Ni/SBA-15

catalyst led to deactivation process. They have obtained best results with Ni/ZrO_2 catalyst showing no deactivation for 20 hours (Nichele *et al.*, 2012).

Glycerol steam reforming reaction is mostly conducted at temperatures above 750 K. High temperature operation leads to active phase sintering so catalyst can deactivate permanently. Nickel, iron, cobalt, and other transition metals can become mobile at temperatures higher than 573 K (Lin, 2013). Iriondo *et al.* (2010) performed glycerol steam reforming reactions over Ni catalysts supported on CeO_2, Al_2O_3, and CeO_2-promoted Al_2O_3. They concluded that nickel-ceria interaction increased the stabilization of active metal particles on catalyst surface. In glycerol steam reforming, in order to prevent from sintering, using CeO_2, TiO_2, or ZrO_2 as support materials is reported to strengthen the interaction between active metal and support (Lin, 2013).

Thyssen *et al.* (2013) performed glycerol steam reforming reactions over Ni catalysts supported by La_2O_3-SiO_2. The catalytic experiments were conducted in a fixed bed reactor containing 150 mg catalyst at 873 K with inlet water to glycerol ratio of 3:1. From their studies, it was shown that the addition of La_2O_3 to Ni catalyst supported by pure SiO_2 favored the production hydrogen and carbon dioxide, while the carbon formation during the reaction was decreased. They explained the decrease in the C content on the active metal by the formation of La carbonate that removed C species over the active metals (Thyssen *et al.*, 2013).

Dieuzeide *et al.* (2013) analyzed the effect of Mg content as a promoter of Ni/γ-Al_2O_3 catalyst in the steam reforming of glycerol. The Mg content has the effects on the textural and structural characteristics of the catalyst, catalytic activity and H_2 selectivity. The catalysts were prepared by the incipient wetness impregnation method. The experiments were carried out in a stainless steel continuous flow fixed bed reactor operating at atmospheric pressure. In each experiment, 45.5 mg of catalyst was inserted to the reactor. Liquid mixture of water and glycerol was fed to the reactor using a syringe pump. Among the catalysts promoted with Mg, the best catalyst activity was achieved with Ni(10)Mg(3)Al catalyst while lowest amount of carbon formation during reaction time on stream was observed on Ni(10)Mg(15)Al catalyst. They concluded that high

contents of Mg inhibited carbon formation and this could be related to that the basic character of the support increased with the Mg content.

2.3. Oxidative Glycerol Reforming for Hydrogen Production

Addition of O_2 to reaction system increases the heat inside the reactor as a result of exothermic nature of oxidation reaction. This favors the glycerol steam reforming which is an endothermic reaction. Therefore, in order to increase H_2 yields, O_2 is co-fed with H_2O to the system under partial oxidation conditions. Moreover, the carbon formation which is commonly observed for glycerol steam reforming reaction especially on Ni-based catalysts decreases in an oxidative environment. Preventing catalyst from coke formation means that catalyst activity remains unchanged for longer periods, and longtime operation is ensured. The chemical expression for oxidative glycerol steam reforming is given as (Lin, 2013):

$$C_3H_8O_3 + \frac{3}{4}O_2 + \frac{3}{2}H_2O \rightarrow 3CO_2 + \frac{11}{2}H_2 \qquad (2.12)$$

By regulating the amount of O_2 and H_2O, the syngas production can be enhanced. The related oxidative glycerol reforming reaction equation is given with parameters “x” and “y” as:

$$C_3H_8O_3 + (\frac{3}{4}\text{-x})O_2 + (\frac{3}{2}\text{-y})H_2O \rightarrow (3\text{-}(2x+y))CO_2 + (2x+y)CO + (\frac{11}{2}\text{-y})H_2 \qquad (2.13)$$

In order to obtained maximum yield of syngas, the parameters x and y should be approximately 3/5 and 5/7, respectively (Lin, 2013).

2.3.1. Catalytic Tests for Oxidative Steam Reforming of Glycerol

Kamonsuangkasem and his friends (2013) carried out experiments on catalytic oxidative steam reforming of glycerol over $Ni/CeZrO_2/Al_2O_3$. They explored the effects of water to glycerol ratio, reaction temperature, and oxygen to glycerol ratio which are regulated as 3, 6 and 9, and 823, 873 and 923 K, and 0.25, 0.50, and 0.75, respectively.

They determined the optimum operating condition for maximum hydrogen selectivity at water to glycerol ratio of 9, oxygen to glycerol ratio of 0.5, and temperature of 923 K. Under these conditions, maximum hydrogen yield and glycerol conversions were obtained as 67% and 69% respectively. Using the promoter of $CeZrO_2$ was said to enhance hydrogen production and inhibit coke formation. The catalytic glycerol steam reforming tests were conducted at an atmospheric pressure in a fixed bed reactor made from a 316-stainless steel tube with an inner diameter of 1.27 cm. They used HPLC pump to inject the aqueous solution to the system. The gas hourly space velocity for catalytic tests was reported as ca. 16,000 L^{-1}. Although they reported some activity results, they did not mention about the blank tests (Kamonsuangkasem *et al.*, 2013).

Turn and his co-workers (2007) conducted experiments on glycerol steam reforming over Ni-based commercial G-91 EW catalysts in the absence and presence of oxygen. They achieved a maximum hydrogen yield of 4.6 mol hydrogen per mole of glycerol, with the absence of oxygen (Turn *et al.*, 2007). Other studies, however, contradicted with the findings of Turn et al. (2007), as the maximum hydrogen yields were achieved with oxygen in the feed. Chang *et al.* (2013) conducted autothermal steam reforming experiments for hydrogen production over packed bed and Pd/Ag alloy membrane reactors. In the membrane reactor, glycerol conversion increased with pressure, but the hydrogen yield declined. In the packed bed reactor, nickel on ceria-alumina gave 85% hydrogen yield with oxygen/glycerol ratio of 0.15 (Chang *et al.*, 2013). Therdthianwong *et al.* (2011) studied the same reaction over nickel on ceria-zirconia, alumina catalyst and with water-to-glycerol ratio of 9 and oxygen-to-glycerol ratio of 0.5. They obtained complete glycerol conversion and 80% hydrogen selectivity (Therdthianwong *et al.*, 2011).

Schmidt and his co-workers (2009) investigated catalytic partial oxidation of glycerol to syngas and non-equilibrium products at temperatures above 823 K and at contact times between 30-90 ms over Rh and Pt based catalysts. They used a nebulizer emitting droplets of fuel and air on the order of 10-100 μm which served an excellent mixing. They used cylindrical ceramic foam monoliths composing 99% α-Al_2O_3, and catalyst were prepared by coating Rh and Pt noble metals over foam monolith. Incipient to wetness impregnation technique is used for coating. The Rh based catalyst showed maximum glycerol conversion of 90% and a 65% H_2 selectivity while steam-to-carbon

ratio was set to 0.66. Another important result was the formation of large amounts of non-equilibrium chemicals such as acrolein, acetaldehyde, and hydroxyacetone over the foam surface; especially for the reactions performed using Pt based catalyst (Schmidt *et al*., 2009). The same group continued their investigations of Rh catalyst supported on ceria-alumina. They observed the long time behavior of the catalyst for glycerol partial oxidation on an autothermal reactor. Catalyst deactivation occurred on a long term operation which lasted for 450 hours. The maximum H_2 selectivity was obtained as 70% at the beginning of the operation, and then started to decrease down to 20% as a result of the catalyst deactivation (Schmidt *et al*., 2010).

Generation of syngas from glycerol partial oxidation using $LaMnO_3$ and $LaNiO_3$-coated monoliths was studied by Lin and Liu (2014). The optimization of the performance of $Pt/LaMnO_3$ was achieved at steam/carbon and C/O_2 ratios of 0.66 and 1.1, respectively, where glycerol conversion reached 98%, yielded a H_2/CO ratio of 2.1, and produced the least hydrocarbon by-products with 6.1% (Lin and Liu, 2014).

Liu and his friends studied the autothermal reforming of glycerol into synthesis gas over BASF Pt and Rh/Pt dual layer monolith catalyst. They used atomizer nozzle to spray the glycerol-water mixture over the monolith. They concluded that the distance between the nozzle and catalyst affected the product distribution. They considered the thermal decomposition of the glycerol, and they called the gap between the nozzle and the catalyst as "non-catalytic/decomposition reaction zone". They had conducted the non-catalytic experiments at temperatures of 673-973 K, at atmospheric pressure, at steam-to-carbon ratio 0.8, oxygen to carbon ratio of 0.15 and GHSV about 15,000 h-1 at STP. It was determined that glycerol thermally decomposed to produce more carbon containing products. Glycerol conversions obtained from blank monolith at 673 and 773 K were lower than the catalytic reactions; however, at 873 and 973 K, the conversions were nearly same. Moreover, at this temperature levels, catalytic activity was observed which was attributed to the appearance of H_2, CO, and CO_2. They concluded that catalytic activity led to increase in CO_2 production as a result of steam reforming reaction or the water gas shift reaction (Liu *et al.*, 2013).

3. EXPERIMENTAL WORK

3.1. Materials

3.1.1. Chemicals

All the chemicals used for preparation of catalytic microchannel reaction system are presented in Table 3.1.

Table 3.1. Chemicals used in experimental tests.

Chemicals	**Specification**	**Source**	**Molecular weight (g/gmol)**
Nickel(II) nitrate hexahydrate	$Ni(NO_3)_2 \cdot 6H_2O$	Sigma-Aldrich	290.79
Gamma alumina (1/8" pellets)	γ-Al_2O_3 225 m^2/g	Alfa Aesar	-
Gamma alumina (3 μm)	γ-Al_2O_3 80-120 m^2/g	Alfa-Aesar	101.96
Glycerol	$C_3H_8O_3$ 99.5% purity	Sigma-Aldrich	92.09
FeCrAlY	FeCrAlY sheets (2 mm x 100 mm x 100 mm)	Goodfellow Cambridge Ltd.	-

3.1.2. Gases and Liquids

The N_2, H_2, O_2, Ar and He are the gases that are directly used in the experiments. Gases such as CO, CO_2, CH_4, C_2H_4, and C_2H_6 are only used for calibration of chromatographs. All gases are supplied by Linde and given in Table 3.2 with their applications. The deionized water is obtained from Zeneer Water Purification System and

its conductivity is less than 0.1 $\mu S.cm^{-1}$. It is also used in catalyst synthesis and in coating the catalyst onto FeCrAlY plates. Glycerol, another reactant used in the system, is obtained from Sigma-Aldrich with 99.5 % purity.

Table 3.2. Specifications and applications of the gases used.

Gas	**Specification**	**Application**
Argon	99.995% (Linde)	GC carrier gas
Helium	99.99% (Linde)	GC carrier gas
Nitrogen	99.99% (Linde)	GC calibration, inert
Oxygen	99.998% (Linde)	GC calibration, reactant gas
Carbon monoxide	99.999% (Linde)	GC calibration
Hydrogen	99.99% (Linde)	GC calibration, reducing agent
Carbon dioxide	99.99% (Linde)	GC calibration
Methane	99.70% (Linde)	GC calibration
Ethane	$5\%C_2H_6+95\%N_2$ (Linde)	GC calibration
Ethylene	$5\%C_2H_4+95\%N_2$ (Linde)	GC calibration

3.2. Experimental Systems

The experimental system used in this research is composed of four sub-systems:

- Catalyst Preparation System: This system is used for preparing the catalysts, being used in the experimental study, via incipient-to-wetness impregnation method.
- Catalyst Characterization System: This system is utilized for characterizing surface structure of used or reduced catalysts and for measuring the metal percentages inside of catalyst by using the method called Scanning Electron Microscopy (SEM) integrated with Energy Dispersive X-ray Spectroscopy (EDX).
- Catalytic Reaction System: This system is used for catalytic activity tests, consisting of mass flow controllers for inlet gases, HPLC pump for water and glycerol mixture feed, reaction furnace controlled by three programmable temperature controllers and a microchannel reactor, together with two cold traps.

- Product Analysis System: Two online gas chromatographs are utilized for analyzing the composition of the product gases.

3.2.1. Catalyst Preparation System

The incipient-to-wetness impregnation technique is used for the preparation of Ni/Al_2O_3 catalysts. This technique is described schematically in Figure 3.1. Retsch UR1 ultrasonic mixer serves a uniform mixing providing well dispersion of the active metal precursor over catalyst support. Other parts of the system involve a vacuum pump connected to a Buchner flask, silicone tubings and a Masterflex computerized-drive peristaltic pump which is used for pumping solution of active metal precursor over the catalyst support.

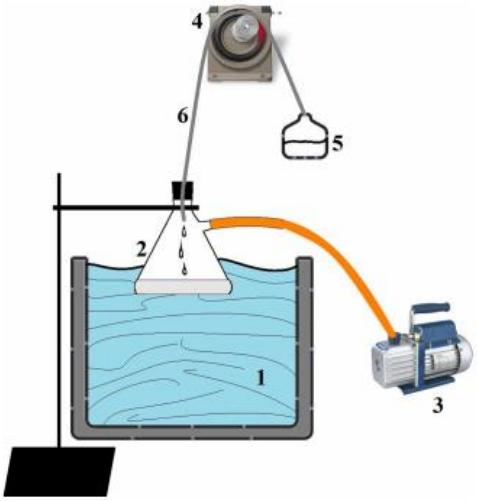

Figure 3.1. Catalyst Impregnation System: 1. Ultrasonic mixer 2. Buchner flask 3. Vacuum pump 4. Peristaltic pump 5.Aqueous catalyst solution 6. Silicon tubing (Karakaya, 2012).

3.2.2. Catalyst Characterization System

The structure and composition of catalyst samples are analyzed at Boğaziçi University Advanced Technologies R&D Center through Backscattering Electron-Scanning Electron Microscopy (BSE-SEM) and Energy Dispersive X-ray Analyses (EDX) using a Philips XL30 ESEM-FEG system.

3.2.3. Catalytic Reaction System

Catalytic reaction system was designed and constructed at Catalyst Technology and Reaction Engineering Laboratory / KB 404 of BU. Department of Chemical Engineering for gas phase glycerol steam reforming (GSR) and oxidative glycerol steam reforming (OGSR) experiments. This system includes; feed preparation, reaction, and product analysis parts which are explained below, in detail.

Figure 3.2. Feed Preparation Part of Glycerol Reforming System.

Feed preparation part is designed and constructed to transport liquid reactants (deionized water and glycerol mixture), inert gas (N_2), reactant gas O_2 for OGSR tests and reducing agent (H_2) into the reaction section (Figure 3.2). Gas regulators provided by Linde are used to regulate the outlet pressures of gaseous species (N_2, H_2, and O_2) from pressurized storage cylinders. Moreover, the flow rates of the gases to the reaction section

are controlled and measured by Bronkhorst F-201CV series digital mass flow controllers (MFC). 1/8” stainless steel tubing is separately used to connect each gaseous species to their individual MFC unit. As a result, the flow rate of each gas can be regulated in the corresponding MFC unit for a desired feed composition by using MFC calibration charts. The calibrations of MFCs for each specific gas are made and given in Appendix A. The liquid reactants (deionized water and glycerol mixture) are fed to the reaction section using a Shimadzu LC-20AD HPLC pump with constant pulse-free flow. The HPLC pump is a very precise and well calibrated apparatus showing exact liquid flow on its digital screen. The liquid mixture is brought to the reaction system horizontally within 1/16” stainless steel tube, and is mixed with the carrier gas N_2 (and with O_2 specifically for OGSR tests). This mixed gas-liquid solution is directly sprayed into a 2.0 cm ID x 80 cm quartz reactor which is placed in the furnace vertically.

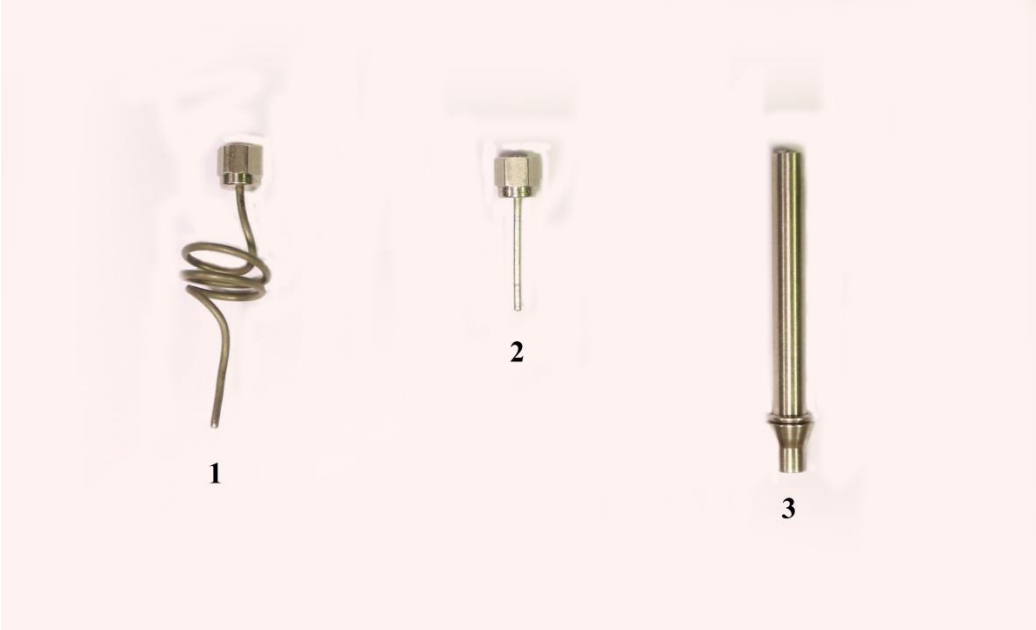

Figure 3.3. Different Configurations to Introduce Liquid Reactant Mixture into Furnace: 1. 1/16" spiral-shaped. 2. 1/16" straight. 3. 1/4" straight.

The mixing of glycerol and water is a very important part of this study in order to obtain the desired S/C ratios. To do so, different configurations for the upstream of the reaction furnace are investigated in order to enhance the mixing of glycerol and water. Some of these configurations are shown in Figure 3.3. The tubing carrying the glycerol

solution from the HPLC pump to entrance of the furnace are first covered with electrical line heater to increase the solution temperature to 125 °C. It was thought that the increase in the temperature would make the flow of the liquid solution inside of the pipe easier because the viscosity of the glycerol would decrease as a result of the temperature increase. Additionally, this heating would help to enhance vaporization of glycerol solution while passing through the first part of the furnace. Moreover, the tubing for the carrier gas N_2 was also covered with electrical line heater and heated up to 125 °C which would also help easier vaporization of the glycerol solution inside the furnace. However, for the proposed configuration, high amount of coke was observed in blank tests. This result most probably stemmed from the fact that at 125 °C, the water in the solution, which has boiling temperature of 100 °C at 1 atm, was vaporized and this led to an increase in its volume and speed compared to liquid glycerol, which has boiling temperature of 290 °C at 1 atm. When glycerol reached the upper zone of the furnace, there would be smaller S/C ratio which would lead to coke formation. After this observation, it was decided not to heat the tubings for liquid and gaseous reactants. Without pre-heating the reactant mixture, it was fed into the reaction system through a 1/4" pipe as seen in Figure 3.3. Because the 1/4" pipe has a large inner diameter, an annular flow regime was achieved and no spraying effect was observed in this configuration. It was seen that the glycerol solution was accumulated on the inner surface of pipe and formed large droplets. When a large droplet fell into the reactor, it spent less time in the upper zone of the furnace. The good mixing and complete vaporization of the glycerol solution within this zone were not guaranteed in this case. Hence, in order to prevent annular flow and obtain a good mixing at the reactor entrance, 1/4" pipe was replaced with a 1/16" pipe. Diameter reduction in the pipe helped to push liquid down, and 1/16" pipe acted as a nozzle. This improvement allowed the glycerol-water mixture to vaporize completely at the upper part of the reactor. Fast vaporization also led to correct adjustment of local S/C ratio over the catalyst surface by serving good mixing. Further improvement was tried by placing a spiral shaped 1/16" pipe (Figure 3.3) to the upper zone of the furnace to improve mixing of the liquid mixture. However, blank tests with this configuration showed coke formation, most probably due to the faster vaporization of water compared to glycerol in the mixture. The mixture flowed through the spiral in the hot zone causing a decrease in the S/C ratio. At the end of these investigations, it was decided to continue to the catalytic experiments with the 1/16” straight pipe.

Figure 3.4. Reaction Part of Glycerol Reforming System.

The experimental tests are conducted in the furnace (PROTHERM PZF 12/50/500) which is shown in Figure 3.4. This furnace includes three zones each of which can be temperature programmed separately. Each zone has its own temperature controllers. The sprayed glycerol mixture is vaporized at the upper part of the furnace. Temperature of this part is set to a temperature between 310-350 °C, which is above the boiling point of the glycerol (290 °C at 1 atm), in order to guarantee complete vaporization of water and glycerol. N_2 (together with O_2 for OGSR tests) and vaporized glycerol-water mixture flow through the middle zone of the furnace where the microchannel reactor is placed. Temperature of middle zone is set as the reaction temperature. After the reaction, the formed products with unconverted reactants enter the bottom zone where temperature is again set to 310 °C which is above the boiling points of the glycerol and any possible liquid products (290 °C at 1 atm). This prevents formation of condensates on the inner

surface of the quartz reactor. After the gas mixture exit the furnace, they enter the first cold trap being placed right below the furnace. The unreacted glycerol, water and/or any other heavy compounds are condensed in cold trap to prevent any condensation in the tubes between the furnace and the product analysis systems.

Figure 3.5. Post-reaction Part of Glycerol Reforming System.

The first cold trap is actually enough to condensate the liquid components. However in order to make sure that no condensate, especially water, enters to the gas chromatographs, a second cold trap is placed inside a Dewar flask which provides a good insulation between the surroundings and the cold trap. Presence of the condensate in the product gases has an adverse effect on gas chromatography settings. A three way valve is placed between these two cold traps, in order to either to trap N_2 in the quartz tube or to send the gas to soap bubble meter for manual check of gas flows or to send the effluent gases to the gas chromatographs.

Figure 3.6. Gas Chromatographs used in Glycerol Steam Reforming System.

Gas chromatographs are used for analyzing the dry product gases, and the first data point is recorded in 30th minute after the reaction is started, then each data point is taken in every 45 minutes until 300 minutes. Reported results are given by calculating the arithmetic averages of the data after the system reaches the state, which approximately corresponds to the 120th minute of the experiment.

3.2.4. Product Analysis System

The effluent stream from the cold traps consists of inert N_2, H_2, CO, CH_4, CO_2, C_2H_4 and C_2H_6 (unconverted O_2 for OGSR tests). The composition of the stream is determined and analyzed via two gas chromatographs (Shimadzu GC-2014 and Shimadzu GC-8A) equipped with two different packed columns. Shimadzu GC-2014 which is equipped with a Molecular Sieve 5A column and a thermal conductivity detector (TCD) is used for detecting and quantifying H_2, N_2, CH_4, O_2 and CO gases. Moreover, Shimadzu GC-8A gas chromatograph which is equipped with a Porapak Q column and a TCD detects and quantifies the gases such as N_2, CH_4, CO_2, C_2H_4 and C_2H_6.

The product stream continuously passes through the column of the Shimadzu GC-8A which has relatively more distance to the reactor exit compared to Shimadzu GC-2014. After gas sampling is made on this chromatograph, the product gas is directed to the Shimadzu GC-2014 using a three way valve. After waiting a minute, sampling loop of this GC is get filled by the product gases, then sample is let to enter the column of the GC, and results are obtained in terms of area under the curves. Sampling procedure of both GC is carried out by a six-way valve and consists of sampling loop of 1 ml for injection of product gas to the column. The operating parameters for gas chromatographs are given in Table 3.3.

Table 3.3. GC operating conditions for product gas analysis.

GC Parameter	**Shimadzu GC-2014**	**Shimadzu GC-8A**
Detector type	Thermal conductivity	Thermal conductivity
Column oven temperature	50 °C	90 °C
Injector temperature	80 °C	90 °C
Detector temperature	150 °C	150 °C
Carrier gas	Argon	Helium
Carrier gas flow rate	25 $mL.min^{-1}$	25 $mL.min^{-1}$
Detector current	50 μA	120 μA
Column packing material	Molecular Sieve 5A (60-80 mesh)	Propak Q (80-100 mesh)
Column tubing material	Stainless steel	Stainless steel
Column ID & length	1/8" OD x 2 m	1/8" OD x 3 m
Sampling loop	1 mL	1 mL

It is essential to make a calibration of the gas chromatographs in order to get clear peaks for each gas, to determine the retention time specific to the gases and the corresponding flow rates of the product gases using the relation between the peak area and the calibration chart. Calibrations are performed using two different ways, first of which is taking the feed samples as known volumetric composition of binary mixture of two gases using the calibrated mass flow controllers. Second one is about injecting known volumes of the gas to columns directly. The computers of the gas chromatographs display the peaks

at the specific retention times for each gas. The curves generate area, and the area is calculated by integrator software. The micromoles of gases versus generated peak area are plotted, and then the calibration curves are obtained as given in Appendix B.

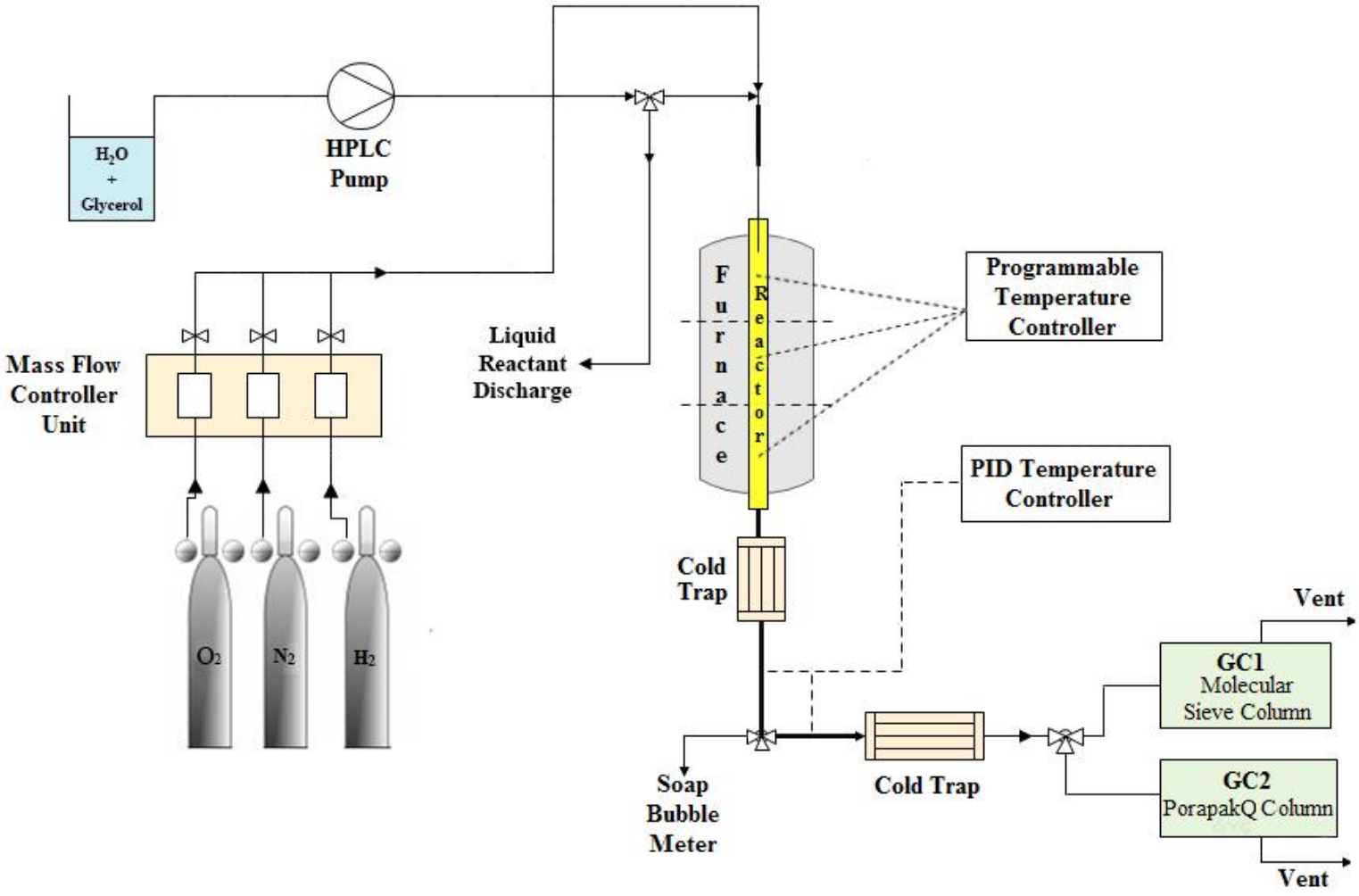

Figure 3.7. Process Flow Sheet of the Reaction System.

3.3. Catalyst Preparation and Pretreatment

The experimental tests of glycerol steam reforming are carried out on Ni/Al_2O_3 catalyst with two different active metal loadings (5% and 10% Ni) and two different configurations (packed and coated catalysts). Additionally, 5 wt.% Ni/Al_2O_3 is used for oxidative steam reforming tests. Catalysts are prepared using the incipient to wetness impregnation method. Catalyst preparation involves support (Al_2O_3) preparation, active catalyst preparation, plate coating for microchannel reactor and pretreatment stages.

3.3.1. Preparation of Support

Catalytic steam reforming and oxidation of hydrocarbons occur at elevated temperatures. That is why the catalyst support must have a good thermal stability, as well as a high surface area. The γ-Al_2O_3 is one of the frequently used support materials because of its high surface area (ca. 150-200 m^2/g). However, it has been reported that the support has lower stability at temperatures greater than 600 °C and it has a tendency to facilitate the carbon formation over the surface of the catalyst in the presence of the steam due to its high acidic characteristic (Ma, 1995). The experimental tests in this study are performed at a maximum of 600 °C. The most stable phase of the alumina is reported as α phase which is obtained after heat treatment to γ-Al_2O_3 up to 1127 °C. However, it turns to have a lower surface area (less than 5 m^2/g) which leads to low dispersion of the active metals over the support (Doesburg et al., 1999). There is an optimization between the catalyst surface and thermal stability due to the phase of the alumina. The δ-phase which is the intermediate phase between γ and α phase has relatively high thermal stability with a decent surface area (Ma, 1995).

Three different procedures were investigated by Avci and co-workers (2004) with various drying and calcination temperatures and durations. The procedure and the BET surface areas of resulting materials are given in Table 3.4.

Table 3.4. Alumina support preparation procedures.

Procedure	**BET surface area (m^2g^{-1})**
Calcination at 1000 °C for 4 h	46.8
Drying of alumina at 150 °C for 2 h Calcination at 900 °C for 4 h	81.6
Drying of alumina at 105 °C for 16 h Calcination at 875 °C for 4 h	73.2

The study revealed that the second procedure resulted in the highest BET surface area. Drying period and time has an effect on BET surface area as seen in the second and third comparison. Longer period of drying at a lower temperature gave a lower surface area, even though the calcination temperature was 25 °C below that of the second procedure. In this study, the second procedure is applied in support preparations.

The catalytic activity tests in this study comprise steam and oxidative steam reforming of glycerol for the parametric and comparative study of packed and coated microchannel reactor configurations. For the preparation of the coated microchannel configuration, 3-μm sized γ-Al_2O_3 are dried at 150°C for 2 hours and calcined at 900°C for 4 hours in accordance with the procedural guidelines given in Table 3.4. The similar procedure is applied for the preparation of the catalysts used in packed microchannel configuration. The difference is the size of the alumina particles. In the preparation of the particulate catalysts suitable for packing into the microchannel, alumina particles are crushed and sieved to 60 – 80 mesh size (250 – 177 μm).

3.3.2. Preparation of Active Catalysts

Incipient-to-wetness impregnation method is used to prepare 5 wt. % Ni/Al_2O_3 and 10 wt. % Ni/Al_2O_3 catalysts for both coated and packed microchannel configurations. All catalyst preparations are made on the bases of 3 grams total weight.

3.3.2.1. Incipient-to-wetness Impregnation of Active Metals over the Al_2O_3. The aqueous solutions of the active metal precursors which are stated in Table 3.1 are prepared by mixing and dissolving the required amount of precursor salt in definite amount of

deionized water (ca. 1 $mL_{solution}$ $g^{-1}_{support}$). For the preparation 3 grams of 5 wt. % Ni/Al_2O_3, 2.85 grams of support and 0.15 grams of active metal are needed, and in order to meet the active metal requirement, 0.743 grams of 20.18 wt.% Ni containing nickel (II) nitrate hexahydrate precursor is dissolved and mixed in 2.85 grams of deionized water. Moreover, for 3 grams of 10 wt. % Ni/Al_2O_3 catalyst, the aqueous solution of the active metal precursor is obtained by mixing and dissolving 1.486 grams of 20.18 wt. % Ni containing nickel (II) nitrate hexahydrate in 2.7 grams of deionized water. The dried and calcined support, either 60-80 mesh (250 – 177 μm) or 3-μm size of δ- Al_2O_3, is placed into the Büchner erlen and mixed ultrasonically for 30 minutes under vacuum. The aqueous solution of the metal precursor is impregnated over the support with the usage of a peristaltic pump (Figure 3.1). The homogenous dispersion of the aqueous solution over support surface is an important aspect in this technique. After impregnation, resulting slurry is let to mix ultrasonically for another 90 minutes under vacuum to enhance the homogenous distribution of the active metal over support surface. After the mixing stage, the catalyst is dried over night at 120 °C (min. 16 hours). As the final step of active catalyst preparation, dry catalyst particles is crushed to obtain finer particles, and this form of the catalyst is calcined at 600 °C for 3 hours.

3.3.2.2. Catalytic Microchannel Synthesis. The catalytic microchannel synthesis requires some chemical as well as mechanical treatments. First step of this synthesis is the manufacturing of a 310-grade cylindrical housing with a diameter of 18.6 mm and a length of 30 mm. Two different shapes of this housing are utilized in catalytic experiments. The shape which is given in Figure 3.8 is used for coated microchannel configurations and it needs one FeCrAlY plate to create a microchannel at the center of the housing. The “H” shaped housing which is given in Figure 3.9 requires two FeCrAlY to form a microchannel and used for packed microchannel configuration. The diameter of the housing is manufactured so that when it is placed to the middle part of the quartz reactor, it prevents by-pass of reactants from the interface of quartz tube and housing. The only space that a reactant molecule can travel is the microchannel at the center of the housing.

The FeCrAlY is a special alloy for catalyst coating. The FeCrAlY sheets are machined into plates with dimension of 2 mm x 5 mm x 20 mm using the wire electro discharge method. These plates are rasped in order to place them inside of the housing.

Once the plate is inserted to the housing, only gap between the inlet and the outlet of the housing is the microchannel at the center. Before coating or packing the catalysts, the plates are cleaned first with distilled water, then ethanol and finally acetone to remove any impurities over the surface. The next step is the calcination of the cleaned plates. Calcination is performed at 900 °C for 2 hours in order to increase the adhesion of the coated catalysts via the formation of the native alumina layer over plate surface.

In the coated microchannel configuration, the plates are coated with calcined 3-μm-sized catalyst powders. Catalyst powders are mixed with a few drops of deionized water at a water-to-powder ratio of 5:1. This mixture is blade coated onto plates until the catalyst weight per surface area reaches ca. 0.02 $g_{cat}cm^{-2}$. However, the blade coating is performed as slurry, so it is hard to estimate whether dry catalyst weight on the surface reaches to 0.02 $g_{cat}cm^{-2}$. In order to meet this constraint, it is found that the weight of the coated slurry must be around 0.035-0.040 $g_{cat}cm^{-2}$. After drying of the coated slurry on the plate surface, the catalyst weight over the plate corresponds approximately to 0.02 $g_{cat}cm^{-2}$. Another requirement is the homogenous coating of the slurry such that it must have same height at each point of plate surface. The plate must be inserted into housing while the catalyst on it is still wet, in order to see whether there are excess catalyst touching the wall of the housing or not and to observe enough space forming catalytic channel. This check is important because for any inconvenience after drying and calcination of the coated plate, the plate does not fit to housing and the catalyst on it may crack, then all step must be repeated one more starting with cleaning the plate.

After coating the slurry over the plate surface, the resulted catalyst coated plates are dried overnight (16 hours) at 120 °C. Then, they are calcined at 600 °C for 3 hours. This is the final treatment of the coated plates before using them in the catalytic tests. The coated plates are inserted to housing, and quartz wool is placed inside of the housing to the bottom side of the plate in order to keep the plate inside of the housing when housing is inserted vertically on the quartz tube. A visual representation of the plate and the housing type is given in Figure 3.8.

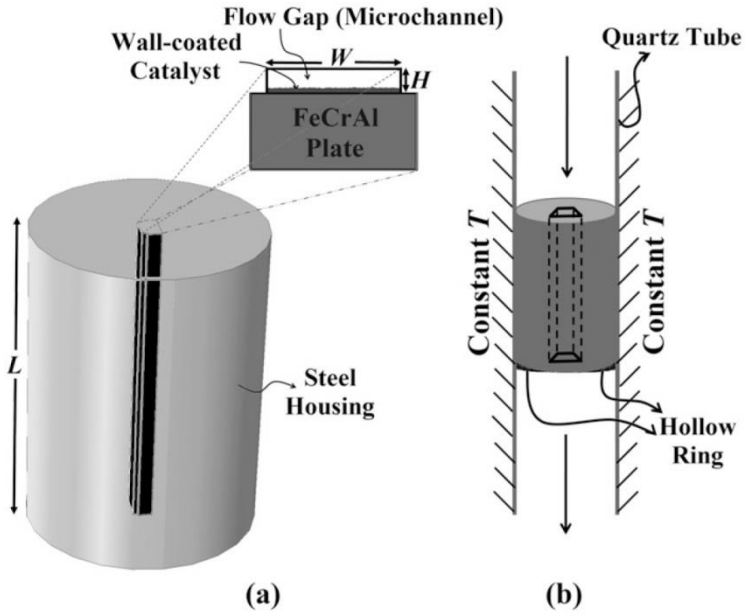

Figure 3.8. Coated Microchannel Reactor Configuration a. Coated microchannel reactor b. Location of steel housing in quartz tube (Karakaya *et al*., 2012).

In packed microchannel configuration, the H type housing, 60-80 mesh (250 – 177 μm) size of 5 wt. % Ni/Al_2O_3 catalyst powders, and two FeCrAlY plates are used. The plates are inserted to the housing forming a microchannel. In order to pack the catalysts to this channel, bottom side of the channel is closed using the quartz wool. The packed microchannel configuration experiment is done to compare the results with coated microchannel configuration. As a result, for a better comparison, the packed amount of the catalyst is determined as giving the same W/F_{A0} (weight of catalyst coated or packed over glycerol fed to the reactor). Other constraints are the ratio of bed length to particle diameter ($L_{tube}/D_{particle}$) and ratio of tube diameter to particle diameter ($D_{tube}/D_{particle}$). As a rule of thumb, $L_{tube}/D_{particle}$ ratio must be higher than 50 and $D_{tube}/D_{particle}$ ratio must be higher than 15 (Simsek *et al.*, 2013). Based on these constraints, the amount of the catalyst is determined and packed to the microchannel formed by plates and housing.

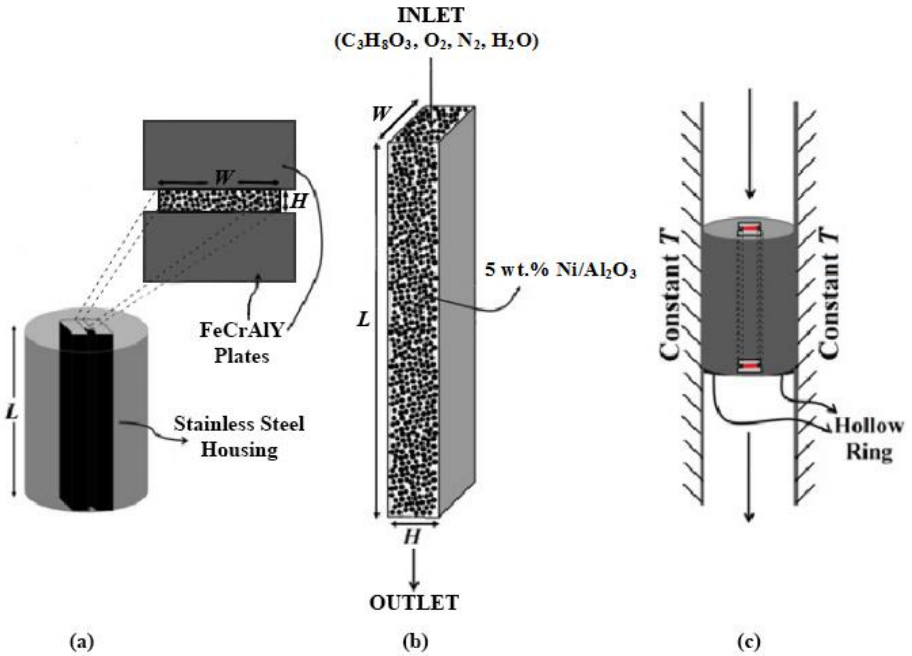

Figure 3.9. Packed Microchannel Reactor Configuration a. H-shaped housing (top and side view) b. Packed catalysts in microchannel c. Location of H-shaped housing in quartz tube (Simsek *et al*., 2013).

3.3.4. Pretreatment

Before starting the experimental tests, the active metals in the coated or packed catalysts must be activated after calcination procedure in order to reduce the active metals from their oxidized states to their metallic states. In order to achieve that, 40 NmL min^{-1} H_2 flow is passed over the catalysts at 800 °C for 2 hours in situ before the reaction tests. The N_2 gas flow is used for increasing the temperature to 800 °C, and for cooling after the reduction.

3.4. Reaction Tests

3.4.1. Blank Tests

Blank tests are done without using the catalyst in order to state that whether the materials of construction (stainless steel tubings, 310-grade stainless steel housing, quartz reactor, FeCrAlY plate and quartz wool) are inert towards the reactants in both steam and

oxidative steam reforming reactions. Blank tests are performed at reaction conditions. This investigation gives that material of construction is not inert. Even at lowest temperature investigated in this study (425 °C), an activity is observed for blank test at this temperature level. Glycerol decomposition depends on temperature, and according to temperature increments from 425 °C to 600 °C, the observed activity increases.

Additional blank experiments are performed in order to determine exact source of the activity. First blank experiment is conducted without including housing and plate. This test shows no activity meaning that stainless steel tubing, quartz reactor and quartz wool are inert for reforming reactions. This result shows that activity stems from plate, housing or the both. One more blank experiment is performed at 425 °C including only housing inside of the quartz reactor. An activity which is less than the activity observed with including all material of construction, and this means that the plate is responsible for this activity difference. In conclusion, it is stated that housing and the plate are not inert towards the reactants. The list of blank tests is given in Table 3.5.

Table 3.5. List of blank tests in microchannel reactor.

#	T (°C)	$C_3H_8O_3/H_2O/N_2/O_2$ (molar ratio)	S/C	Liquid feed ($NmL.min^{-1}$)	N_2 gas feed ($NmL.min^{-1}$)	Total flow ($NmL.min^{-1}$)
1	425	1 / 15 / 16 / 0	5	0.0421	48	96
2	450	1 / 15 / 16 / 0	5	0.0421	48	96
3	475	1 / 15 / 16 / 0	5	0.0421	48	96
4	500	1 / 15 / 16 / 0	5	0.0421	48	96
5	550	1 / 15 / 16 / 0	5	0.0421	48	96
6	600	1 / 15 / 16 / 0	5	0.0421	48	96
7	500	1 /15 / 14.67 / 1.33	5	0.0421	44	96
8	550	1 /15 / 14.67 / 1.33	5	0.0421	44	96
9	600	1 /15 / 14.67 / 1.33	5	0.0421	44	96

In the case of oxidative steam reforming, blank tests are again conducted at three temperature levels in order to see how oxygen affects the activity on housing and the plate. The last three rows of Table 3.5 correspond to oxidative blank tests. Outcomes of the blank tests are given and discussed in Chapter 4.

3.4.2. Steam Reforming of Glycerol in Microchannel Reactor

Glycerol steam reforming tests are performed in gas phase over the coated or packed catalysts inside of the housing placed in the quartz tube. The plates are coated with 3-μm size of 5 wt. % Ni/Al_2O_3 and 10 wt. % Ni/Al_2O_3 catalysts, and packing of catalyst is performed with 60-80 mesh (250 – 177 μm) size of 5 wt. % Ni/Al_2O_3 catalyst particles. A small piece of quartz wool is inserted into the bottom of the housing to stabilize the position of the coated plate or the packed catalysts in the housing. In all experimental tests, quartz wools with a thickness of approximately 1.0 cm are placed below the bottom end and above the housing entrance. The quartz wool which is over the hollow ring in the middle of the quartz tube helps to keep the housing stationary at the desired position at the second zone of the furnace which has a temperature set as the reaction temperature. The other 1.0 cm-thick quartz wool is placed on top of the housing and it is necessary in reactions with high coking rate, like glycerol steam reforming, for understanding whether coking occurs before reactants reach the catalytic zone. After each experimental test, these quartz wools are examined for coke formations and kept with reacted catalysts for further investigations. This configuration is also valid for oxidative steam reforming tests and prevents bypass of the reactants through the gap between the housing and the tube. Moreover, the material of construction of housing (310-grade steel) expands as temperature increases, and the expansion also prevents bypass. The quartz tube including housing is placed into the furnace having three zones which can be regulated separately using three different PID temperature controllers. The temperature measurement of this furnace works with a precision of ±1.0 °C. Once the temperature of the first zone is set to 310 °C, all the reactants turn into gas phase thanks to the nozzle apparatus at the entrance. Second zone is set to the reaction temperature, and gas phase reactions occur at this temperature level.

The catalytic performance tests for the steam reforming of glycerol are conducted to investigate the effects of active metal loadings, temperature, S/C ratio, total flow and the reactor configurations. For different temperature levels (425, 450, 475, 500, 550 and 600 °C), S/C ratio and total flow are kept constant at 5 and 96 NmL min^{-1} respectively during experiments. For different S/C ratios (3, 4, 5, and 6), two temperature levels (500 °C and 600 °C) and two catalysts (5 wt% $Ni\text{-}Al_2O_3$ and 10 wt% $Ni\text{-}Al_2O_3$) are investigated while

the total flow is kept constant at 96 NmL min^{-1} in each experimental sets. The effect of the total flow rate (64, 96, 128, and 160 NmL min^{-1}) is also investigated over two catalysts with different metal loadings (5 wt% Ni-Al_2O_3 and 10 wt% Ni-Al_2O_3) at 600 °C with S/C ratio of 5. The reactor configurations (packed or coated microchannel) are compared at three temperature levels (475 °C, 500 °C, and 550 °C), and at three S/C ratios (3, 4, and 5) while keeping the W/F_{A0} ratio same in both configurations. All experimental parameters for steam reforming reactions over 10 wt.% Ni/Al_2O_3 and 5 wt.% Ni/Al_2O_3 are given in Table 3.6.

Glycerol conversion, product selectivity and yield are the calculated parameters. All liquid products formed by decomposition of the glycerol, that are condensed and collected in the cold traps, are neglected in the conversion calculations. Glycerol conversions are calculated based on number of moles of carbon entering to the system (glycerol feed) and the moles of carbon present in product gases detected by Molecular Sieve 5A and Porapak Q columns (CH_4, CO, CO_2, C_2H_4 and C_2H_6). All calculations are performed on dry basis and reported in Section 4 with graphs showing the effect of experimental parameters.

Table 3.6. Experimental roadmap of Ni-based catalyst for glycerol steam reforming.

#	Catalyst	Reactor Conf.	T (°C)	S/C	Liquid feed (NmL min^{-1})	N_2 feed (NmL min^{-1})	Total flow (NmL min^{-1})
1	10 wt.% Ni/Al_2O_3	Coated	425	5	0.0421	48	96
2	10 wt.% Ni/Al_2O_3	Coated	450	5	0.0421	48	96
3	10 wt.% Ni/Al_2O_3	Coated	475	5	0.0421	48	96
4	10 wt.% Ni/Al_2O_3	Coated	500	5	0.0421	48	96
5	10 wt.% Ni/Al_2O_3	Coated	500	4	0.0355	57	96
6	10 wt.% Ni/Al_2O_3	Coated	500	3	0.0288	66	96
7	10 wt.% Ni/Al_2O_3	Coated	550	5	0.0421	48	96
8	10 wt.% Ni/Al_2O_3	Coated	600	5	0.0421	48	96

Table 3.6. Experimental roadmap of Ni-based catalyst for glycerol steam reforming (cont.).

#	Catalyst	Reactor Conf.	T (°C)	S/C	Liquid feed (NmL min-1)	N2 feed (NmL min-1)	Total flow (NmL min-1)
9	10 wt.% Ni/Al_2O_3	Coated	600	4	0.0355	57	96
10	10 wt.% Ni/Al_2O_3	Coated	600	3	0.0288	66	96
11	10 wt.% Ni/Al_2O_3	Coated	500	6	0.0487	39	96
12	10 wt.% Ni/Al_2O_3	Coated	600	5	0.0325	32	64
13	5 wt.% Ni/Al_2O_3	Coated	425	5	0.0421	48	96
14	5 wt.% Ni/Al_2O_3	Coated	450	5	0.0421	48	96
15	5 wt.% Ni/Al_2O_3	Coated	475	5	0.0421	48	96
16	5 wt.% Ni/Al_2O_3	Coated	500	5	0.0421	48	96
17	5 wt.% Ni/Al_2O_3	Coated	500	4	0.0355	57	96
18	5 wt.% Ni/Al_2O_3	Coated	500	3	0.0288	66	96
19	5 wt.% Ni/Al_2O_3	Coated	550	5	0.0421	48	96
20	5 wt.% Ni/Al_2O_3	Coated	600	5	0.0421	48	96
21	5 wt.% Ni/Al_2O_3	Coated	600	4	0.0355	57	96
22	5 wt.% Ni/Al_2O_3	Coated	600	3	0.0288	66	96
23	5 wt.% Ni/Al_2O_3	Coated	600	5	0.0562	64	128
24	5 wt.% Ni/Al_2O_3	Coated	600	5	0.0702	80	160
25	5 wt.% Ni/Al_2O_3	Coated	500	6	0.0487	39	96
26	5 wt.% Ni/Al_2O_3	Coated	600	5	0.0325	32	64
27	5 wt.% Ni/Al_2O_3	Packed	475	5	0.0421	48	96
28	5 wt.% Ni/Al_2O_3	Packed	500	5	0.0421	48	96
29	5 wt.% Ni/Al_2O_3	Packed	550	5	0.0584	66.7	133.3

Table 3.6. Experimental roadmap of Ni-based catalyst for glycerol steam reforming (cont.).

#	Catalyst	Reactor Conf.	T (°C)	S/C	Liquid feed (NmL min-1)	N2 feed (NmL min-1)	Total flow (NmL min-1)
30	5 wt.% Ni/Al_2O_3	Packed	500	4	0.0286	46	77.4
31	5 wt.% Ni/Al_2O_3	Packed	500	3	0.0232	53.2	77.4
32	5 wt.% Ni/Al_2O_3	Packed	500	6	0.0487	39	96

3.4.3. Oxidative Steam Reforming of Glycerol in Microchannel Reactor

This study mainly focused on glycerol steam reforming, however, the carbon formation over the catalyst surface is one of the main conclusions, and it is one of the reasons for catalyst deactivation. The other possible reason of deactivation is stated as active phase sintering. The challenge of coke formation can be tackled by adding oxidant to eliminate the carbon from the system, and that is why, oxidative steam reforming tests are conducted.

Oxidative steam reforming of glycerol in a microchannel reactor is not investigated in literature. In general, relatively few studies have focused on OGSR compared to GSR. In this study, OGSR reactions are performed over 5 wt. % Ni/Al_2O_3 catalyst with coated microchannel configuration. The investigated parameters are temperature, and the C/O ratio. In order to compare the results with steam reforming reactions, total flow rate kept constant at 96 Nml/min. Experimental tests of OGSR are given in Table 3.7.

Table 3.7. Experimental roadmap for oxidative glycerol steam reforming.

#	T (°C)	C/O	S/C	Liquid feed ($NmL\ min^{-1}$)	O_2 flow (Nml/min)	N_2 flow ($NmL\ min^{-1}$)	Total flow ($NmL\ min^{-1}$)
1	500	1.125	5	0.0421	4	44	96
2	550	1.125	5	0.0421	4	44	96
3	600	1.125	5	0.0421	4	44	96
4	550	0.75	5	0.0421	6	42	96
5	550	2.25	5	0.0421	2	46	96

3.4.4. Measurement procedure of catalyst activities

In order to quantify activities of catalyst in both GSR and OGSR tests, the parameters such as “glycerol conversion”, “product selectivity” and “product yield” are defined. Glycerol conversion is defined based on carbon balance, and there is an assumption that there is no liquid product being formed by catalytic reactions. Moreover, the formed carbon over catalyst surface is not taken into account. According to these assumptions, glycerol conversion is calculated using Equation 3.1.

$$X_{glycerol} = 100 \times \frac{\text{moles of carbon in gaseous products}}{3 \times \text{moles of glycerol in the feed}} \tag{3.1}$$

The other parameter is the selectivity of each species, and it is calculated by dividing the molar amount of the gaseous species in the product stream by the molar amount of glycerol converted:

$$\text{Selectivity}_i = \frac{\text{moles of species "i" in gaseous products}}{\text{moles of glycerol converted}} \tag{3.2}$$

Glycerol conversion is much higher in OGSR compared to GSR. The product selectivity in this case, is lower because of higher conversions. However, the produced amount of gases is very high than GSR tests. In order to make correct analysis, the yield, that is the ratio of moles of produced product to the glycerol feed, is also defined to compare the produced amounts in GSR and OGSR.

$$\text{Yield}_i = \frac{\text{moles of species "i" in gaseous products}}{\text{moles of glycerol feed}} \tag{3.3}$$

4. RESULTS AND DISCUSSION

4.1. Results of Glycerol Steam Reforming Experiments

The present work involves a parametric study about microchannel enabled reforming of glycerol to hydrogen over Ni-based catalysts. Temperature, S/C ratio, total reactant flow rate and reactor configurations are the investigated parameters and results of these investigations are presented in this section. The experimental results, including those of blank tests, are given in terms of glycerol conversion and gaseous product selectivity for each experiment. Moreover, SEM and EDX analysis of spent and reduced Ni/Al_2O_3 catalysts are done in order to investigate any changes in the surface morphology and to examine carbon formation.

4.1.1. Effect of Temperature on GSR

Temperature is an important parameter for chemical reactions as well as for glycerol steam reforming. Steam reforming is endothermic so that any increase in temperature leads to higher conversion of the reactants. The investigated temperature levels for this study are 425, 450, 475, 500, 550, and 600 °C. Two different catalysts (5 wt. % Ni/Al_2O_3 or 10 wt.% Ni/Al_2O_3) are used in the experimental tests while keeping the S/C ratio (S/C) at 5, N_2 flow rate at 48 NmL min^{-1}, and total flow rate at 96 NmL min^{-1}. The blank experiments without the catalyst are also compared with the results of the coated microchannel configuration.

The product gas is analyzed using the results obtained from Molecular Sieve 5A (for H_2, N_2, CH_4, CO) and Porapak Q columns (for C_2H_4 and C_2H_6). The glycerol conversion is calculated using the expression given in Equation 3.1. It is assumed that no liquid product is formed in the catalytic experiments.

Experimental results show that temperature is an important parameter affecting the conversion of the glycerol such that increasing the temperature results a considerable increase in glycerol conversion. Less than 2% conversion over 5 wt. % Ni/Al_2O_3, 10 wt% Ni/Al_2O_3 catalysts and in blank tests is observed at temperatures below 500 °C. In investigated temperature interval, there is not a considerable effect of active metal loading

on conversion. The temperature of 550 °C represents a point where conversions start to increase. At this temperature, glycerol conversions are calculated as 4.38 %, 4.42 %, and 2.88 % for 10 wt. % Ni/Al_2O_3, 5 wt. % Ni/Al_2O_3 catalysts and blank tests, respectively. Another 50 °C increase in the temperature (600 °C) displays a drastic increase in glycerol conversions. The conversions at this temperature are stated as 20.92 %, 19.44 %, and 15.90 % for 10 wt.% Ni/Al_2O_3, 5 wt.% Ni/Al_2O_3 catalysts and blank tests, respectively. The difference in the glycerol conversions obtained from two different metal loadings is very small, which is also an indication of the fact that the active metal content does not affect the conversion. Moreover, it is believed that increasing the metal content may favor active metal migration over the surface that decreases number of active sites.

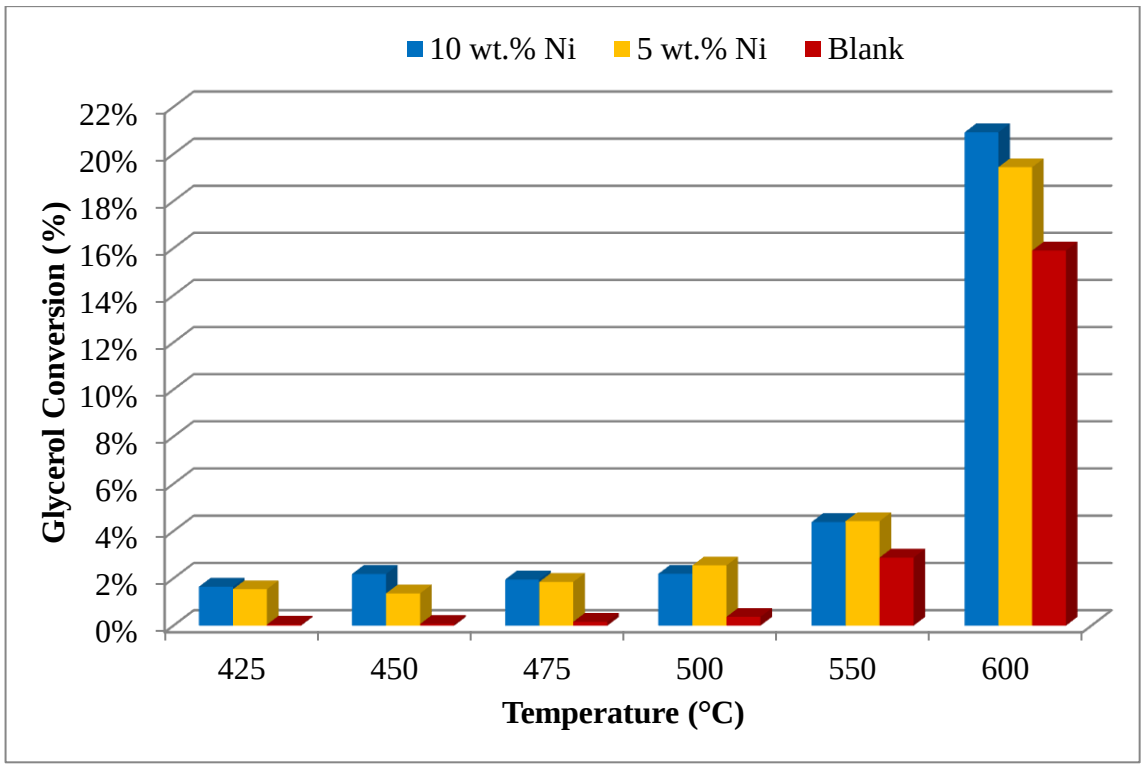

Figure 4.1. Glycerol Conversion vs Temperature for GSR (S/C = 5, N_2 flow = 48 NmL min^{-1}, Total flow = 96 NmL min^{-1}).

The parametric study for temperature change clearly indicates that there is a direct proportionality between temperature and conversion. In fact, this is an expected response of the system because steam reforming is an endothermic reversible reaction, so any heat input will shift the reaction equilibrium to the product side favoring higher conversion of the reactants and increased formation of the products. Moreover, results shows that the

active metal content has no considerable effect on glycerol conversion, which can also be explained by the smaller metal particle sizes and better metal dispersion obtained with less Ni loading. Another interesting behavior of the system is observed in the conversions obtained in the blank tests. The conversions in blank test increase up to 15.90 % which indicates that the metal housing, made of 310-grade stainless steel, is not inert for this system. The composition of the 310-grade stainless steel includes about 25% chromium and 20% nickel in its structure (Goodfellow, 2014; Sandmeyer, 2014). The presence of nickel is thought to be responsible for observing some activities in the blank tests. Additionally, the homogenous dissociation of glycerol molecule, which has a relatively big structure (compared to methane), results in the formation of the carbon containing products such as CH_4, C_2H_4 and C_2H_6.

The other experimental parameter calculated is the selectivity of the product gases (H_2, CH_4, CO, CO_2, C_2H_4 and C_2H_6) being defined as the ratio of the mole of product formed divided by the moles of the glycerol converted (Equation 3.2). The selectivity of all products at different reaction temperature is given in Figure 4.2 and Figure 4.3 for 10 wt.% Ni/Al_2O_3 and 5 wt.% Ni/Al_2O_3 catalysts, respectively. It is observed that there is a concave behavior of CO, CH_4, and C_2H_4 selectivity and a convex behavior of H_2 and CO_2 selectivity with respect to temperature. It is also noted that 475 °C is a turning point at which local maxima and minima points are located. It is seen that maximum H_2 selectivity can be obtained at this temperature level.

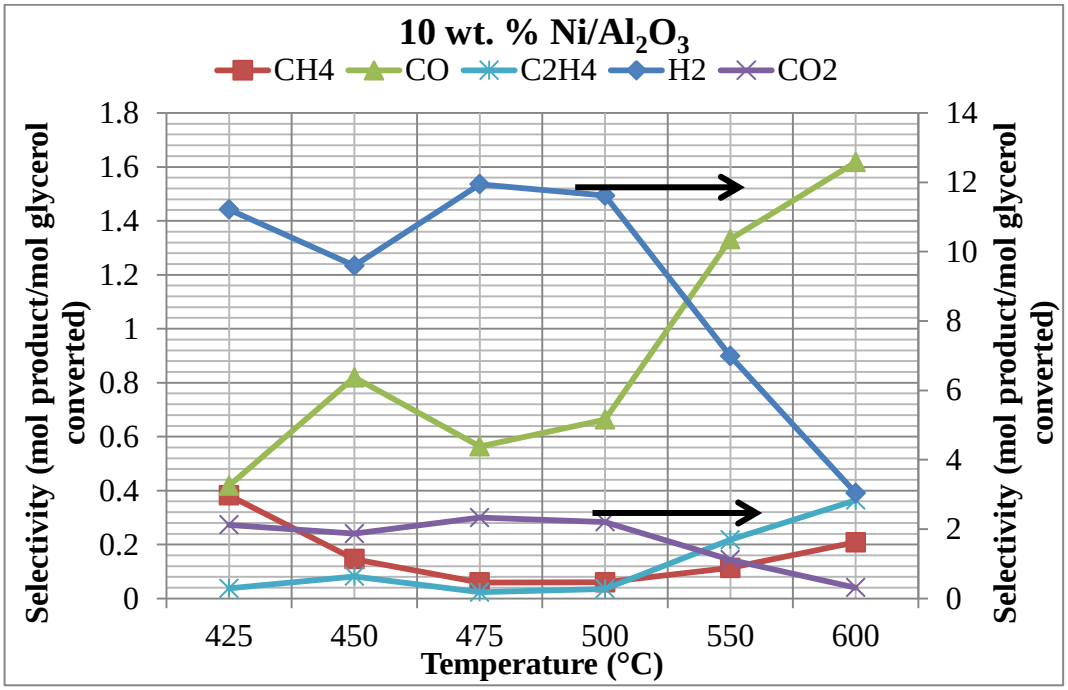

Figure 4.2. Selectivity of Products over 10 wt% Ni/Al_2O_3 vs Temperature (S/C = 5, N_2 flow = 48 NmL min^{-1}, Total flow = 96 NmL min^{-1}).

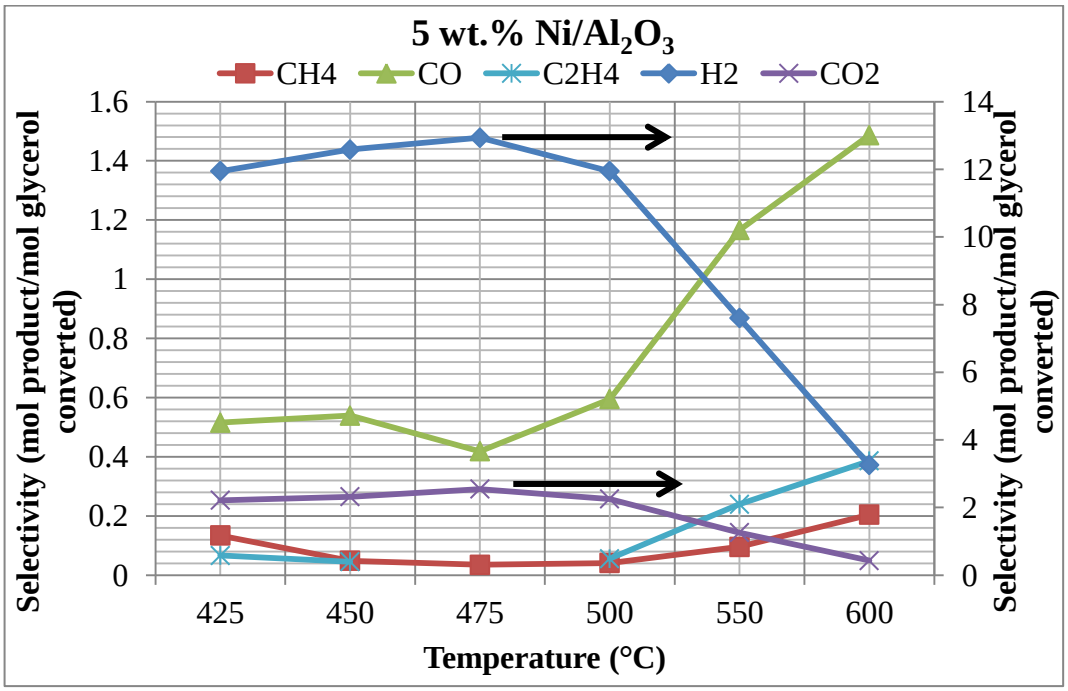

Figure 4.3. Selectivity of Products over 5 wt% Ni/Al_2O_3 vs Temperature (S/C = 5, N_2 flow = 48 NmL min^{-1}, Total flow = 96 NmL min^{-1}).

The mechanism of the glycerol steam reforming involves pyrolysis of glycerol (Reaction 2.1), water gas shift reaction (Reaction 2.2), and dehydrogenation reactions (Reaction 2.11) which are the main routes of H_2 production. Pyrolysis of glycerol yields CO and H_2 as products and it is considered as the first step for glycerol steam reforming reaction mechanism. Water gas shift reaction is another source of H_2 production in which CO reacts with H_2O producing H_2 and CO_2. The last source of H_2 production in this mechanism is the dehydrogenation reactions which are related with the dehydrogenation of glycerol or intermediate products formed from glycerol itself. H_2 selectivity at different temperatures over 10 wt.% Ni/Al_2O_3 catalyst, 5 wt.% Ni/Al_2O_3 catalyst, and for blank tests is given in Figure 4.4.

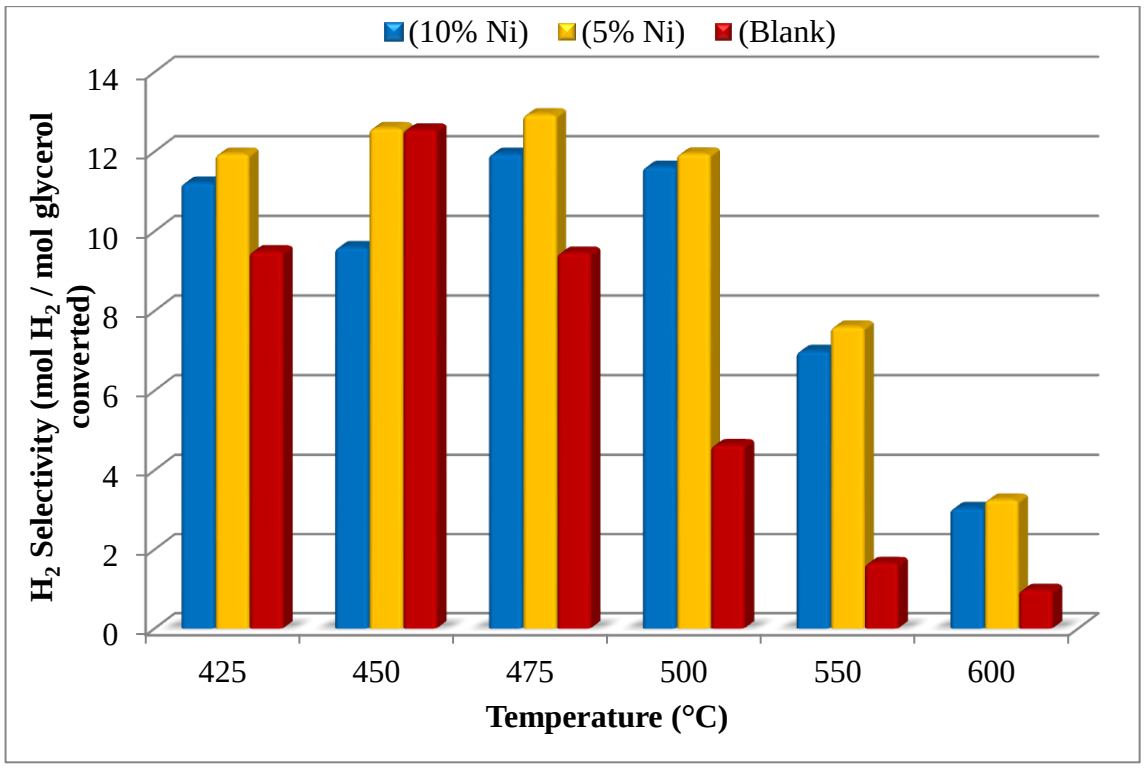

Figure 4.4. H_2 Selectivity vs Temperature for GSR (S/C = 5, N_2 flow = 48 NmL min^{-1}, Total flow = 96 NmL min^{-1}).

H_2 selectivity over 10 wt. % Ni/Al_2O_3 gives the maximum selectivity at 475 °C as 11.94. Above 475 °C, an increase in temperature leads to a decrease in H_2 selectivity from 11.94 (at 475 °C) to 3.04 (at 600 °C). On the other hand, the maximum H_2 selectivity on 5 wt. % Ni/Al_2O_3 is observed at 475 °C as 12.93. The temperature increase for this case also

leads to a decrease in H_2 selectivity (12.93 at 475 °C to 3.25 at 600 °C). The main conclusion that can be obtained from the comparison of two different catalysts is that both catalysts (10 wt.% Ni/Al_2O_3 and 5 wt.% Ni/Al_2O_3) give maximum H_2 selectivity at 475 °C and the 5 wt.% Ni/Al_2O_3 is more selective at each temperature level compared to 10 wt.% Ni/Al_2O_3 in terms of H_2 production which can possibly be explained by improved Ni dispersion in the 5 wt.% Ni/Al_2O_3 and the higher chance of sintering in the 10 wt.% Ni/Al_2O_3 catalyst by migration of the Ni particles on the catalyst surface. Blank tests show that the maximum H_2 selectivity is obtained at 450 °C as 12.55, after this temperature level, the selectivity starts to decrease up to 0.97 at 600 °C. Although glycerol conversions increase exponentially with temperature, the produced amount of H_2 does not increase that much. The general trend observed in these experimental sets is that the H_2 selectivity is higher on 5 wt.% Ni/Al_2O_3 than 10 wt.% Ni/Al_2O_3, and 10 wt.% Ni/Al_2O_3 gives more H_2 selectivity compared to blank configuration.

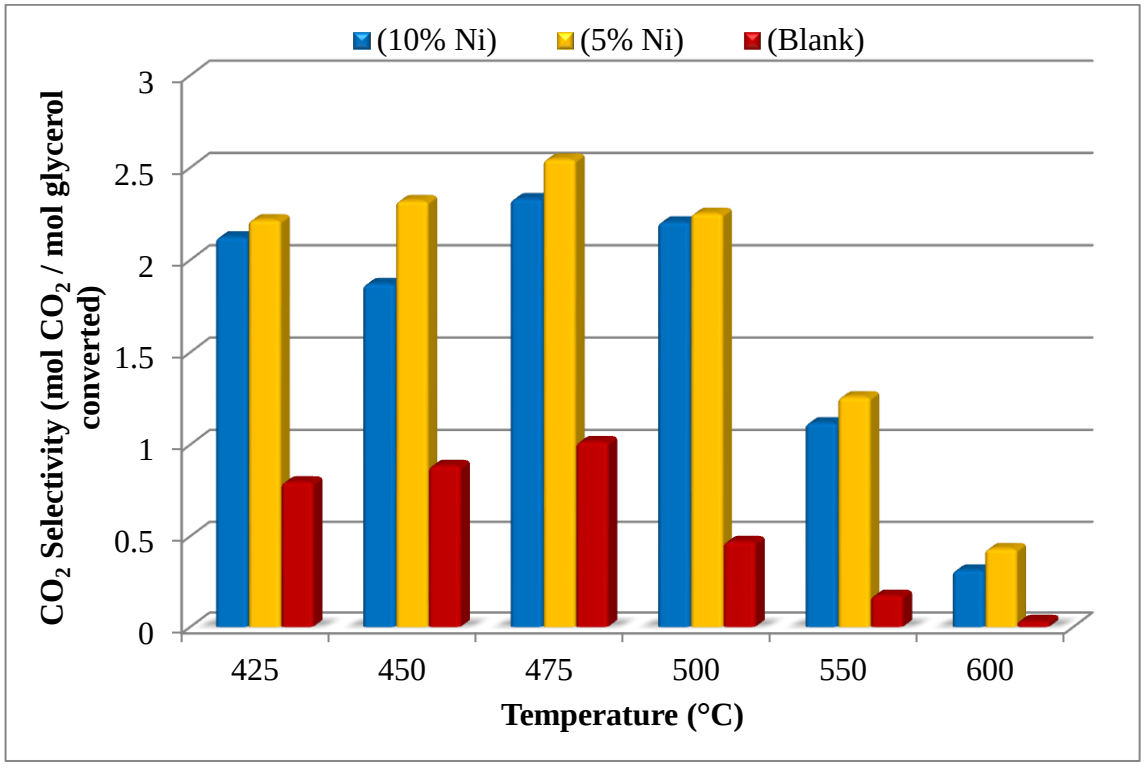

Figure 4.5. CO_2 Selectivity vs Temperature for GSR (S/C = 5, N_2 flow = 48 NmL min^{-1}, Total flow = 96 NmL min^{-1}).

The change in the CO_2 selectivity as a function of temperature is given in Figure 4.5. The change in the CO_2 selectivity shows a trend that is very similar to that of H_2. Water gas shift reaction is responsible for this similar behavior. In reforming reaction, there is no any external O_2 source which produces CO_2 by reacting with hydrocarbons. Moreover, there is no mechanism suggesting the removal of CO_2 as a side product. As a result, the CO_2 formation is the result of the water gas shift reactions only in which CO reacts with H_2O to produce H_2 and CO_2. This reaction also explains the positive relation between the selectivities of H_2 and CO_2. Water gas shift reaction is slightly exothermic reactions, so any increase in the temperature does not favor the forward reaction to produce H_2 and CO_2. Although the produced amount of the CO_2 increases slightly according to increase in temperature, this increase is very small compared to the increase in the glycerol conversion. As a result of these facts, selectivity of CO_2 decreases in the temperature interval of 475 °C to 600 °C. The maximum CO_2 selectivities are calculated at 475 °C as 2.54, 2.33, and 1.01 for 5 wt. % Ni/Al_2O_3 catalyst, 10 wt. % Ni/Al_2O_3 catalyst, and blank tests, respectively.

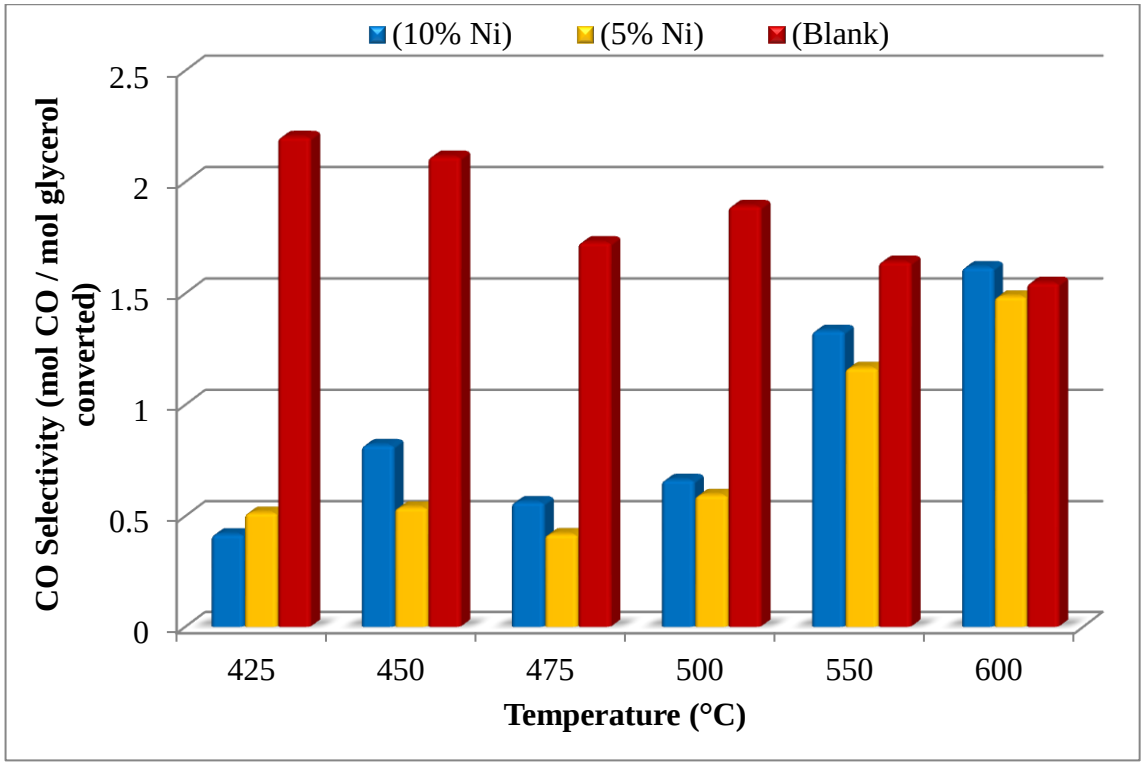

Figure 4.6. CO Selectivity vs Temperature for GSR (S/C: 5, N_2 flow = 48 NmL min^{-1}, Total flow = 96 NmL min^{-1}).

The change in CO selectivity as a function of temperature is given in Figure 4.6. It is observed that there is an inverse relation between the CO selectivity obtained from catalytic reactions and blank tests. As the temperature increases the CO selectivity decreases in blank experiments. Whereas, in catalytic experiments CO selectivity increases with temperature over both catalysts. The maximum CO selectivity in blank tests is observed at 425 °C as 2.20, and it decreases slightly to 1.55 at 600 °C. The CO selectivity is higher over the 10 wt. % Ni/Al_2O_3 catalyst than 5 wt. % Ni/Al_2O_3 for almost all temperature (except at 425 °C). The maximum CO selectivity for catalytic reactions is observed at the highest reaction temperature (600 °C) as 1.62 and 1.49 for 10 wt. % Ni/Al_2O_3 and 5 wt. % Ni/Al_2O catalysts, respectively. There are two reasons of increase in CO selectivity with temperature. The first one is the pyrolysis of glycerol (Reaction 2.1), and the second one is the water gas shift reaction (Reaction 2.2). Pyrolysis reaction produces CO and H_2 as products and it is treated as the first step of glycerol steam reforming reaction mechanism. Glycerol pyrolysis is an endothermic reversible process, and an increase in the temperature favors the forward reaction resulting in more CO production. In the case of water gas shift, CO is present in the reactant side of the reaction equation. Thermodynamically, reverse water gas shift becomes favorable with temperature due to exothermic nature of the reaction. These two mechanisms favor formation of CO, and this is also observed in experimental results. In general, there is an opposite relation in the response of the CO selectivity compared to H_2 and CO_2 selectivity which is also a result of water gas shift reaction.

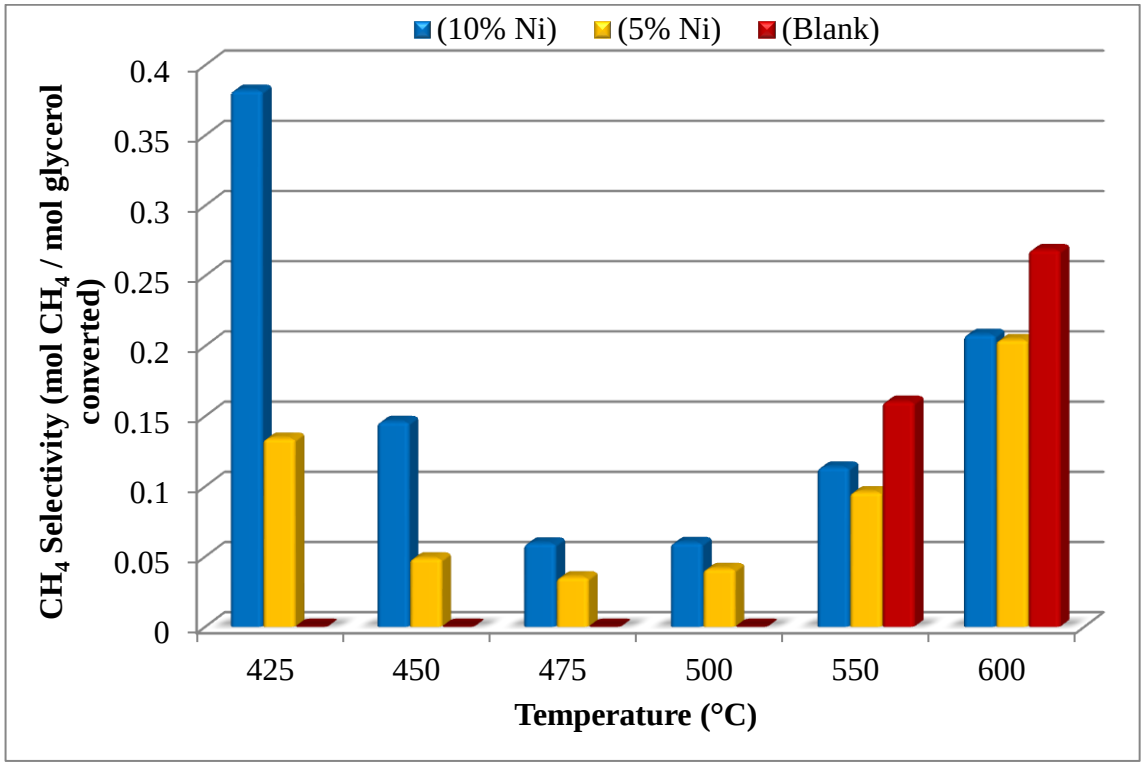

Figure 4.7. CH_4 Selectivity vs Temperature for GSR (S/C = 5, N_2 flow = 48 NmL min^{-1}, Total flow = 96 NmL min^{-1}).

The change in CH_4 selectivity with temperature is presented in Figure 4.7. In general, methane selectivities are very small. For the catalytic experiments, a parabolic shape is observed such that there is decrease in the CH_4 selectivity from 425 °C to 475 °C, above which it starts to increase until the temperature reaches 600 °C. The selectivity on 10 wt. % Ni/Al_2O_3 catalyst is higher than the selectivity on 5 wt. % Ni/Al_2O_3 at each temperature. The CH_4 selectivity for the blank experiment is zero at the temperature interval 425 °C – 500 °C, and then it increases up to 0.27 at 600 °C. The possible sources of methane productions are given in the Reaction 2.5-2.7. Although it is very complicated to state which reaction dominates the formation methane at the given temperature interval, it can be said that according to Reaction 2.6, the increase in the CO which is observed in experimental tests leads to production of methane. In general, increase in temperature results in more hydrocarbon formation because of decomposition of glycerol. This is also valid for oxidative steam reforming reactions Additionally, dehydrogenation, dehydration and CO removal reactions occur during glycerol steam reforming which may end up with additional CH_4 produced (Lin, 2013). Blank tests result in higher CH_4 selectivity. Possible

reason of lower CH_4 selectivity in catalytic tests may be explained by the catalytic activity which may cause methane steam reforming reactions.

$$C + 2H_2 \leftrightarrow CH_4 \quad (2.5)$$

$$CO + 3H_2 \leftrightarrow CH_4 + H_2O \quad (2.6)$$

$$CO_2 + 4H_2 \leftrightarrow CH_4 + 2H_2O \quad (2.7)$$

The changes in C_2H_4 and C_2H_6 selectivities as a function of the temperature are given in Figure 4.8 and Figure 4.9, respectively. The C_2H_4 and C_2H_6 are the by-products formed from (mostly liquid) intermediate products through dehydration, dehydrogenation and CO removal reactions (Lin, 2013).

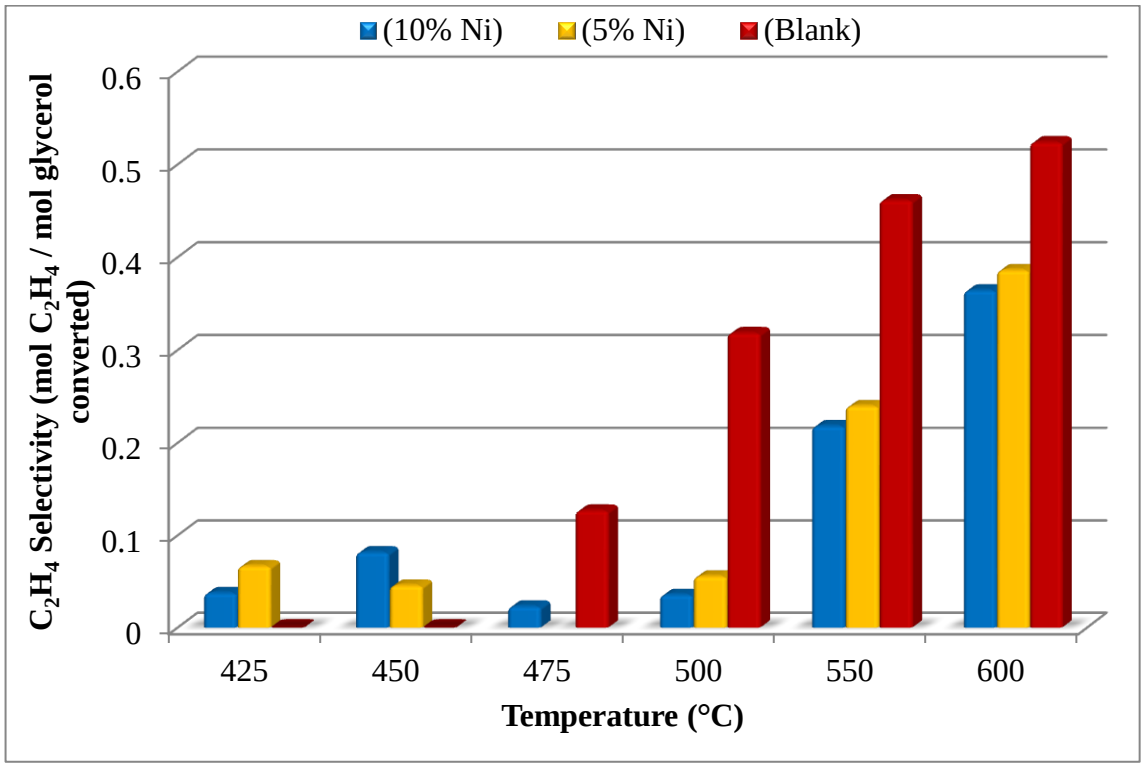

Figure 4.8. C_2H_4 Selectivity vs Temperature for GSR (S/C = 5, N_2 flow = 48 NmL min^{-1}, Total flow = 96 NmL min^{-1}).

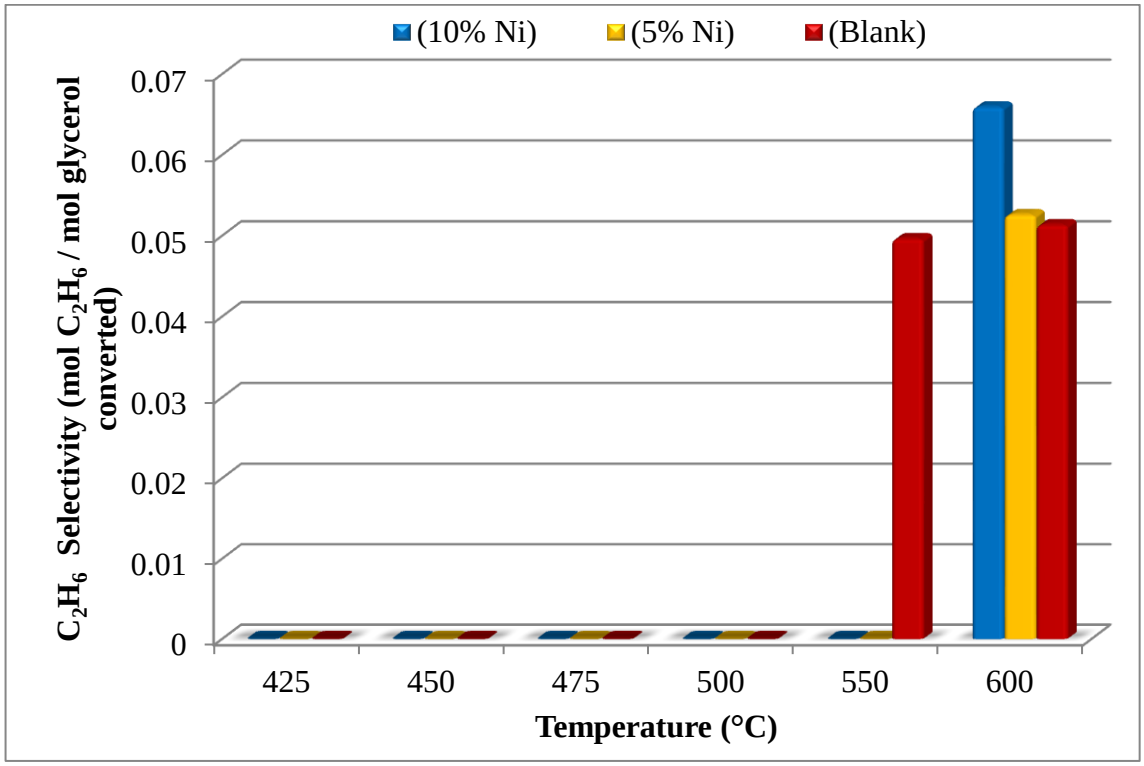

Figure 4.9. C_2H_6 Selectivity vs Temperature for GSR (S/C = 5, N_2 flow = 48 NmL min^{-1}, Total flow = 96 NmL min^{-1}).

As the size of the hydrocarbon increases the corresponding selectivity decreases as in the cases of methane, ethylene, and ethane. The C_2H_4 selectivity shows similar trend with CH_4 selectivity given in Figure 4.7. The C_2H_4 selectivity increases after 475 °C until it reaches to its maximum values as 0.36, 0.39, and 0.52 at 600 °C for 10 wt.% Ni/Al_2O_3 catalyst, 5 wt.% Ni/Al_2O_3 catalyst and blank tests, respectively. The C_2H_6 selectivity is very small compared to other hydrocarbons in the system, and it has a maximum value at 600 °C as 0.066 over the 10 wt.% Ni/Al_2O_3. Blank tests show higher selectivities especially in case of C_2H_4, which is attributed to the Ni driven coking over the metallic housing.

4.1.2. Effect of S/C Molar Ratio on GSR

The second parameter that is investigated in the experimental tests is the molar ratio of S/C in feed. The S/C ratio is an important parameter because steam is the reactant of reforming and ,for the cases of Ni-based catalysts, presence of steam in the reaction medium can affect the catalyst structure and prevents the coke formation to some extent.

The effect of S/C is investigated for two temperatures (500 °C and 600 °C) and on two catalysts (10 wt. % Ni/Al_2O_3 and 5 wt. % Ni/Al_2O_3) by keeping total flow rate at 96 NmL min^{-1} and glycerol feed flow rate at 3 NmL min^{-1}. Steam amount is fed with desired S/C ratio, and N_2 is added to system as balance gas to keep total flow rate constant. The investigated S/C ratios are 3, 4, 5, and 6 for the tests conducted at 500 °C on both catalysts. For the tests conducted at 600 °C, the ratios are 3, 4, and 5. The corresponding flow rates and the ratios of the feed stream ($C_3H_8O_3/H_2O/N_2$) are summarized in the Table 3.6. Glycerol conversion and gaseous product selectivies are reported in this section.

The change in glycerol conversion with respect to the S/C ratio is given in Figure 4.10 for both catalysts at 500 °C. For 5 wt% Ni/Al_2O_3 catalyst, conversions increase with higher amounts of steam in the feed until S/C is 5, at which glycerol conversion is 2.55%, and further increase in the steam amount (S/C=6) decreases conversion to 1.97%. A similar trend is observed for 10 wt. % Ni/Al_2O_3, over which conversion as S/C=5 is found to be 2.19% and further increase in the steam amount did not increase the conversion.

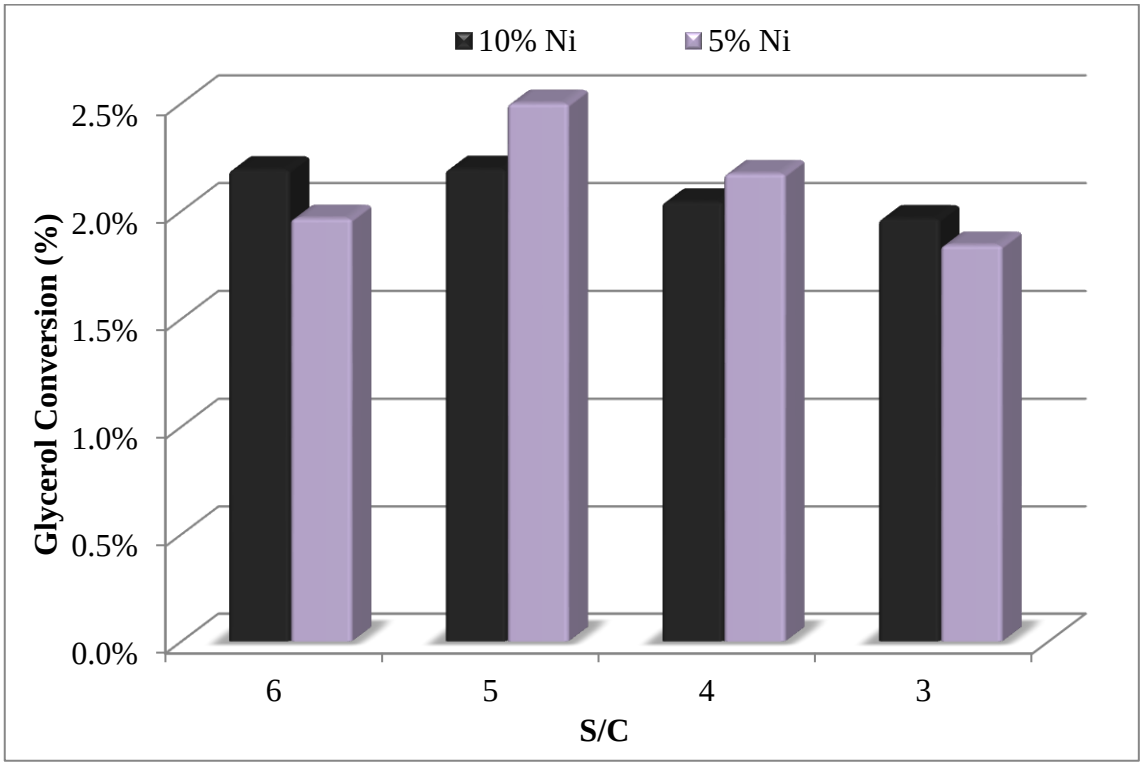

Figure 4.10. Glycerol Conversion vs S/C Molar Ratio (T = 500 °C, Total flow = 96 NmL min^{-1}).

The reaction tests are also conducted at 600 °C on both catalysts for the S/C ratios of 3, 4, and 5. The results of these experiments are given in Figure 4.11. For the 5 wt. % Ni/Al_2O_3 catalyst, conversion is slightly increased from 17.94% at S/C ratio of 3 to 19.44% at S/C ratio of 5. In the case of 10 wt.% Ni/Al_2O_3, the glycerol conversions stay almost the same with respect to the S/C ratio. The conversions are 21.07%, 19.73%, and 20.92% for S/C ratios of 3, 4, and 5, respectively. In general, conversions are very small at 500 °C. It can be concluded that 500 °C is not enough to see the effect of the steam content because of the very small fluctuations in conversions, which can be within the limits of experimental error. As expected, conversions obtained at 600 °C are relatively higher than obtained at 500 °C. Steam is the reactant of glycerol steam reforming which is reversible. The increase in the steam amount shifts the reaction towards products resulting in an increase in the conversion. However, for the case of Ni-based catalysts, sintering in the presence of the steam is also an important parameter which deactivates the catalysts and decreases conversions. These opposing effects can be responsible for the fact that glycerol conversion stays more or less constant at 600 °C with respect to S/C ratio. Additionally, this result can possibly be explained by the non-monotonic dependence of reaction rate on steam.

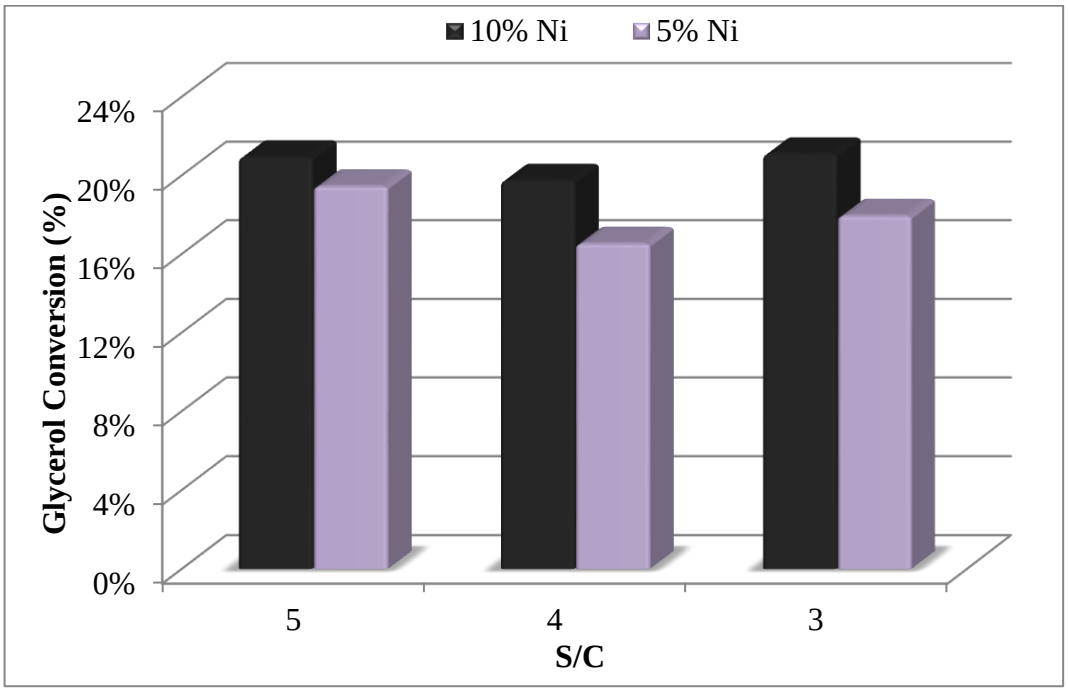

Figure 4.11. Glycerol Conversion vs S/C Molar Ratio (T = 600 °C, Total flow = 96 NmL min^{-1}).

The change in H_2 selectivity with respect to S/C ratio at 500 °C and 600 °C is given in Figure 4.12 and Figure 4.13, respectively. According to Figure 4.12, H_2 selectivity over 5 wt.% Ni/Al_2O_3 at 500 °C increases with respect to increase in the S/C ratio. The selectivity is 10.75 at S/C ratio of 3, and it increases to 18.22 when the S/C ratio is 6. However, the reaction tests conducted on 10 wt. % Ni/Al_2O_3 give a different result. The selectivities are 12.33, 12.81, 11.61, and 10.66 for the S/C ratios of 3, 4, 5, and 6. The increase in the steam amount, in this case, does not lead to increase in H_2 selectivity. 5 wt. % Ni/Al_2O_3 is more selective to hydrogen production at higher S/C ratios (5 and 6), whereas, at lower S/C ratios (3 and 4), 10 wt. % Ni/Al_2O_3 is more selective towards the production of hydrogen. This can be explained by the surface structural change of the catalysts in the presence of the steam. The agglomeration of active metals on the surface is also related with the composition of the active metal. More active metal on the surface results in formation of bigger clusters that decrease the active sites, and in turn decreases the production of hydrogen in steam reforming reactions.

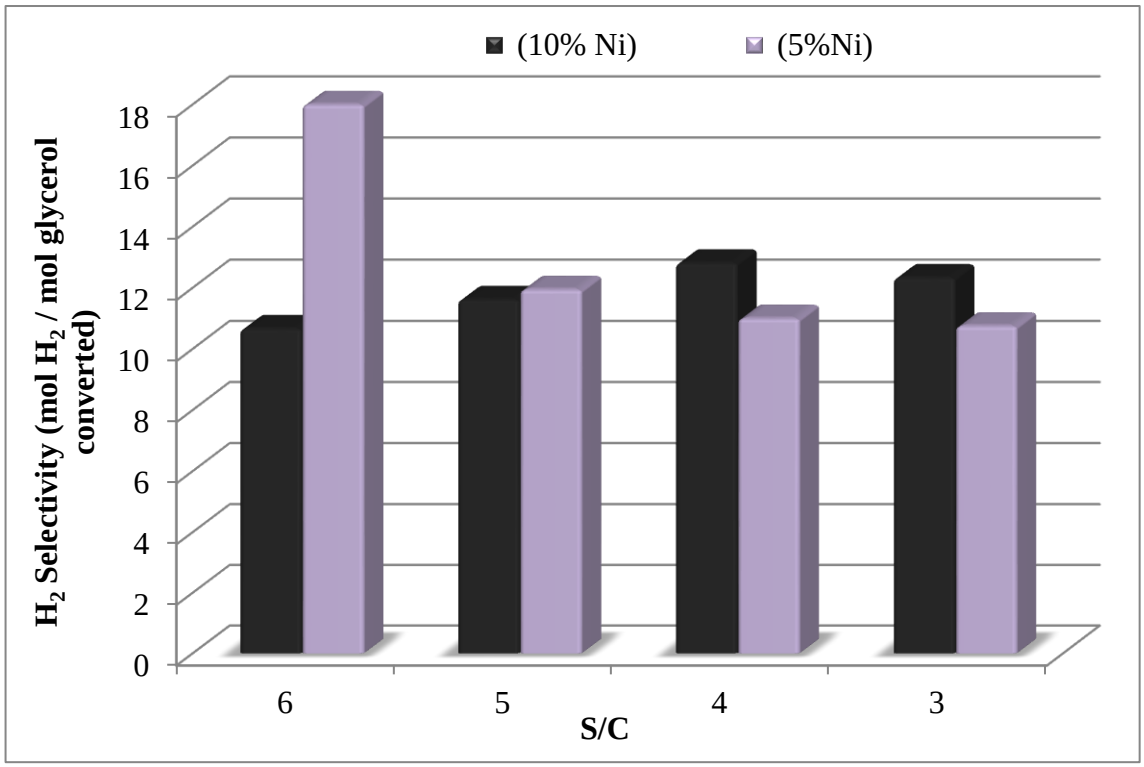

Figure 4.12. H_2 Selectivity vs S/C Ratio (T = 500 °C, Total flow = 96 NmL min^{-1}).

H_2 selectivity at 600 °C is given in Figure 4.13 for both catalysts. The results show that, selectivity on 5 wt. % Ni/Al_2O_3 increases with respect to increase in the steam content. The selectivity at S/C ratio of 3 is calculated as 2.35, and it increases to 3.25 at S/C ratio of 5. For the case of 10 wt. % Ni/Al_2O_3, it can be concluded that the selectivity increases with respect to S/C ratio. The increase in the hydrogen selectivity is explained by the effect of water gas shift reaction. As the steam increases, the forward water gas shift reaction is favored, so more hydrogen is produced. The decrease in hydrogen selectivity as a result of temperature increase from 500 °C to 600 °C is also seen for all S/C ratios, and the reasons for this behavior is explained in Section 4.1.1.

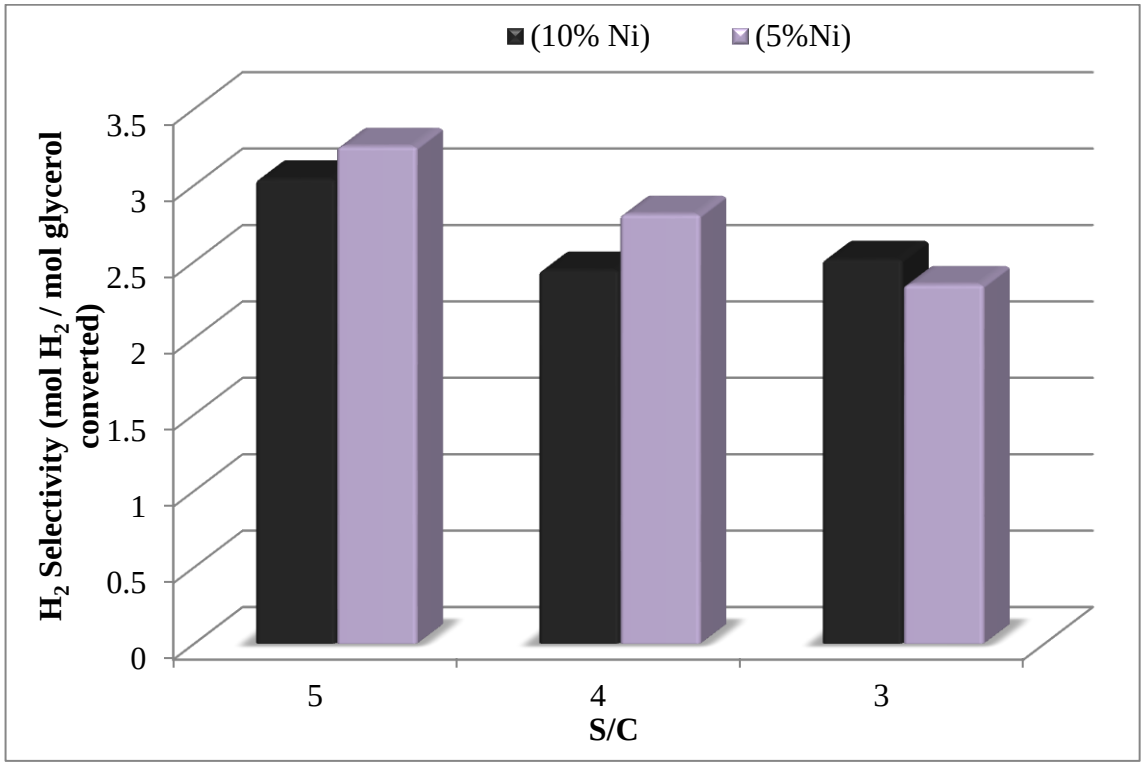

Figure 4.13. H_2 Selectivity vs S/C Ratio (T = 600 °C, Total flow = 96 NmL min^{-1}).

CO selectivity at 500 °C for both catalysts is given in Figure 4.14. CO selectivity over both catalyst decreases as S/C ratio increases from 3 to 5. For 5 wt. % Ni/Al_2O_3 catalyst, the selectivity is 0.84 at S/C ratio of 3, and it decreases to 0.59 at S/C ratio of 5. The selectivity of CO over 10 wt. % Ni/Al_2O_3 is 1.07 at S/C ratio of 3, and it is 0.66 when the S/C ratio is increased to 5. Further increase in the steam (S/C=6) leads to an increase in the selectivities such that it becomes 1.09 and 0.91 for 5 wt. % Ni/Al_2O_3, and 10 wt. %

Ni/Al_2O_3 catalyst, respectively. The decrease in the CO selectivity may stem from the water gas shift reaction. CO is the reactant of this reaction, and the shift towards products with steam addition leads to increased CO consumption. Increase in the CO selectivity with steam maybe explained by Reaction 2.6 which is an equilibrium reaction consuming CO and H_2 while producing methane and steam. If the steam amount increases, this reaction may dominate the overall mechanism and lead to more production of CO.

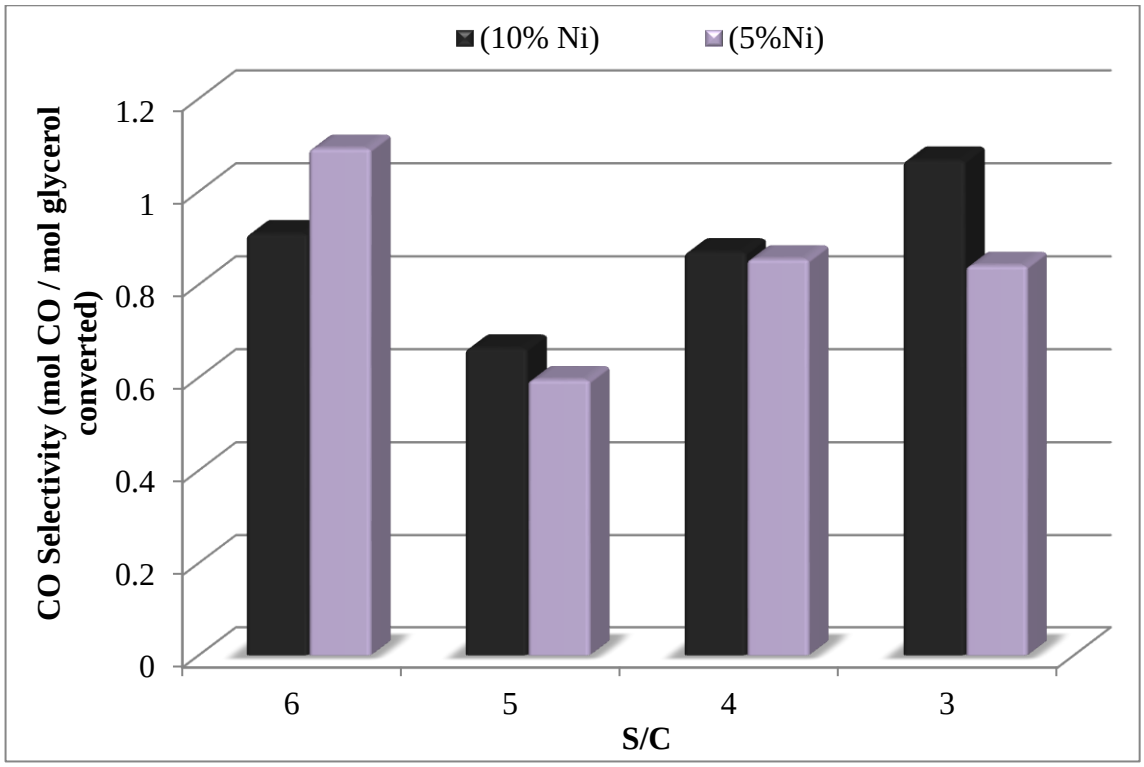

Figure 4.14. CO Selectivity vs S/C Ratio (T = 500 °C, Total flow = 96 NmL min^{-1}).

CO selectivity at 600 °C for both catalysts is given in Figure 4.15 for the cases in which the S/C ratio is set to 3, 4, or 5. For 5 wt. % Ni/Al_2O_3, CO selectivity increases slightly with S/C ratio. At S/C ratio of 3, the selectivity is 1.42, and for S/C ratio of 5, the selectivity is 1.49. In the case of 10 wt. % Ni/Al_2O_3 catalysts, CO selectivities are given as 1.64, 1.51, and 1.62 for S/C ratios of 3, 4, and 5, respectively. CO selectivity on both catalysts at 600 °C does not change significantly with S/C ratio. This may be due to water gas shift and Reaction 2.6 in which CO is in the reactant side and the steam in the product side. There may be a balance between reactions such that increase in the steam amount will decrease the CO amount according to the water gas shift, on the other hand, the other

reaction (Reaction 2.6) favors the production of CO when the amount of steam increases in the reaction medium. Moreover, exothermicity of the water gas shift favors the production of CO in the case of addition of more external heat to the system and increasing the temperature from 500 °C to 600 °C.

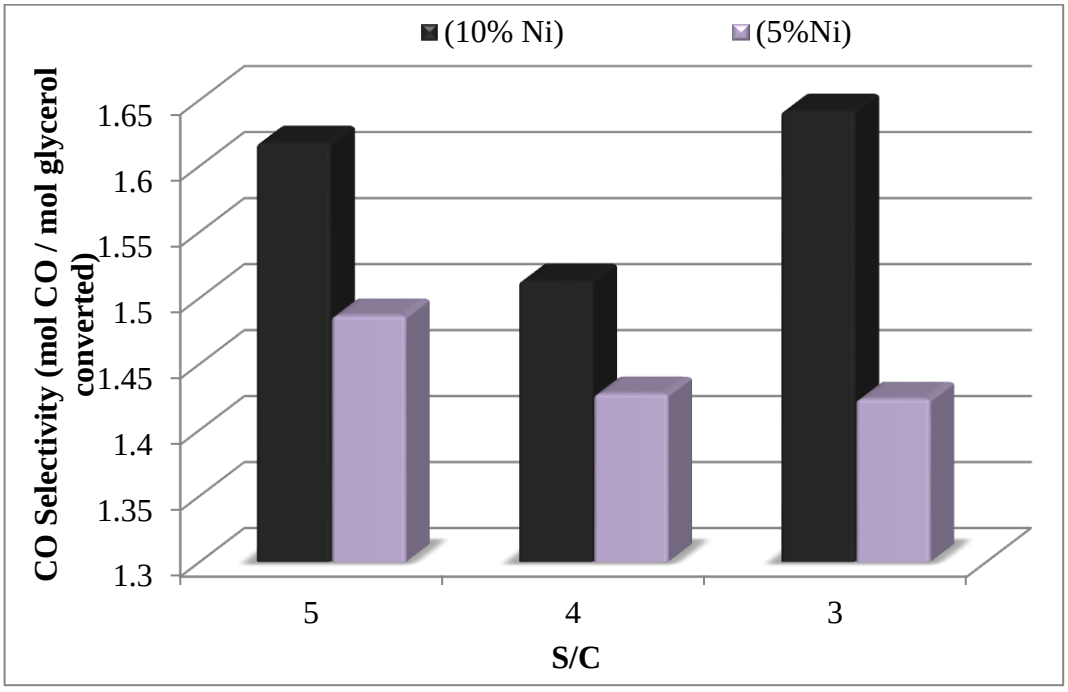

Figure 4.15. CO Selectivity vs S/C Ratio (T = 600°C, Total flow = 96 NmL min^{-1}).

The relation between the S/C ratio and the CO_2 selectivity over two catalysts at 500 °C is given in Figure 4.16. CO_2 selectivity over 5 wt. % Ni/Al_2O_3 catalyst is found to increase with S/C ratio. CO_2 selectivity is 2.04 at S/C ratio of 3, and it increases to 3.67 when S/C ratio is set to 6. CO_2 selectivity over 10 wt. % Ni/Al_2O_3 catalyst increases from 1.82 to 2.20 upon changing S/C ratio from 3 to 5 and further increase in steam leads to slight decrease in the selectivity which is 1.95. The increase in CO_2 selectivity is the result of the water gas shift reaction; as the steam amount increases, the reaction shifts to the product side forming more CO_2. The selectivities over both catalysts are almost equal to each other when the S/C ratio is 3, 4, and 5. However, there is a considerable difference between the selectivities when S/C ratio is set to 6. At this S/C ratio, CO_2 selectivity is 3.62 for 5 wt. % Ni/Al_2O_3, and 1.95 for 10 wt. % Ni/Al_2O_3. This difference may be the result of agglomeration of active metals in the presence of the steam.

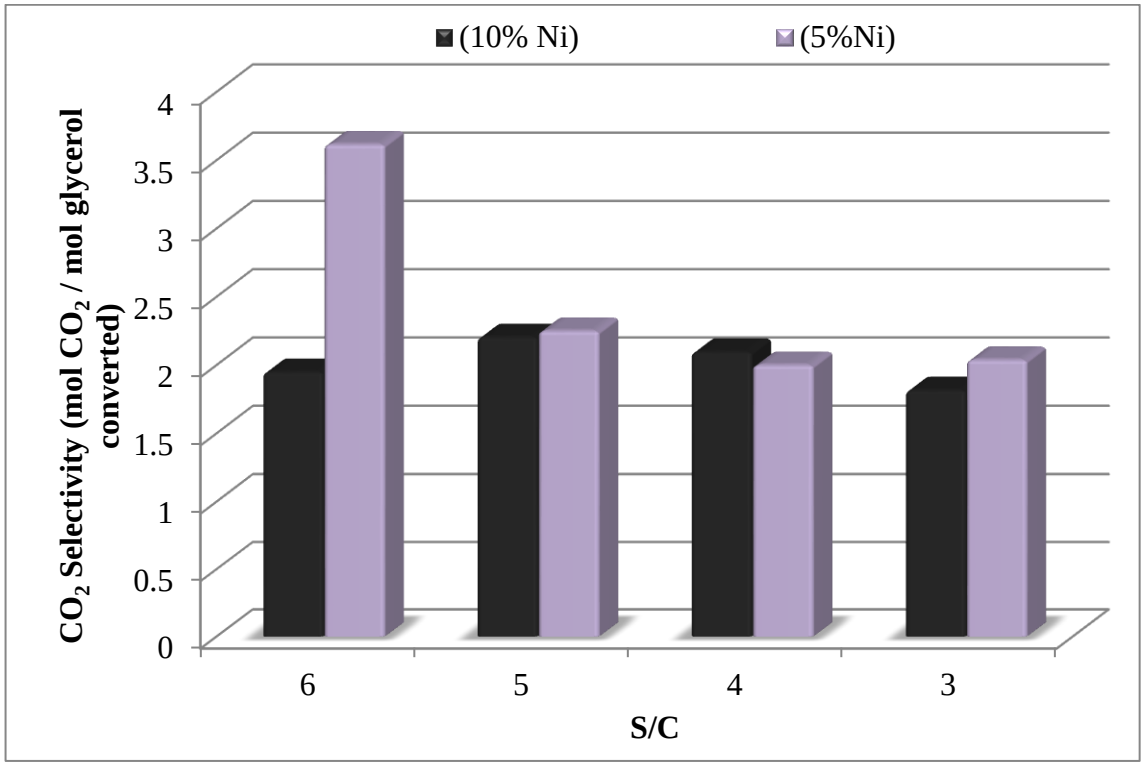

Figure 4.16. CO_2 Selectivity vs S/C Ratio (T = 500°C, Total flow = 96 NmL min^{-1}).

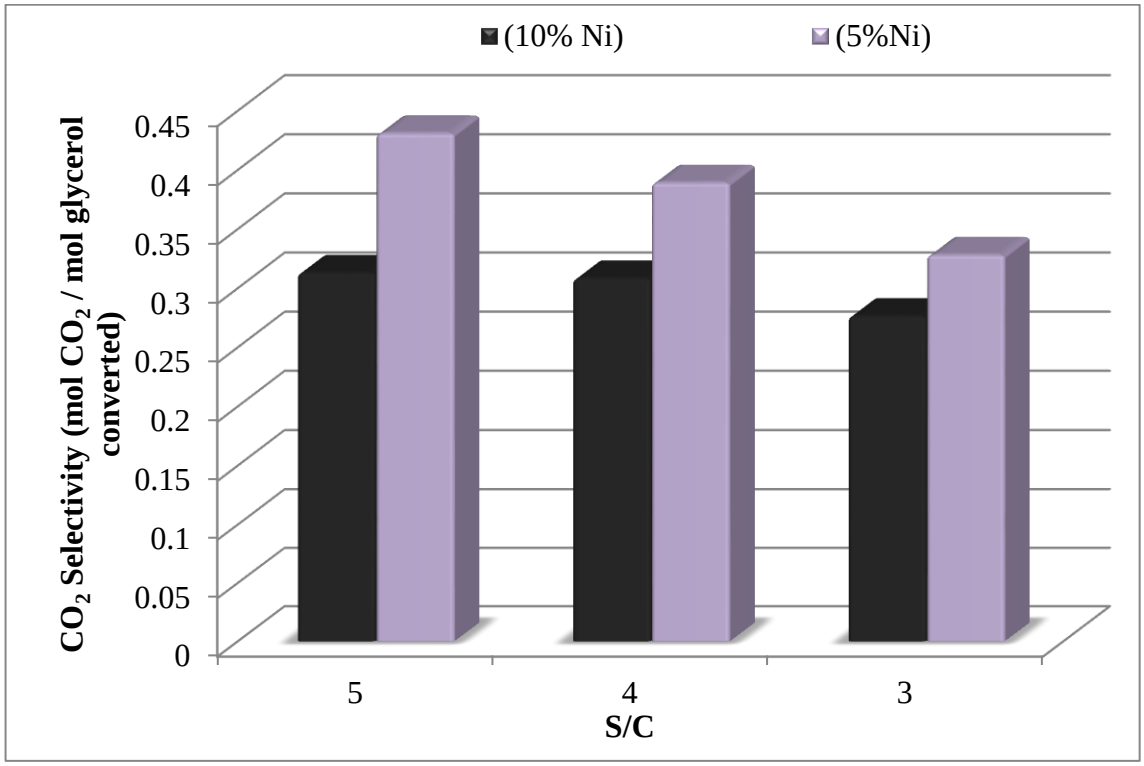

Figure 4.17. CO_2 Selectivity vs S/C Ratio (T = 600 °C, Total flow = 96 NmL min^{-1}).

The effect of S/C ratio on CO_2 selectivity at 600 °C is shown in Figure 4.17. For both catalysts, as S/C ratio increases, the CO_2 selectivity increases accordingly. The CO_2 selectivity over 5 wt. % Ni/Al_2O_3 is reported as 0.32 and 0.43 for S/C ratio of 3 and 5, respectively. CO_2 selectivity over 10 wt. % Ni/Al_2O_3 increases slightly from 0.28 to 0.31 when S/C ratio is changed from 3 to 5. 5 wt.% Ni/Al_2O_3 catalyst is more selective for the production of CO_2 compared to 10 wt. % Ni/Al_2O_3.

The CH_4 selectivities at 500 °C and 600 °C are given in Figure 4.18 and Figure 4.19, respectively over both catalysts. CH_4 selectivity over 5 wt.% Ni/Al_2O_3 catalyst is found to increase with S/C ratio. However, there is not a clear profile for the selectivities over 10 wt. % Ni/Al_2O_3. At 500 °C, the maximum methane selectivity is attained over the 5 wt.% Ni/Al_2O_3 catalyst for S/C ratio of 6 as 0.08. Temperature is an important parameter for methane and other hydrocarbons in GSR reactions. The corresponding peaks for these hydrocarbons at low temperature were not seen without zooming to the post run graph obtained from gas chromotographs. The peaks at low temperatures were mostly drawn manually. This can also lead to the fluctuations in the results.

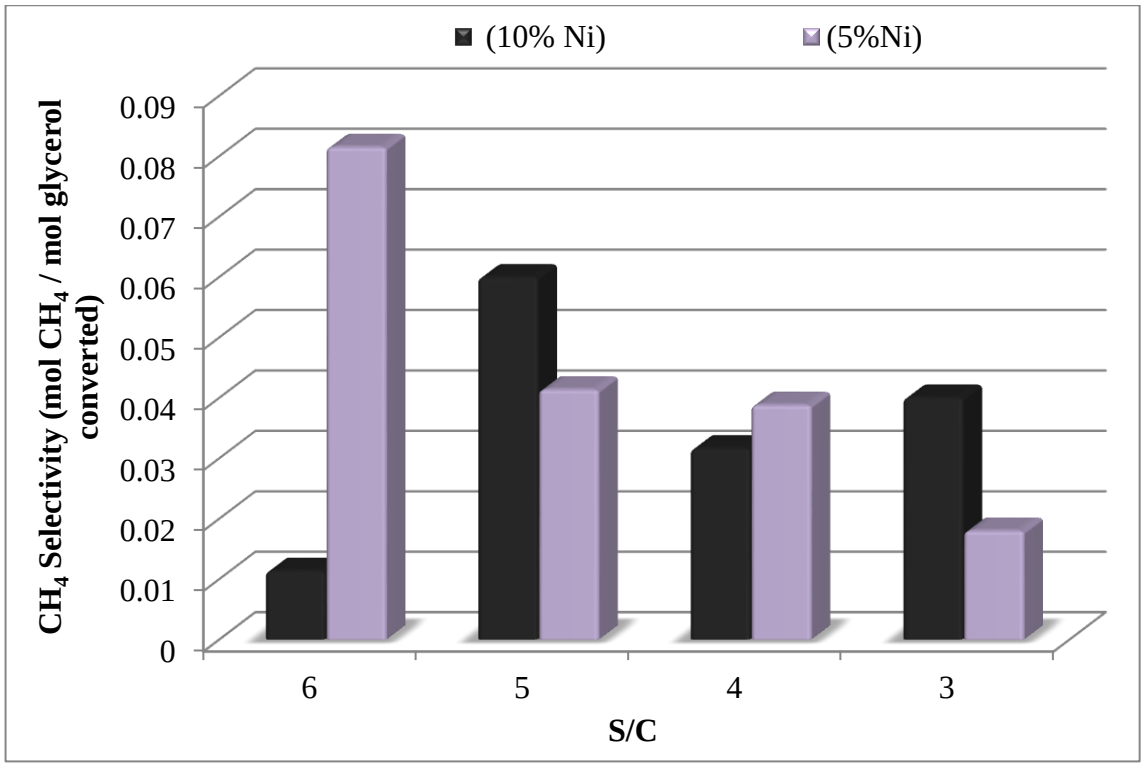

Figure 4.18. CH_4 Selectivity vs S/C Ratio (T = 500°C, Total flow = 96 NmL min^{-1}).

Figure 4.19 gives the CH_4 selectivities over both catalysts at 600 °C with the S/C ratios of 3, 4, and 5. As the temperature is increased to 600 °C, the selectivity of the CH_4 increased considerably compared to the selectivities at 500 °C. CH_4 selectivity over the 5 wt.% Ni/Al_2O_3 catalyst is 0.21, 0.19, and 0.20 for S/C ratios of 3, 4, and 5, respectively. The other catalyst gives the CH_4 selectivities as 0.23, 0.21, and 0.21 for S/C ratios of 3, 4, and 5, respectively. It is concluded that the S/C ratio does not affect CH_4 selectivity significantly. There are several mechanisms that may lead to methane formation or consumption. One of them is the reaction of carbon (coke) with H_2 to produce methane. The increase in the steam amount will increase the production of hydrogen. As the H_2 amount increases, the probability of the contact of H_2 molecules and carbon deposited on the surface increases, which may result in CH_4 formation as Reaction 2.5 suggests. On the other hand, increasing the steam in the system reduces the coke formation significantly in reforming. As steam is increased, less coke is present, so the reaction of H_2 and carbon to give CH_4 may be suppressed.

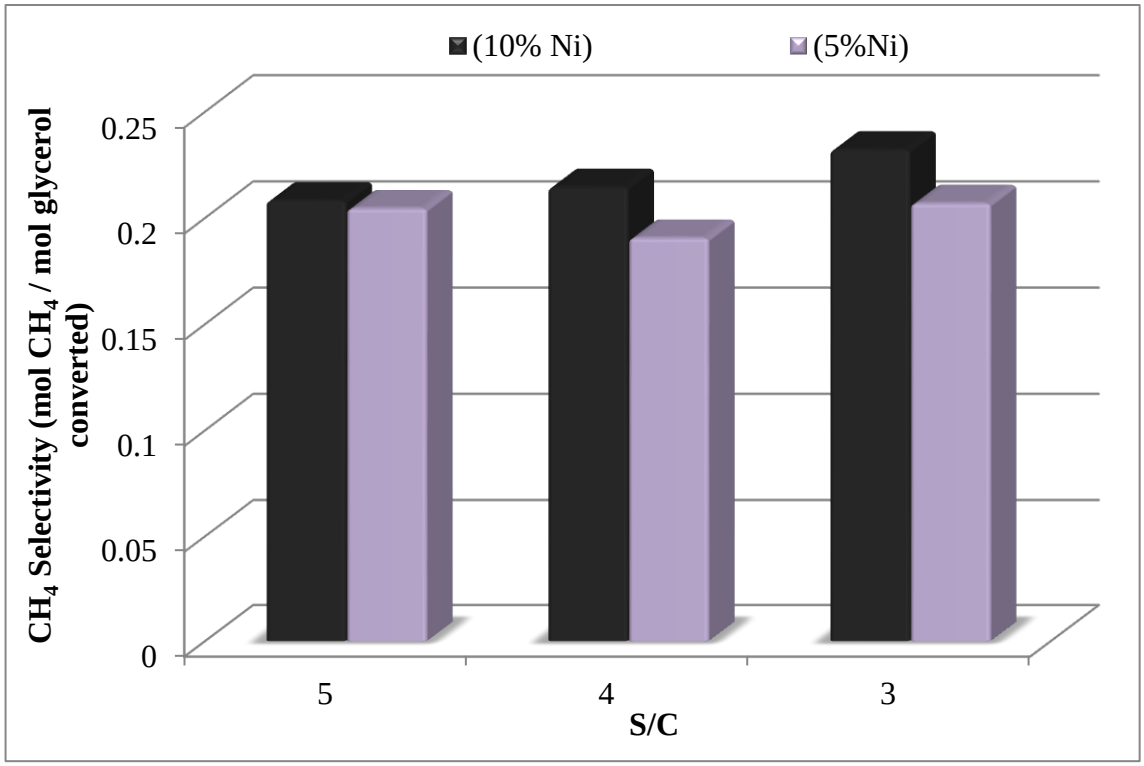

Figure 4.19. CH_4 Selectivity vs S/C Ratio (T = 600°C, Total flow = 96 NmL min^{-1}).

Effect of S/C ratio on C_2H_4 selectivity over both catalysts at 500 °C is shown in Figure 4.20. It is seen that C_2H_4 selectivity over 5 wt.% Ni/Al_2O_3 catalyst increases with

increase in S/C ratio. The selectivities over 5 wt. % Ni/Al_2O_3 are reported as 0.051, 0.052, 0.056, and 0.11 for the S/C ratios of 3, 4, 5, and 6, respectively. 10 wt.% Ni/Al_2O_3 catalysts is less selective toward the production of ethylene than 5 wt.% Ni/Al_2O_3. Moreover, C_2H_4 selectivity over both catalysts at 600 °C is given in Figure 4.21. Based on the trend in Figure 4.21, the ethylene selectivity is decreasing with increase in S/C ratio. Ethylene is the side product of the steam reforming reaction of glycerol, and the higher formation of ethylene means higher formation of carbon in the system. Coke formation is suppressed by addition of more feed to the system. A reaction environment with high steam content may favor the decomposition of glycerol to byproducts (like ethylene) less, which may result in reduced coke formation.

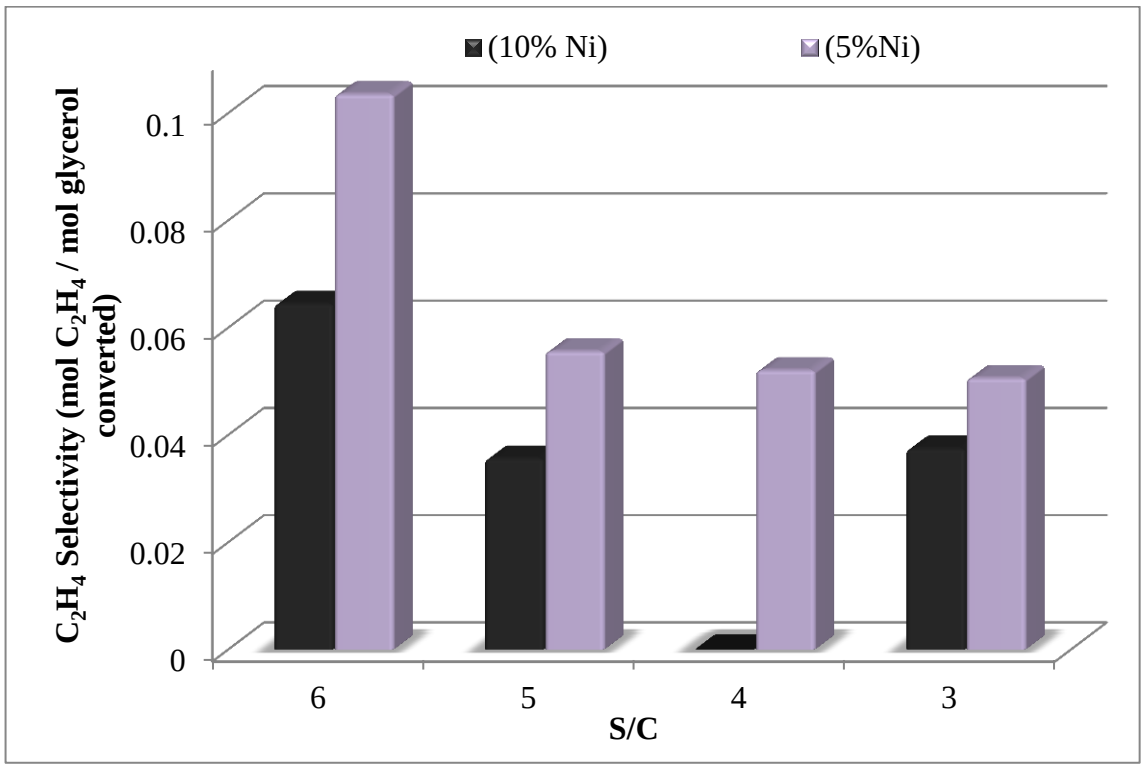

Figure 4.20. C_2H_4 Selectivity vs S/C Ratio (T = 500 °C, Total flow = 96 NmL min^{-1}).

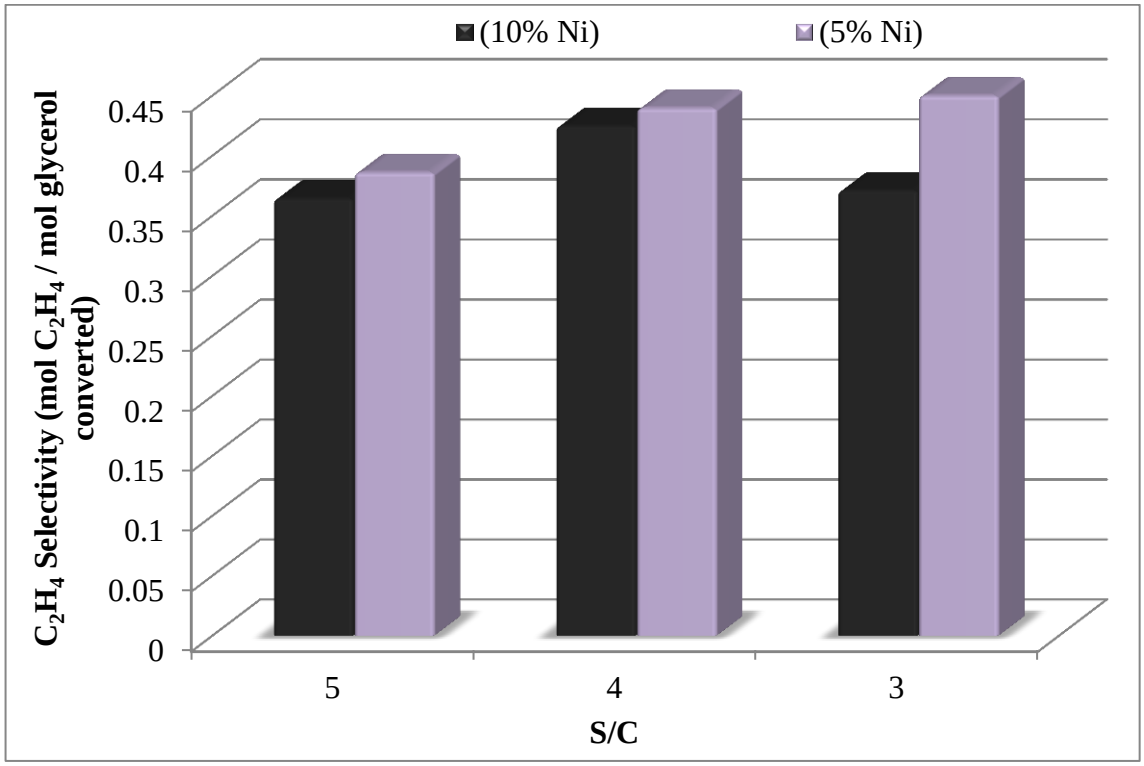

Figure 4.21. C_2H_4 Selectivity vs S/C Ratio (T = 600°C, Total flow = 96 NmL min^{-1}).

There is no C_2H_6 production at 500 °C for S/C ratios 3, 4, 5, and 6 on both catalysts. C_2H_6 selectivity is observed at 600 °C for S/C ratios 3, 4, and 5. Figure 4.22 gives the C_2H_6 selectivity versus S/C ratio over both catalysts. Selectivities are really low even if the reaction tests are conducted at highest temperature. C_2H_6 selectivity over 5 wt.% Ni/Al_2O_3 shows a decreasing trend with the S/C ratio (0.62 at S/C ratio of 3, 0.52 at S/C ratio of 5). However, C_2H_6 selectivity over 10 wt.% Ni/Al_2O_3 increases with the S/C ratio (0.53 at S/C ratio of 3, 0.66 at S/C ratio of 5). The decrease in the selectivities can be explained by the fact that increasing steam content in the reactor may inhibit the byproducts (like C_2H_6), which have the potential to decompose into carbon. It is visually confirmed that high S/C ratios dampen coke formation. This observation supports the decreasing C_2H_6 selectivities at high steam amounts via suppressed glycerol decomposition.

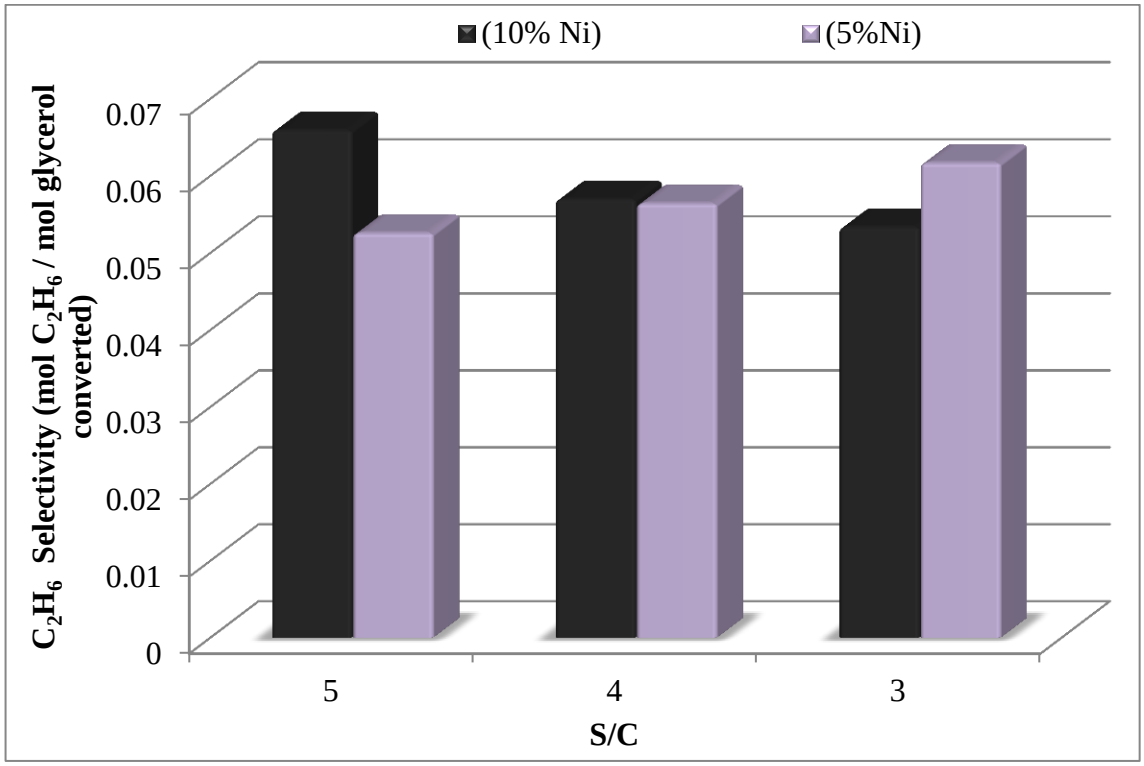

Figure 4.22. C_2H_6 Selectivity vs S/C Molar Ratio (T = 600 °C, Total flow = 96 NmLmin^{-1}).

4.1.3. Effect of Total Flow Rate on GSR

Another parameter that is investigated in this study is the effect of total flow rate. This parameter is investigated over 5 wt.% Ni/Al_2O_3 and 10 wt.% Ni/Al_2O_3 at 600 °C, and the S/C ratio is kept constant at 5. There are four experiments over 5 wt.% Ni/Al_2O_3 catalyst in which the total flow rate is regulated as 64 NmL min^{-1}, 96 NmL min^{-1}, 128 NmL min^{-1} and 160 NmL min^{-1}.

Glycerol conversions over 5 wt.% Ni/Al_2O_3 with respect to total flow rate are given in Figure 4.23. It is seen that the glycerol conversion increases exponentially with decreasing the total flow rate. The conversions over 5 wt.% Ni/Al_2O_3 catalyst are reported as 13.3%, 13.5%, 19.4%, and 33.8% for total flow rates of 160 NmL min^{-1}, 128 NmL min^{-1}, 96 NmL min^{-1} and 62 NmL min^{-1}, respectively. There are two important parameters affecting the result of this investigation, one of them being the time that reactants spent on the catalyst surface, and the other being the amount of the reactant fed to the reactor. As the flow rate decreases, the contact time for the reactants over the catalyst surface increases which leads to higher conversions. For higher flow rates, reactants spent less time over the

surface of catalyst, and this explains why the glycerol conversion is less at high flow rates. Moreover, increasing the flow rate further (which means increasing the reactant amount and decreasing the time those reactants spent on the catalyst surface) does not have a significant effect on glycerol conversion. It is concluded that glycerol conversion remains unchanged at higher flow rates (160 NmL min^{-1} and 128 NmL min^{-1}), but it increases as the total flow rate decreases as a result of the fact that the time those reactants spent in the reactor increases.

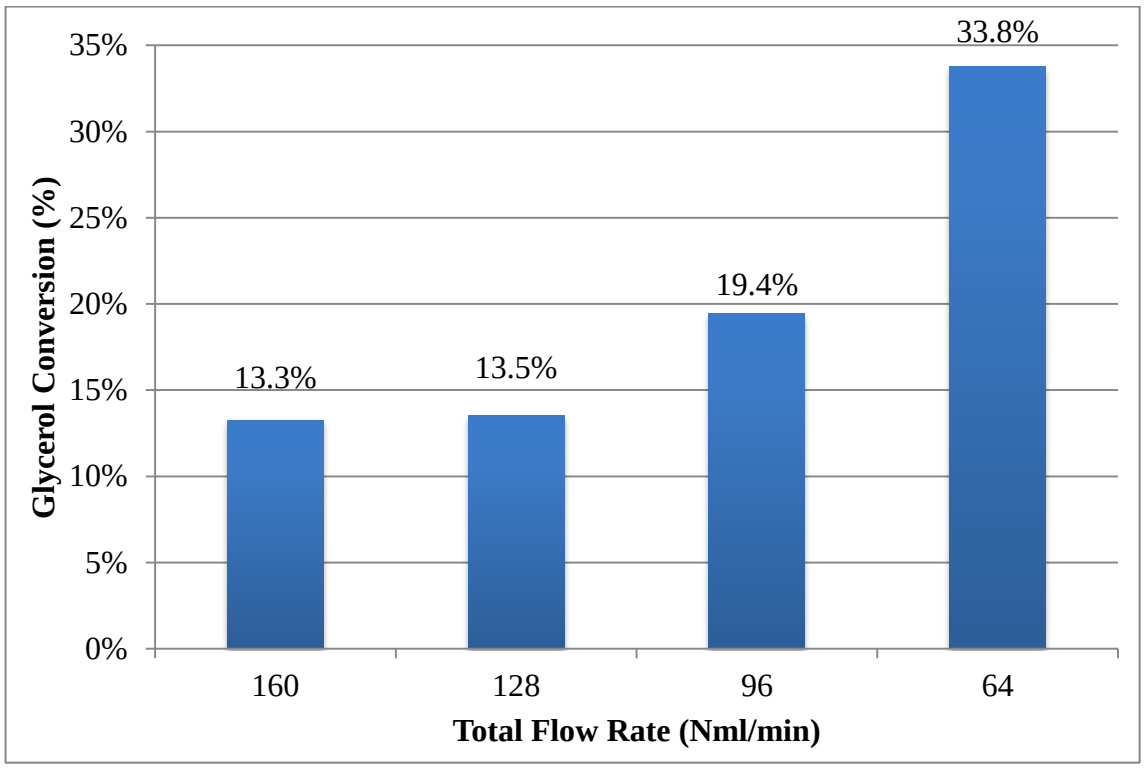

Figure 4.23. Glycerol Conversion vs Total Flow Rate (T = 600 °C, S/C = 5, 5 wt.% Ni/Al_2O_3).

H_2 selectivity over 5 wt.% Ni/Al_2O_3 for different total flow rates is given in Figure 4.24. It is concluded that H_2 selectivity increases as total flow rate decreases. H_2 selectivities over 5 wt.% Ni/Al_2O_3 catalyst are reported as 2.64, 3.24, 3.25, and 4.10 for total flow rates of 160 NmL min^{-1}, 128 NmL min^{-1}, 96 NmL min^{-1} and 62 NmL min^{-1}, respectively. At higher flow rates, the conversions are lower compared to lower flow rates. Glycerol conversion appears in the denominator of the selectivity expression. This indicates that the produced amount of hydrogen increases significantly as the total flow rate decreases. At lower flow rates, even if the amount of the reactants are less, the contact

time effect is dominant, and H_2 selectivity becomes higher in low flow rates. As a result of contact time, glycerol steam reforming reaction is enhanced and it produces more hydrogen.

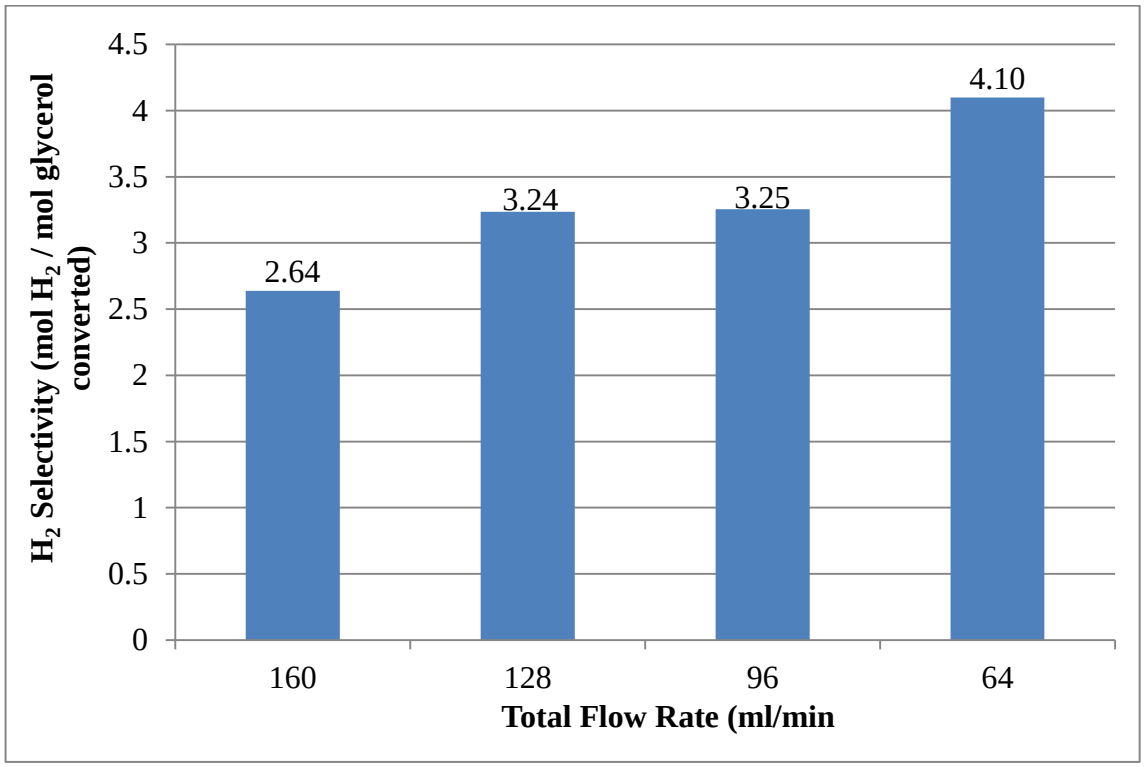

Figure 4.24. H_2 selectivity vs Total Flow Rate (T = 600°C, S/C = 5, 5 wt.% Ni/Al_2O_3).

The selectivities of other gaseous products are given in Figure 4.25. In general, it is concluded that all selectivities increase as the total flow rate decreases. The time that the reaction mechanism takes place over the catalyst surface increases, and that is why more amount of product is obtained at lower flow rates. The most significant increase in the selectivity is observed for CO. CO selectivities over 5 wt.% Ni/Al_2O_3 catalyst are reported as 1.42, 1.40, 1.49, and 2.28 for total flow rates of 160 NmL min^{-1}, 128 NmL min^{-1}, 96 NmL min^{-1} and 62 NmL min^{-1}, respectively. CO is the reactant of the water gas shift in which the hydrogen exists on the product side. Based on Figure 4.24, hydrogen amount also increases as the total flow rate decreases. This increase in hydrogen favors the backward water gas shift reaction resulting in more CO formation. Another reason of the increase in CO selectivity can be stated as the pyrolysis of the glycerol which produces

hydrogen and CO. Increasing the contact time, increases the conversion of the glycerol in pyrolysis reaction which lead to more production of both H_2 and CO.

CO_2 selectivity over 5 wt.% Ni/Al_2O_3 catalyst is also given with respect flow rates in Figure 4.25. CO_2 selectivities are reported as 0.37, 0.46, 0.43, and 0.56 for total flow rates of 160 NmL min^{-1}, 128 NmL min^{-1}, 96 NmL min^{-1} and 62 NmL min^{-1}, respectively. In general, CO_2 selectivity takes its highest value at the lowest flow rate. This is mainly the result of the contact time which allows more conversions of the reactants in glycerol steam reforming. However, CO_2 selectivity does not show an increasing trend with decreasing the flow rate, and it can be concluded that, in overall, the selectivity does not increase too much. The reason for the change in CO_2 production in glycerol steam reforming mechanism is water gas shift reaction. This reaction includes CO and H_2O in the reactant side, and H_2 and CO_2 in the product side. The results of the total flow rate investigation point out an increase in both CO and H_2 production which may result in no more production or consumption of CO_2.

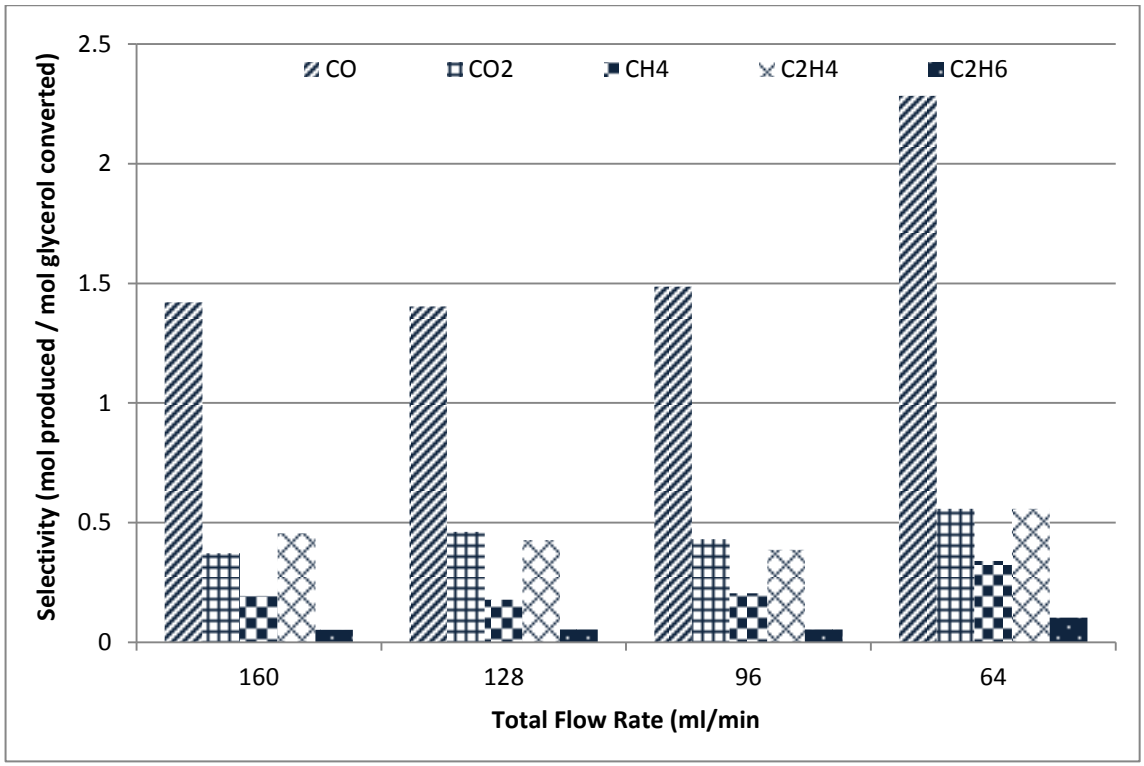

Figure 4.25. Selectivity of Gaseous Products vs Total Flow Rate (T = 600°C, S/C = 5, 5 wt.% Ni/Al_2O_3).

Selectivity of produced hydrocarbons (CH_4, C_2H_4, and C_2H_6) reaches maximum levels at lowest flow rate (64 Nml/min). CH_4 selectivities are 0.19, 0.18, 0.20, and 0.34, C_2H_4 selectivities are 0.46, 0.43, 0.39, and 0.56, and C_2H_6 selectivities are given as 0.05, 0.05, 0.05, and 0.10 for total flow rates of 160 NmL min^{-1}, 128 NmL min^{-1}, 96 NmL min^{-1} and 62 NmL min^{-1}, respectively. Although the changes in selectivities are minor, in general, the selectivities are higher at the lowest flow rate, and the only reason for that is the increase in the contact time. These are carbon including molecules and the conversion is calculated based on the carbon balance. The increase in the production of this species directly affects the conversion and that is why conversion increases exponentially with decreasing the flow rate.

4.1.4. Effect of Reactor Configuration on GSR

Reactor configuration is an important parameter that affects conversions and product distributions. In this study, performance of packed microchannel is compared with the coated microchannel (see Section 3.3.2.2 for the description of microchannel configurations). 5 wt.% Ni/Al_2O_3 catalyst is utilized in both configuration, the only difference is the size of the catalyst powders. In packed microchannel, the housing is packed with 60-80 mesh size of 5 wt.% Ni/Al_2O_3 catalyst. 5 wt.% Ni/Al_2O_3 catalyst is chosen for the comparison because it is concluded that metal loading does not have a significant effect on conversion. Moreover, 5 wt.% Ni/Al_2O_3 catalyst gives higher H_2 selectivity and it is more stable towards the agglomeration of active metals compared to 10 wt.% Ni/Al_2O_3 catalyst.

Glycerol conversion according to reactor configurations and blank experiments at three different temperature levels are given in Figure 4.26. In all three configurations, the temperature increase leads to increase in glycerol conversion. In coated microchannel, the conversions are 2.88%, 3.77%, and 4.42% at temperatures of 475 °C, 500 °C, and 550 °C, respectively. In packed microchannel, the glycerol conversions changes as 0.37%, 1.87%, and 2.55% at temperatures of 475 °C, 500 °C, and 550 °C, respectively.

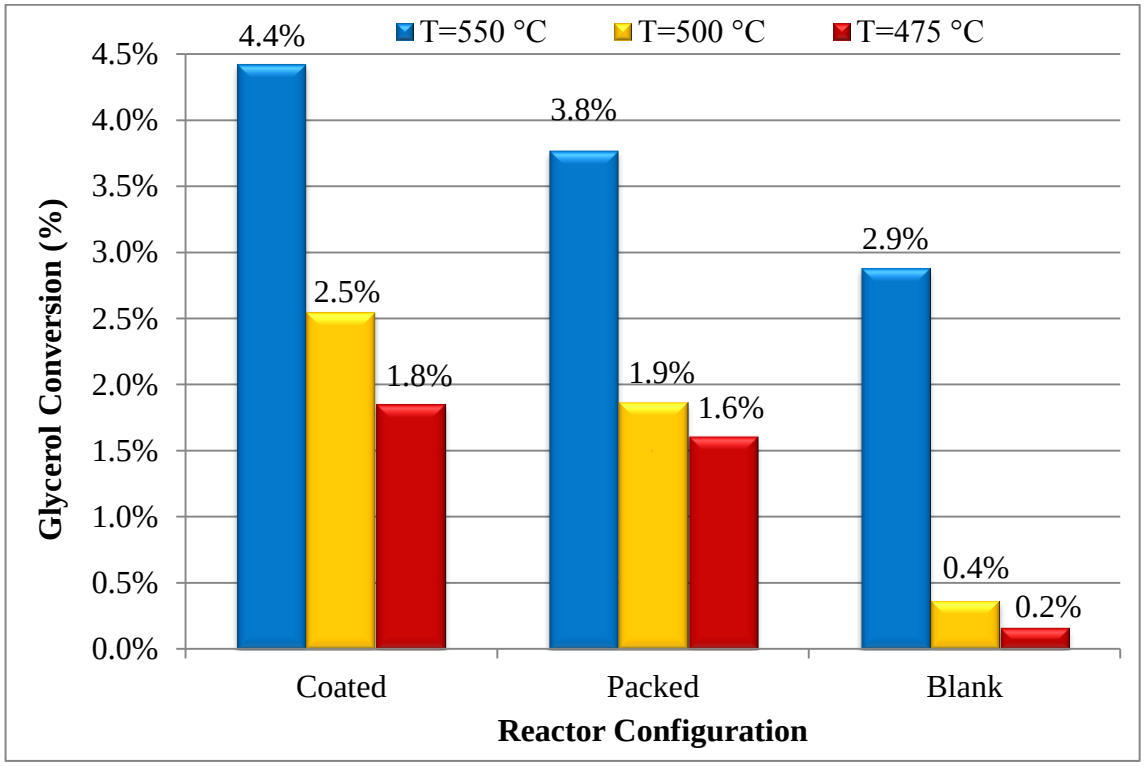

Figure 4.26. Glycerol Conversion vs Reactor Configuration (S/C = 5, 5 wt.% Ni/Al_2O_3, Total flow = 96 NmL min^{-1}).

Coated configuration gives conversions higher than those observed in packed configuration and in blank tests. The reason of this observation is believed to be better utilization of the catalyst bed due to higher heat transfer rates involved.

H_2 selectivity over 5 wt.% Ni/Al_2O_3 catalyst for three configurations are given in Figure 4.27. The effect of temperature on hydrogen selectivity is given in detail in Section 4.1. The decrease in H_2 selectivity in all configurations with respect to temperature increase can be explained by the water gas shift reaction. At high temperatures, water gas shift reaction shifts to reactant sides consuming H_2 and CO_2, and producing CO and H_2O. The decrease in CO_2 and increase in CO is verified in Figure 4.28 and Figure 4.29. H_2 selectivities at 475 °C are reported as 9.46, 11.44, and 12.93 for blank, packed, and coated configurations, respectively. At 500 °C, selectivities decrease to 4.62, 10.23, and 11.95 for blank, packed, and coated configurations, respectively. Moreover, the selectivities at 600 °C are given as 1.65, 6.55, and 7.60 for blank, packed, and coated configurations, respectively.

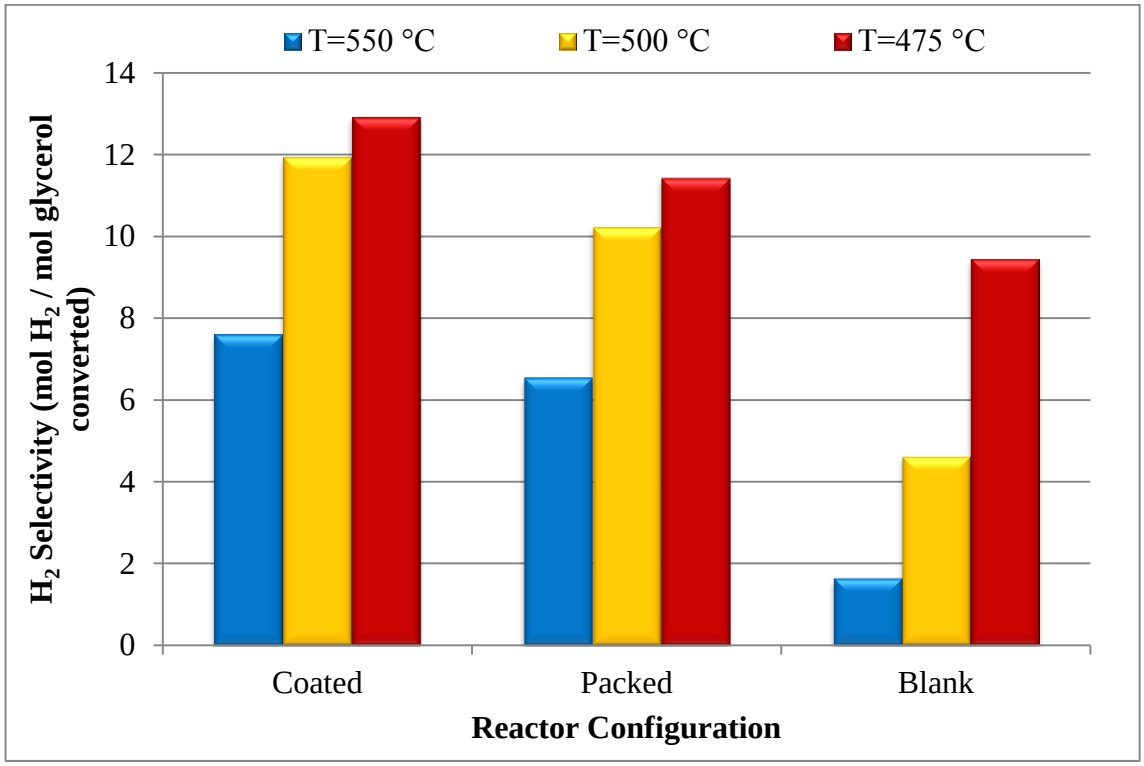

Figure 4.27. H_2 Selectivity vs Reactor Configuration (S/C = 5, 5 wt.% Ni/Al_2O_3, Total flow = 96 NmL min^{-1}).

At all temperature levels, the coated microchannel shows higher selectivity towards to production of hydrogen than two other configurations. The effect of catalyst on hydrogen production is observed because the selectivities in both coated and packed microchannels are higher than the blank tests' results. Coated microchannel configuration shows high hydrogen selectivity because it has better heat distribution over the surface favoring the steam reforming reaction that is producing hydrogen.

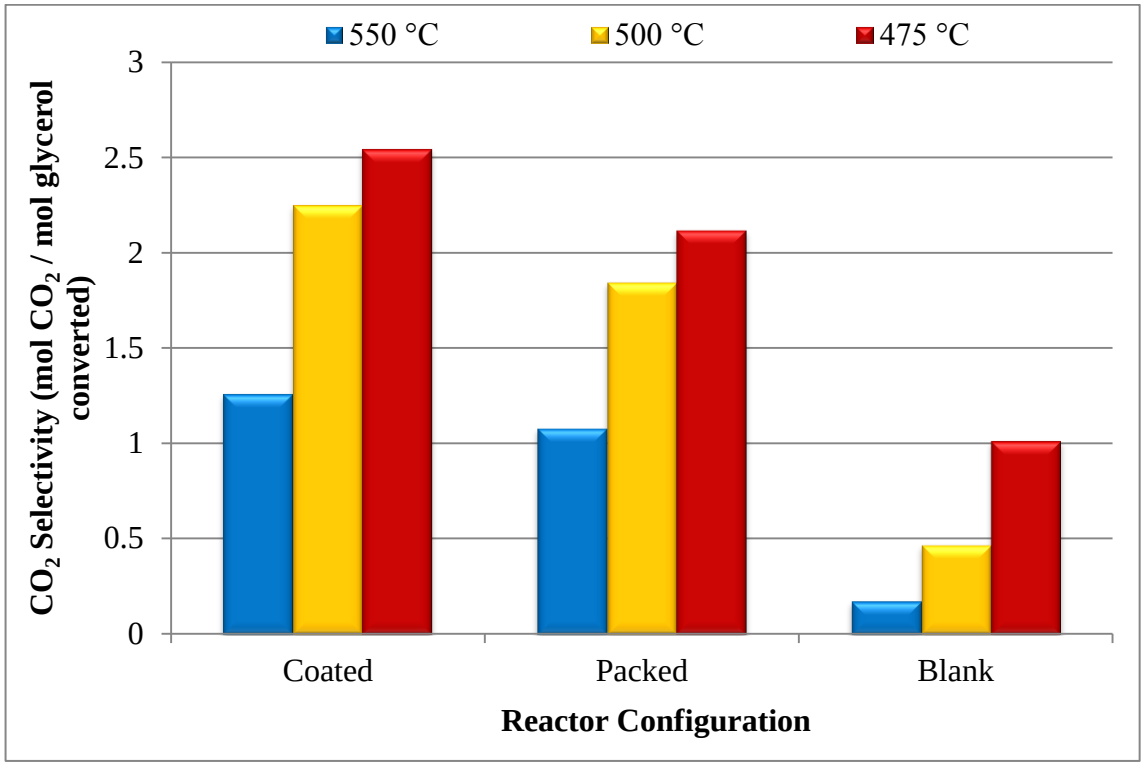

Figure 4.28. CO_2 Selectivity vs Reactor Configuration (S/C = 5, 5 wt.% Ni/Al_2O_3, Total flow = 96 NmL min^{-1}).

The change in CO selectivity is given for three configurations at three temperature levels in Figure 4.29. 5 wt.% Ni/Al_2O_3 catalyst (packed or coated) has lower CO selectivity compared the blank tests' results. In catalytic systems, the water gas shift reaction takes place and consumes the CO. The effect of the catalyst is higher in coated microchannel configuration than packed microchannel. The maximum selectivity on coated microchannel at 550 °C is 1.17 whereas it is 1.34 in packed microchannel.

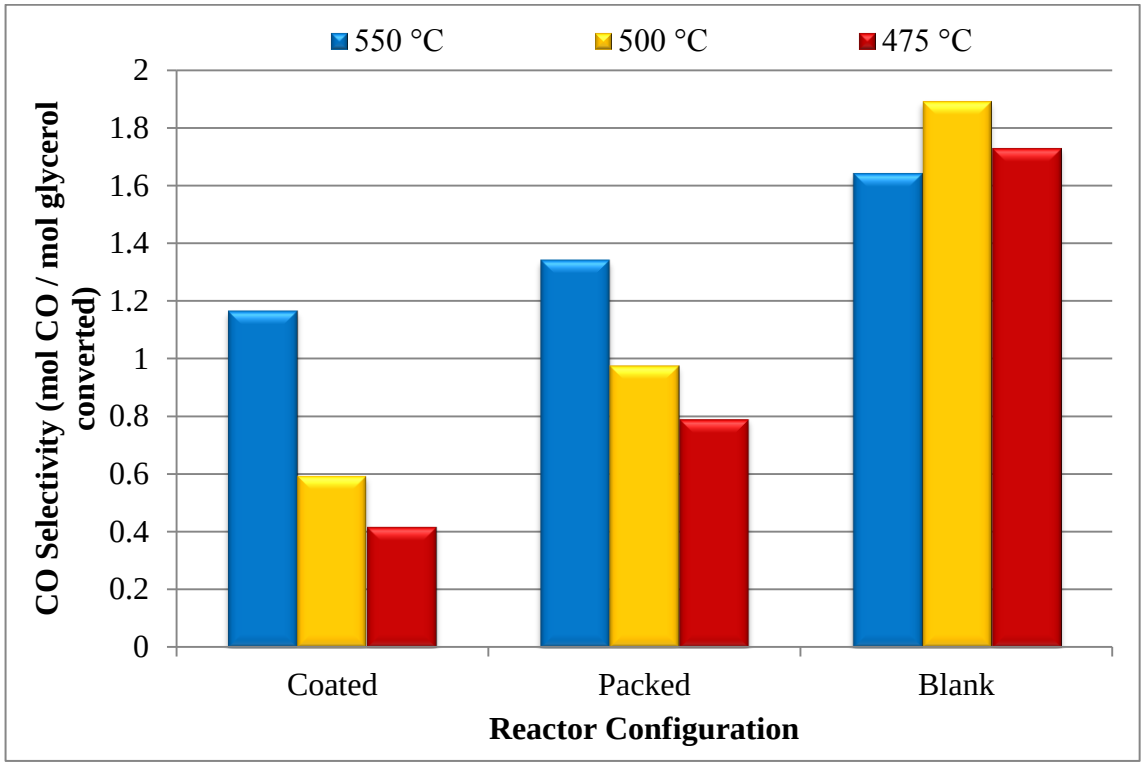

Figure 4.29. CO Selectivity vs Reactor Configuration (S/C = 5, 5 wt.% Ni/Al_2O_3, Total flow = 96 NmL min^{-1}).

4.2. Results of Oxidative Glycerol Steam Reforming Experiments

Oxidative glycerol steam reforming (OGSR) tests are conducted to investigate the effect of adding oxygen to the feed on catalyst performance. The tests are conducted over 5 wt.% Ni/Al_2O_3 at three temperatures (500, 550, and 600 °C) while C/O molar ratio, S/C molar ratio and the total feed flow rate are kept constant at 1.125, 5 and 96 Nml/min, respectively. The results are compared with those of steam reforming tests performed at the same conditions. Oxygen content in feed is the other parameter investigated in OGSR. The C/O molar ratio is changed as 0.75, 1.125 and 2.25 while temperature, S/C molar ratio and total feed flow rate are kept constant at 550 °C, 5 and 96 Nml/min, respectively. The blank tests for oxidative steam reforming reactions are also performed and results are given and discussed in Section 4.2.3.

4.2.1. Effect of Temperature on OGSR

Results of temperature investigation based on glycerol conversion and comparison between GSR and OGSR are given in Figure 4.30.

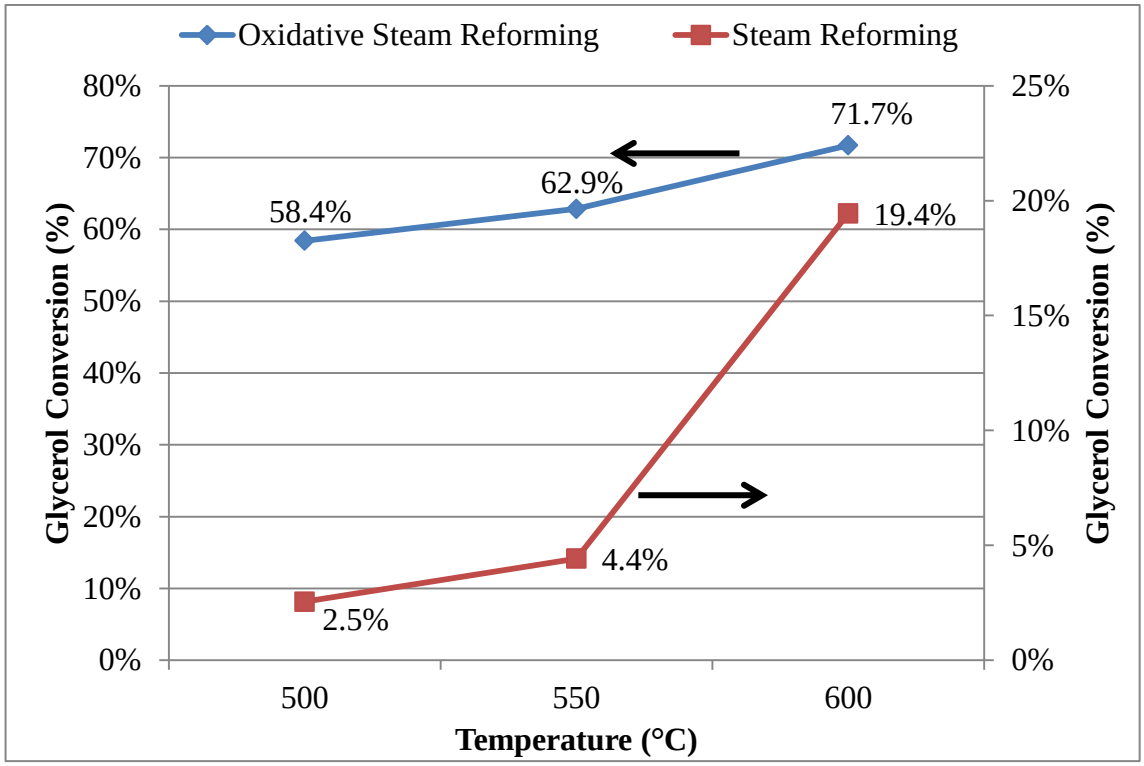

Figure 4.30. Glycerol Conversion vs Temperature for OGSR and GSR (S/C = 5, C/O = 1.125, N_2 flow = 44 NmL min^{-1}, Total flow = 96 NmL min^{-1}).

Glycerol conversion for OGSR is calculated as 58.4%, 62.9%, and 71.7% at 500, 550, and 600 °C, respectively. There is an increase in glycerol conversion with temperature. At the same temperatures, conversions obtained in OGSR tests are significantly higher than those obtained in GSR tests. Adding oxidant helps to burn off the coke formed over 5 wt.% Ni/Al_2O_3, and the elimination of coke in the system prevents catalyst deactivation. Burning the carbon with oxygen leads to formation of more carbon compounds in the product stream which increases the conversions. Moreover, the produced amount of carbon containing products in OGSR is very high compared to GSR tests. Table 4.1 gives product yields for OGSR and GSR at three temperature levels. The highest increase in product yield is observed for CO yield which is 0.015 in GSR tests whereas it is 1.155 in OGSR tests. In general, the most significant changes for product yields are

observed for CO and CO_2 yields. The increase in carbon containing species can be explained by Reaction 2.13 in which CO and CO_2 are the products. Moreover, the presence of O_2 in the system increases the decomposition and oxidation of glycerol over the housing.

Table 4.1. Gaseous product yields in OGSR and GSR at three temperatures

		Product Yields (mol product/mol glycerol fed)					
	T (°C)	**H_2**	**CH_4**	**CO**	**CO_2**	**C_2H_4**	**C_2H_6**
GSR	500	0.304	0.001	0.015	0.057	0.001	-
	550	0.336	0.004	0.052	0.056	0.011	-
	600	0.633	0.040	0.289	0.084	0.075	0.010
OGSR	500	0.770	0.033	1.155	0.531	0.011	0.005
	550	0.668	0.058	1.332	0.431	0.023	0.008
	600	1.094	0.084	1.261	0.661	0.058	0.014

H_2 selectivity for OGSR and GSR are given in Figure 4.31. It is clearly seen that the selectivities are much higher in GSR than OGSR. This is the result of glycerol conversion which is very low in GSR tests and this makes the selectivities higher. A better comparison can be done by investigating the product yields. According to the results given in Table 4.1, H_2 yields are ca. two times higher in OGSR, meaning that produced amount of H_2 as a result of same glycerol input is higher in OGSR.The possible reason of increase in the yields of CO and H_2 can be given as the partial oxidation which directly leads to production of these species. Moreover, O_2 may burn the coke to produce CO, and this CO further reacts with steam to produce H_2 via water gas shift. There may also be a production of H_2 from methane steam reforming, because CH_4 is another product whose yield increases by addition of O_2. H_2 selectivity in OGSR is slightly increases from 1.32 at 500 °C to 1.53 at 600 °C despite of the increase in glycerol conversions from 58.4% to 71.7%, and this is a clear indication of more H_2 yield.

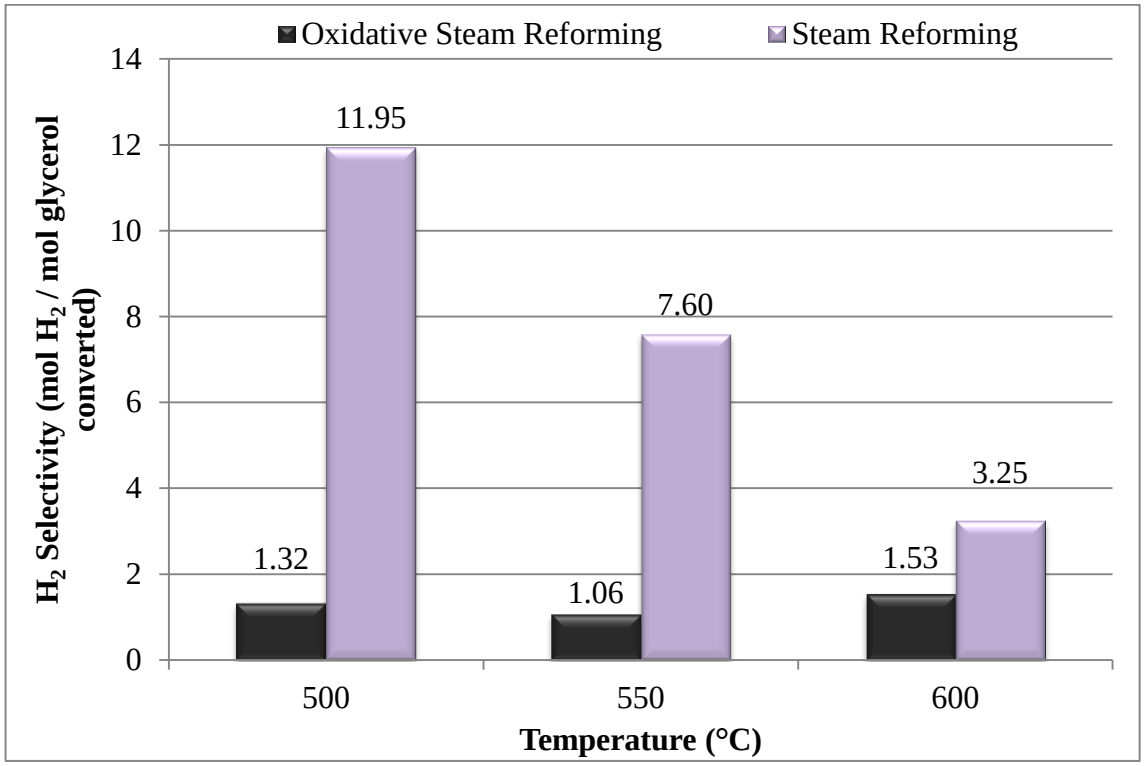

Figure 4.31. H_2 Selectivity vs Temperature for OGSR and GSR (S/C = 5, C/O = 1.125, N_2 flow = 44 NmL min^{-1}, Total flow = 96 NmL min^{-1}).

CO_2 selectivity with respect to temperature is given in Figure 4.32. The CO_2 selectivity for OGSR stays nearly constant with respect to temperature increase despite of increase in conversion. On the other hand, in GSR, there is a considerable decrease in the selectivity as temperature increases, and the reason of this trend is explained in Section 4.1.1. In the case of OGSR, there is not a considerable effect of temperature increase in the selectivity. At 600 °C, CO_2 selectivity in OGSR is higher than the selectivity in GSR. At other temperature levels, GSR gives higher CO_2 selectivity than OGSR. There is a considerable increase in CO_2 yields as a result of O_2 addition as seen from Table 4.1. The increase in the yield can be explained by oxidative glycerol steam reforming reaction equation which produces CO_2 from the reaction of oxygen with steam and glycerol. Moreover, burning carbon in the system leads to more formation of this product.

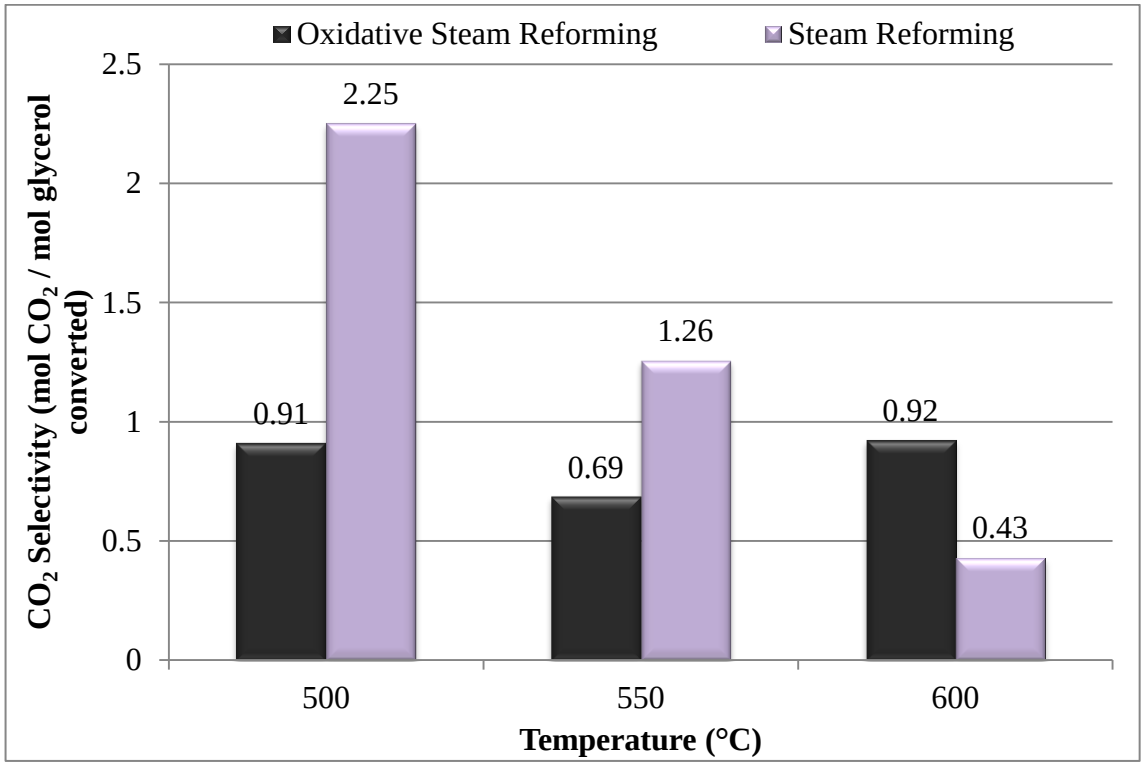

Figure 4.32. CO_2 Selectivity vs Temperature for OGSR and GSR (S/C = 5, C/O = 1.125, N_2 flow = 44 NmL min^{-1}, Total flow = 96 NmL min^{-1}).

CO selectivity with respect to temperature for OGSR and GSR is given in Figure 4.33. It is seen that as temperature increases, CO selectivity does not change significantly in OGSR, however, in GSR, there is an obvious increase in CO selectivity. The gap between CO selectivities in OGSR and GSR decreases as temperature increases. CO yields are given in Table 4.1, and it is seen that the CO yield in OGSR are very high considering the yields in GSR. The result of this difference can be explained by the presence of Reaction 2.13 which is taking place when the system contains oxygen.

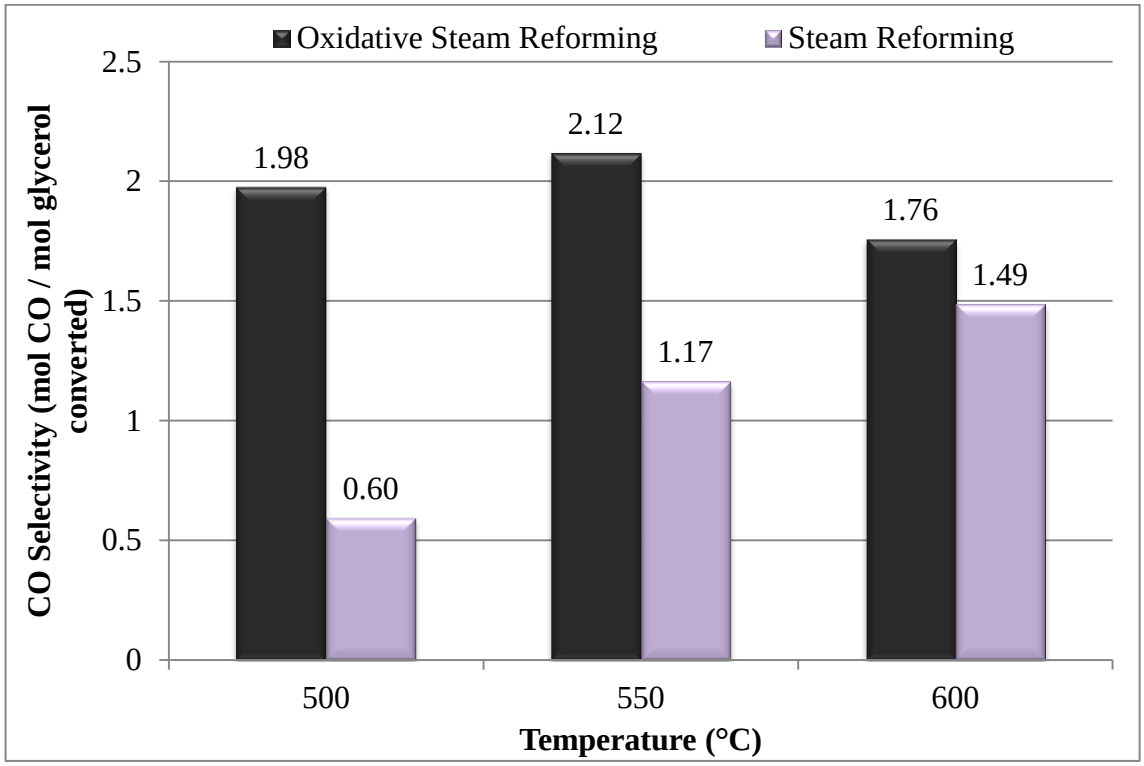

Figure 4.33. CO Selectivity vs Temperature for OGSR and GSR (S/C = 5, C/O = 1.125, N_2 flow = 44 NmL min^{-1}, Total flow = 96 NmL min^{-1}).

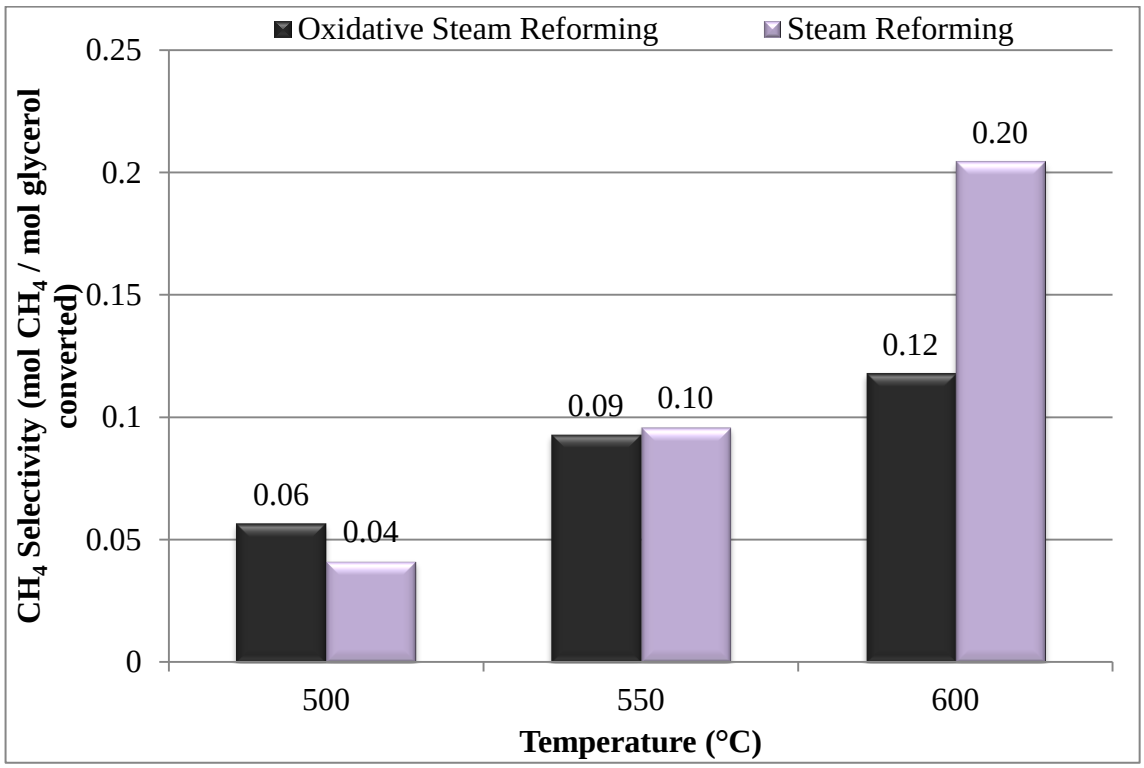

Figure 4.34. CH_4 Selectivity vs Temperature for OGSR and GSR (S/C = 5, C/O = 1.125, N_2 flow = 44 NmL min^{-1}, Total flow = 96 NmL min^{-1}).

CH_4 selectivity for GSR and OGSR is given in Figure 4.34. CH_4 selectivity in OGSR increases slightly (from 0.06 to 0.12) with temperature. This is a clear indication of more methane production in the system, because conversion also increases with temperature. This conclusion is supported with CH_4 yield which is given in Table 4.1. The CH_4 yields are reported as 0.033, 0.058, and 0.084 at 500, 550, and 600 °C, respectively. This trend is also valid for other hydrocarbons (C_2H_4 and C_2H_6) that the presence of the oxygen and higher temperature levels increases the decomposition of glycerol. This decomposition produces more hydrocarbons in the system.

Figure 4.35 and Figure 4.36 show the C_2H_4 selectivity and C_2H_6 selectivity for OGSR and GSR, respectively. The results indicate that selectivity increases with temperature. GSR seems to be more selective for ethylene production. The lower conversion in GSR seems to be responsible for this difference. The yields for these hydrocarbons are higher in OGSR than the yields in GSR (Table 4.1).

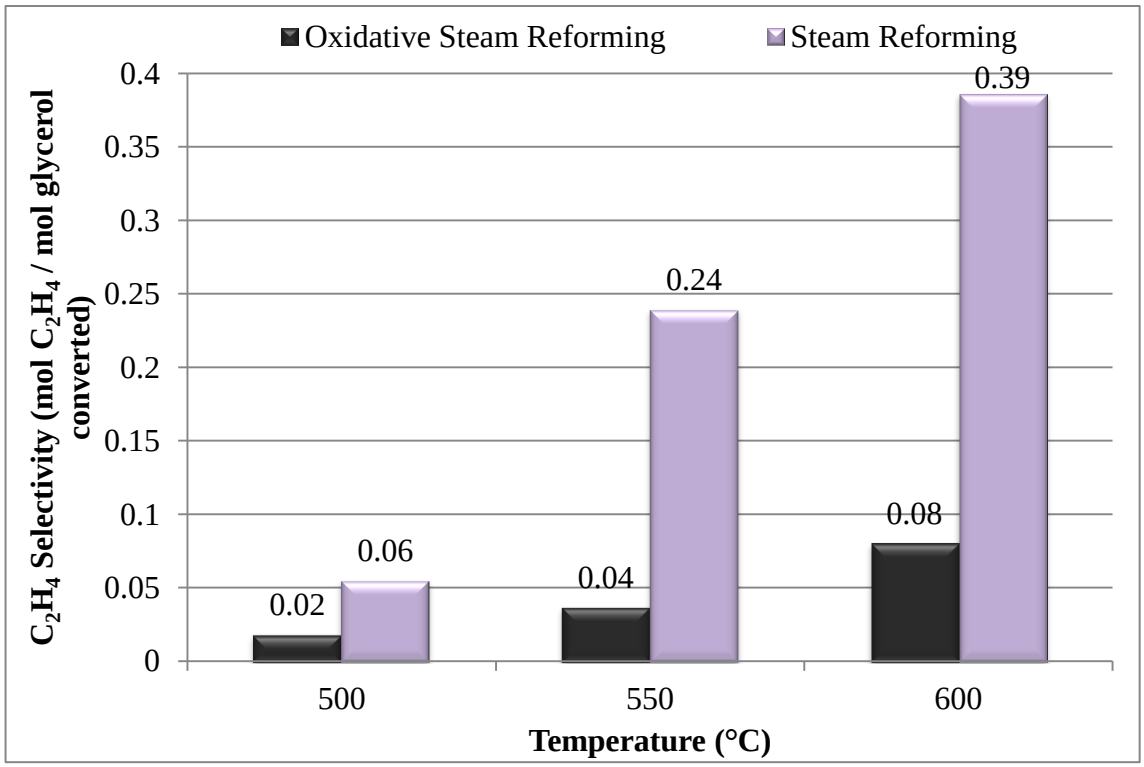

Figure 4.35. C_2H_4 Selectivity vs Temperature for OGSR and GSR (S/C = 5, C/O = 1.125, N_2 flow = 44 NmL min^{-1}, Total flow = 96 NmL min^{-1}).

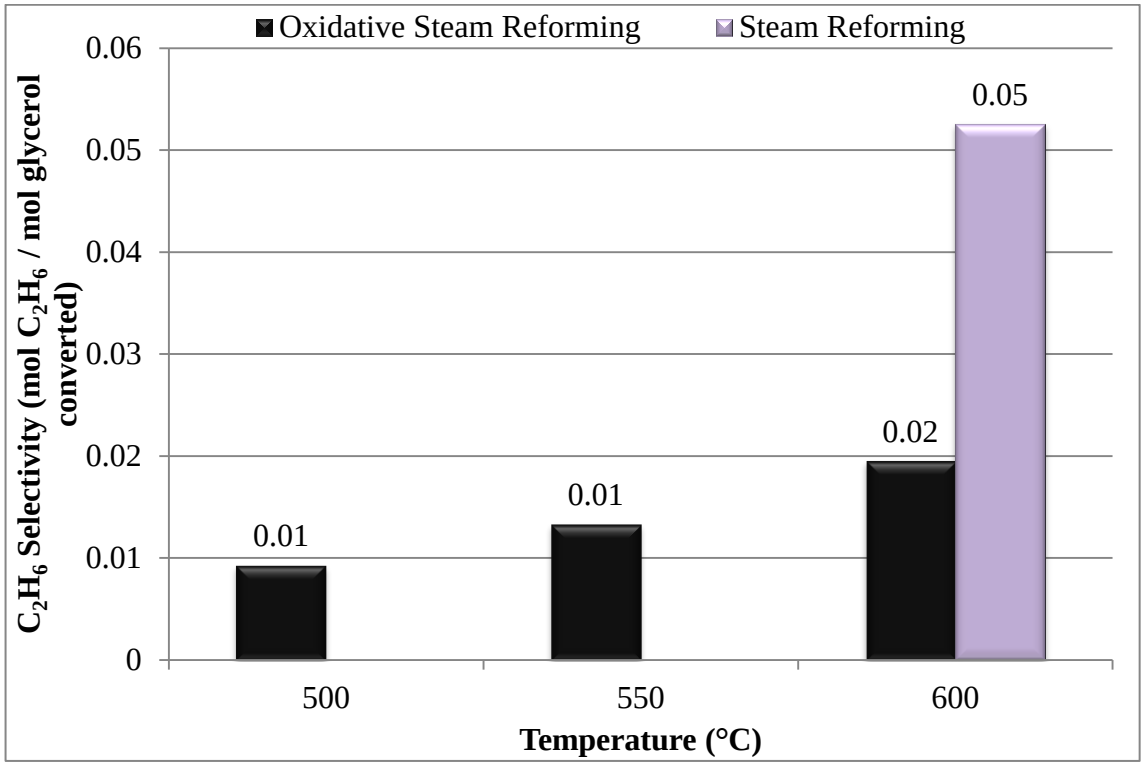

Figure 4.36. C_2H_6 Selectivity vs Temperature for OGSR and GSR (S/C = 5, C/O = 1.125, N_2 flow = 44 NmL min^{-1}, Total flow = 96 NmL min^{-1}).

4.2.2. Effect of C/O Molar Ratio on OGSR

In OGSR tests, it is mainly concluded that oxygen has increased the conversions as well as the yield of each product. After this conclusion, it is decided to make a study to see the effect of oxygen amount in the conversions and selectivities. This time, the C/O molar ratio is changed as 0.75, 1.125, and 2.25 corresponding to O_2 flow rates of 2, 4, and 6 Nml/min, respectively, while keeping S/C molar ratio, total flow rate, the glycerol flow rate and temperature at 5, 96 Nml/min, 3 Nml/min and 550 °C, respectively.

Figure 4.37 is given for glycerol conversion with respect to C/O molar ratio. It is seen that as the C/O molar ratio decreases, glycerol conversion increases. The glycerol conversions are reported as 44.3%, 62.9% and 71.9% for C/O ratios of 2.25, 1.125 and 0.75, respectively. Decreasing C/O molar ratio from 2.25 to 1.125, leads to 18.6% conversion increase. However, the conversion increase is 9% for decrease in C/O ratio from 1.125 to 0.75. The increase in the O_2 amount favors the total oxidation of glycerol which increases the CO_2 selectivity and the yield.

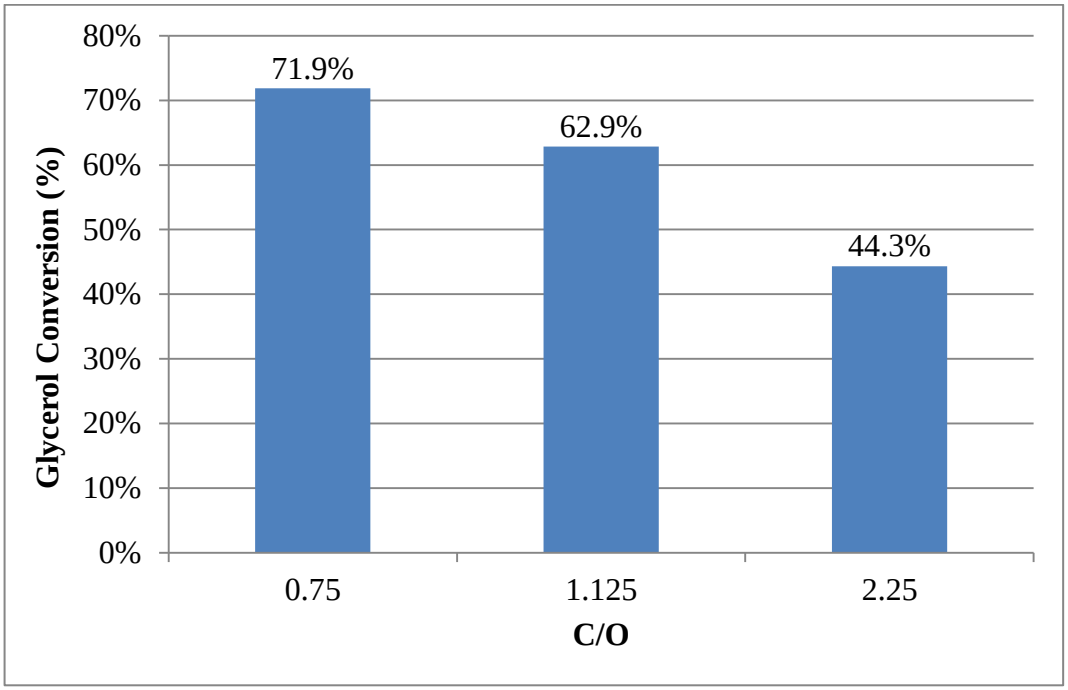

Figure 4.37. Glycerol Conversion vs C/O Ratio for OGSR and GSR (S/C = 5, T = 550 °C, Total flow = 96 NmL min^{-1}).

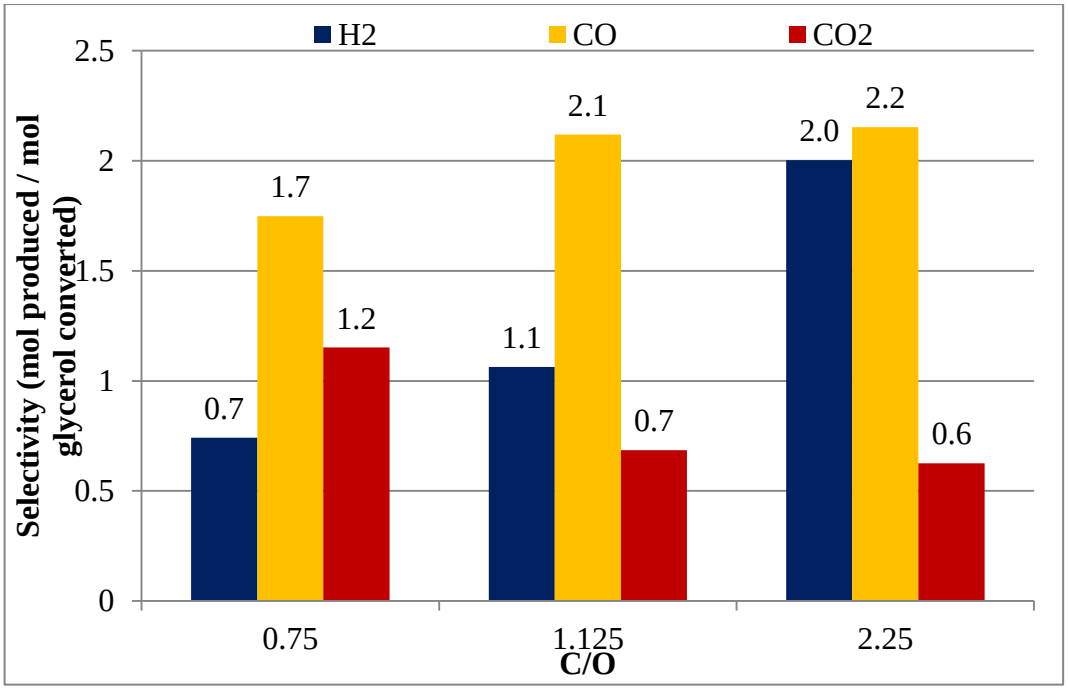

Figure 4.38. H_2, CO, and CO_2 Selectivity vs C/O Ratio for OGSR and GSR (S/C = 5, T = 550 °C, Total flow = 96 NmL min^{-1}).

H_2, CO, and CO_2 selectivities are given as a function of C/O molar ratio in Figure 4.38. H_2 and CO selectivities increase as the molar ratio of C/O increases, whereas CO_2 selectivity decreases at higher C/O molar ratios. In order to make a correct analysis of these trends, the yields are also given in Table 4.2. It is clearly seen that H_2 yield increases whereas CO_2 yield decreases according to increase in C/O molar ratio. Based on Reaction 2.13, the increase in O_2 content means a decrease in the parameter "x" appearing in a function as stoichiometric coefficient for O_2. This directly indicates that the coefficients in product side are affected in such a way that the coefficient of CO_2 increases. Additionally, increasing O_2 content favors the total oxidation of glycerol. There remains less glycerol for steam reforming reaction, and this decreases the H_2 yield and selectivity.

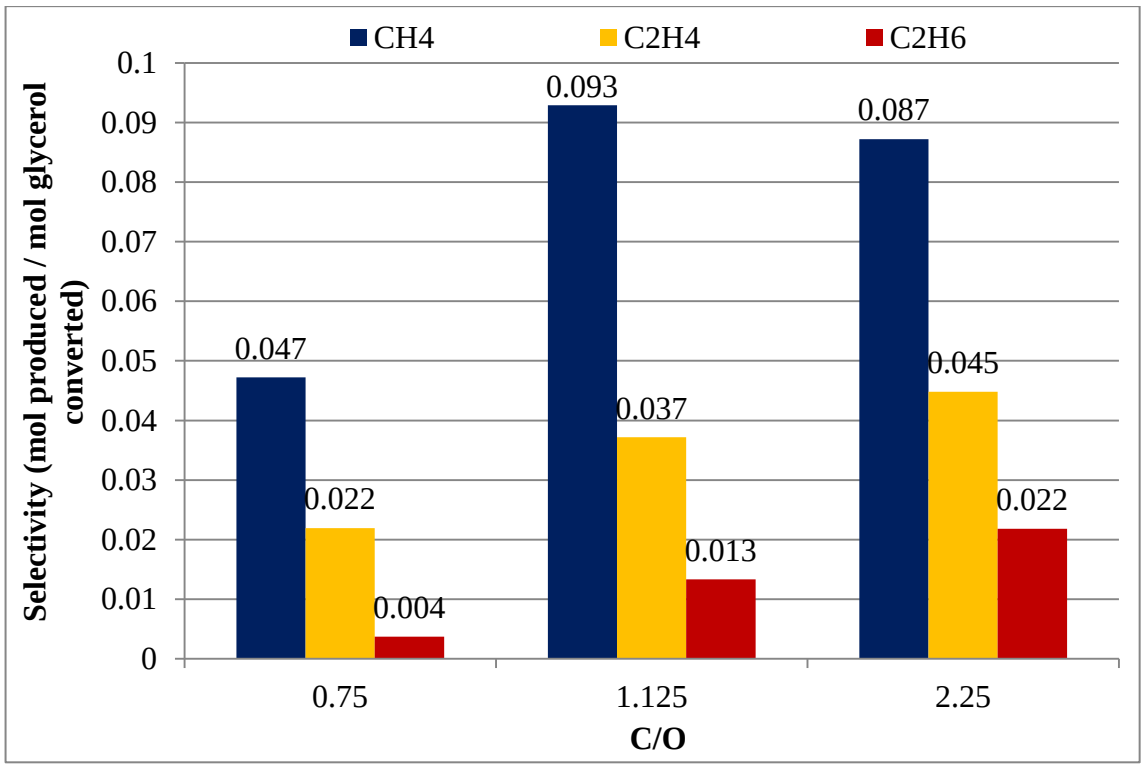

Figure 4.39. CH_4, C_2H_4, and C_2H_6 Selectivity vs C/O Ratio for OGSR and GSR (S/C = 5, T = 550 °C, Total flow = 96 NmL min^{-1}).

The changes in hydrocarbon selectivities according to C/O molar ratio are given in Figure 4.39. Increasing the O_2 content in the system leads to decrease in the selectivities of hydrocarbons. Moreover, in general, the hydrocarbon yields are decreasing as C/O molar ratio decreases. These results can be explained by the total oxidation mechanism occurring

also for these hydrocarbons. The produced CO_2 from total oxidation of these products leads further increase in CO_2 selectivity and yield.

Table 4.2. Gaseous product yields in OGSR at three C/O molar ratios.

	Product Yields (mol product/mol glycerol fed)					
C/O	**H_2**	**CH_4**	**CO**	**CO_2**	**C_2H_4**	**C_2H_6**
0.75	0.533	0.034	1.257	0.828	0.016	0.003
1.125	0.668	0.058	1.332	0.431	0.023	0.008
2.25	0.888	0.039	0.954	0.277	0.020	0.010

4.2.3. Blank Tests for OGSR

The main part of this study is the GSR tests. In GSR tests, blank tests are conducted and it is concluded that the material of construction of housing and plate are not inert towards the reactants. Additionally, introducing O_2 to the system leads to higher conversions. As a result, it is required to see the activity of housing and plate for OGSR tests. Blank tests for OGSR are done at three temperatures (500, 550, and 600 °C), and the reported parameters are glycerol conversion, selectivity and yields of the products.

Glycerol conversion with respect to temperature in OGSR and blank tests are given in Figure 4.40. It is seen that, at each temperature, blank tests result in higher conversions than the catalytic reactions. The main reason of the difference in conversions can be explained by the increase of carbon containing products yields except for CO_2 as given in Table 4.3. Moreover, partial oxidation mechanism is likely to take place even if there is no catalyst in the system.

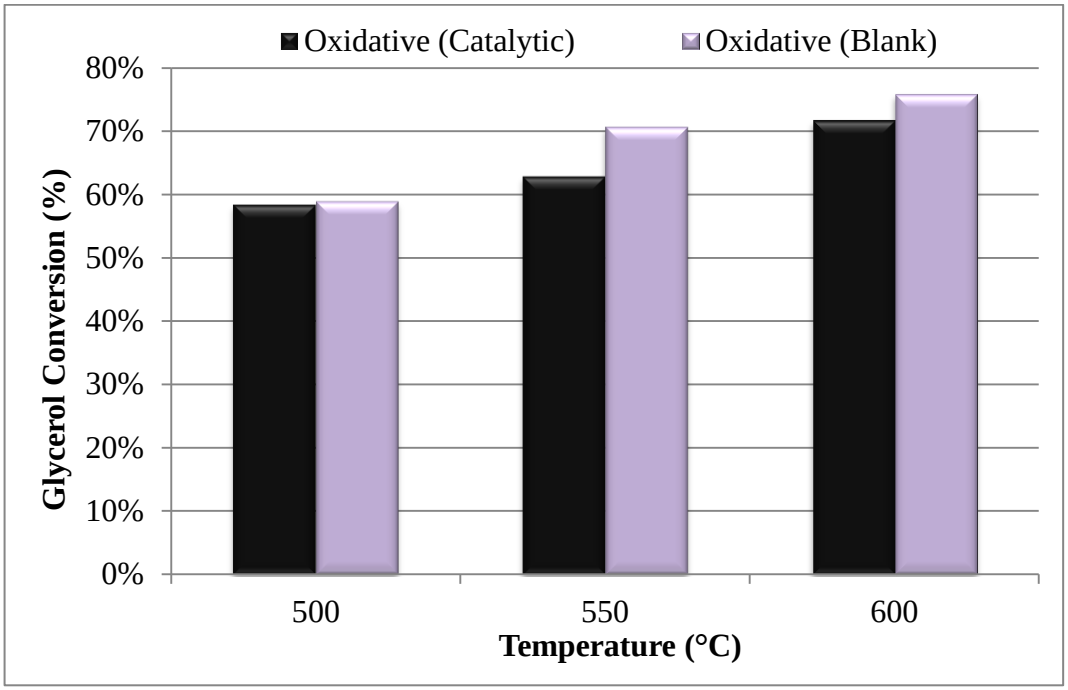

Figure 4.40. Glycerol Conversion vs Temperature for OGSR and Blank Tests (S/C = 5, C/O = 1.125, Total flow = 96 NmL min^{-1}).

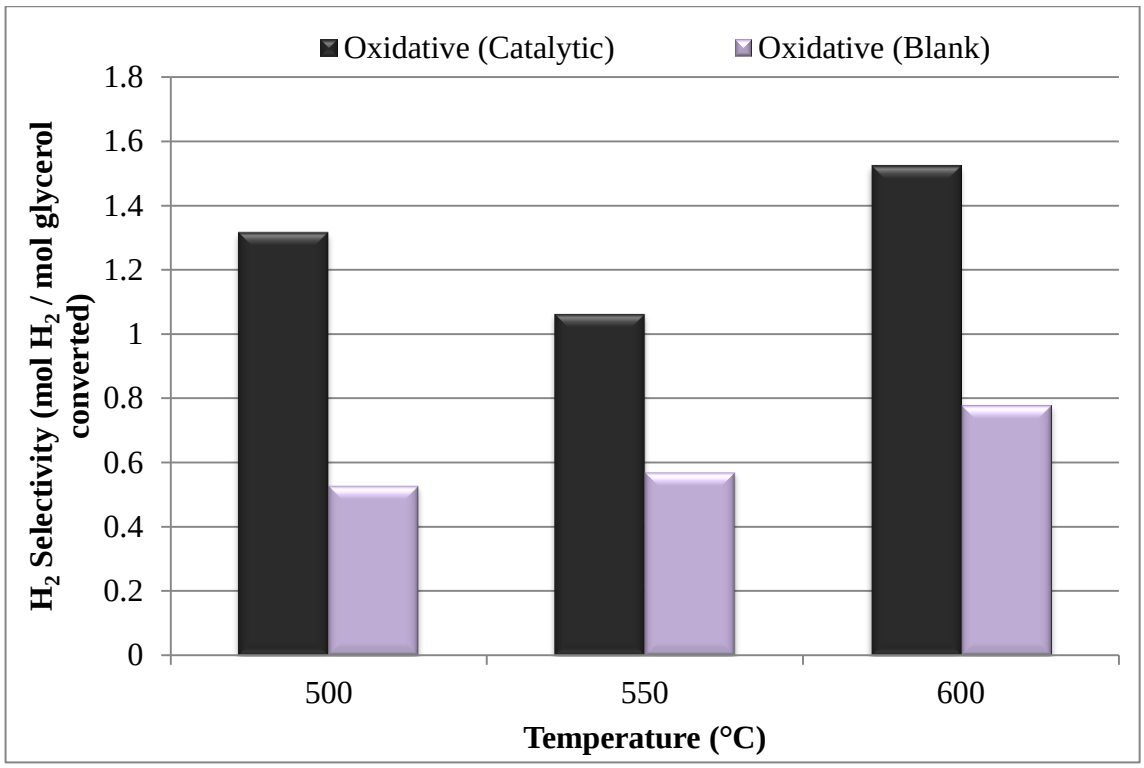

Figure 4.41. H_2 Selectivity vs Temperature for OGSR and Blank Tests (S/C = 5, C/O = 1.125, Total flow = 96 NmL min^{-1}).

The main objective of this study is to produce H_2. In GSR tests, it is seen that housing and plate also lead to an activity of producing H_2. This is also valid for the blank test conducted for OGSR. H_2 selectivity is a clear indication of catalytic activity. This selectivity over catalyst and uncoated plate for OGSR tests is given in Figure 4.41. The selectivities obtained over catalytic surface are higher than the selectivity in blank tests. Moreover, H_2 yield caused from catalytic activity is almost twice higher than the yield in blank tests. The reason of the catalytic activity over housing surface is explained as the presence of Ni metal in construction of stainless steel housing.

CO and CO_2 selectivities are given in Figure 4.42 based on the reaction temperature. CO selectivity over catalytic surface is lower than the blank experiments. On the other hand, CO_2 selectivity increases as a result of catalytic activity. This may be explained by water gas shift reaction which takes place on the catalyst surface. This reaction leads to decrease in CO amount while increasing the CO_2 and H_2 amounts.

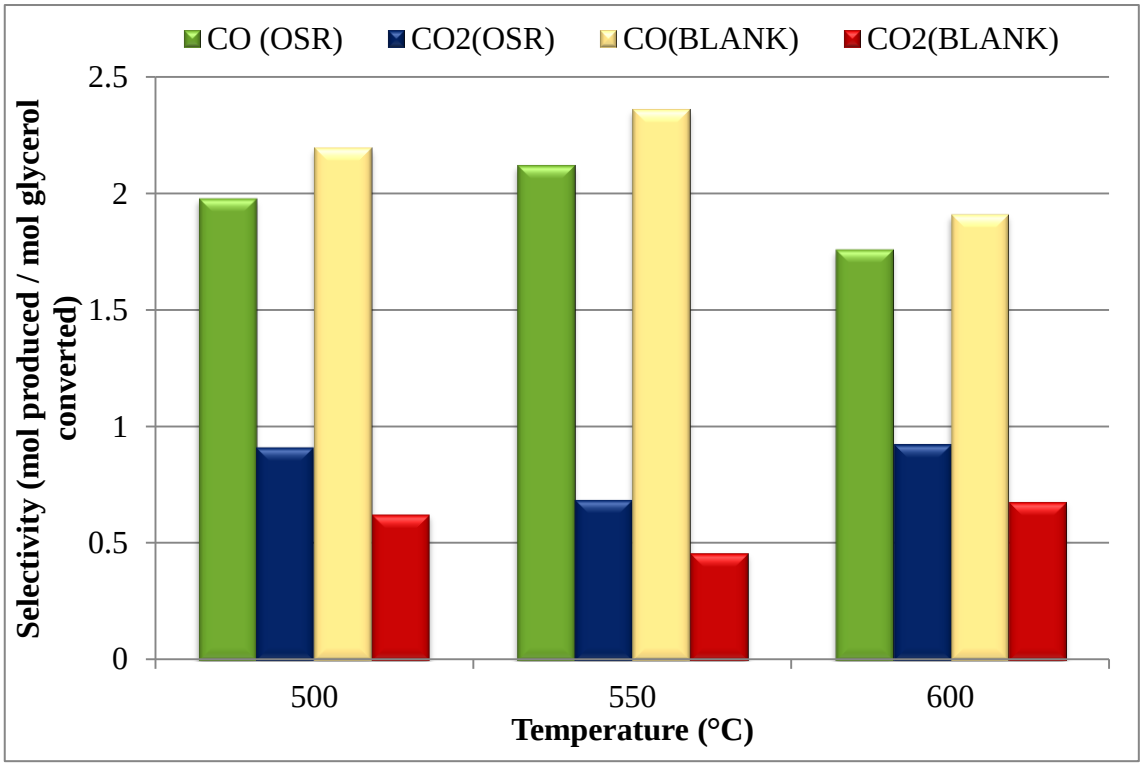

Figure 4.42. CO and CO_2 Selectivities vs Temperature for OGSR and Blank Tests (S/C = 5, C/O = 1.125, Total flow = 96 NmL min^{-1}).

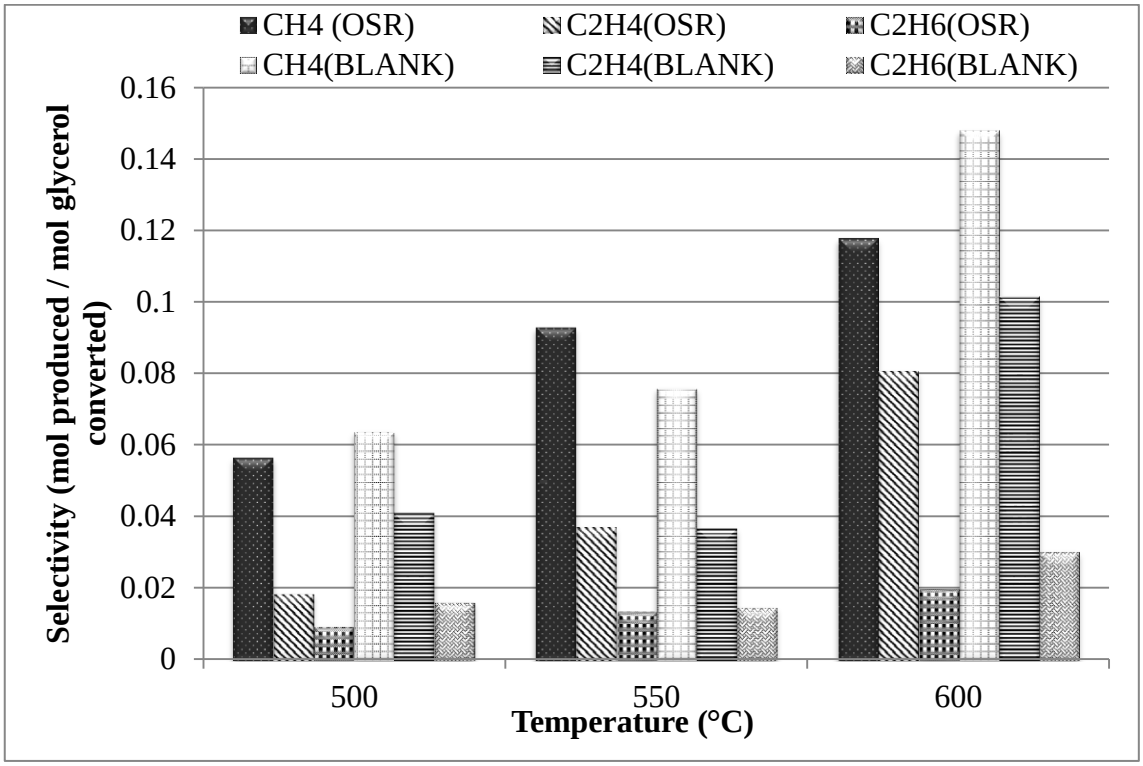

Figure 4.43. CH_4, C_2H_4, and C_2H_6 Selectivities vs Temperature for OGSR and Blank Tests (S/C = 5, C/O = 1.125, Total flow = 96 NmL min^{-1}).

The selectivities of hydrocarbons are presented as a function of temperature in Figure 4.43. The main conclusion from the figure is that catalytic activity leads to decrease in hydrocarbon selectivities. Higher conversions in blank tests are mainly stems from this trend. Moreover, the yields of these hydrocarbons are given in Table 4.3, and they are higher in the absence of catalyst.

Table 4.3. Gaseous product yields in OGSR and blank tests at three temperature.

		Product Yields (mol product/mol glycerol fed)					
	T(°C)	**H_2**	**CH_4**	**CO**	**CO_2**	**C_2H_4**	**C_2H_6**
Oxidative Steam Reforming	500	0.770	0.033	1.155	0.531	0.011	0.005
	550	0.668	0.058	1.332	0.431	0.023	0.008
	600	1.094	0.084	1.261	0.661	0.058	0.014
Blank Tests	500	0.311	0.038	1.295	0.367	0.024	0.009
	550	0.403	0.054	1.669	0.324	0.026	0.010
	600	0.591	0.112	1.450	0.513	0.077	0.023

Blank tests for OGSR reactions give higher conversions and lower H_2 yield and selectivity compared to catalytic OGSR tests. The reasons for these are attributed to the decomposition of glycerol to hydrocarbons and partial oxidation of glycerol to produce H_2 over housing. In order to support these reasons, a blank test is conducted at 600 °C without housing and plate. It contains only the quartz wools. The obtained glycerol conversion is given in Figure 4.44. It is seen that the conversions are increased to 79% at which there is only quartz wool in the system. The reason of higher conversions is the increase in carbon containing products yields. The yield values are given in Table 4.4. From this figure, it is again proposed that decomposition of glycerol at this occurs.

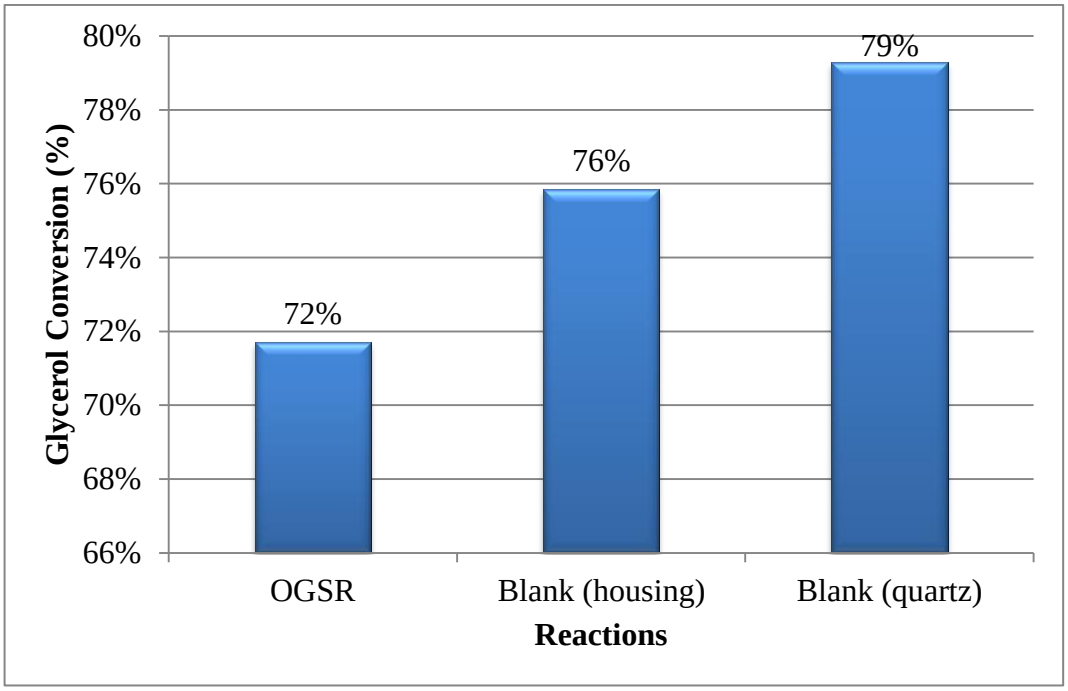

Figure 4.44. Glycerol Conversion vs Temperature for OGSR and Blank Tests (T = 600 °C, S/C = 5, C/O = 1.125, Total flow = 96 NmL min^{-1}).

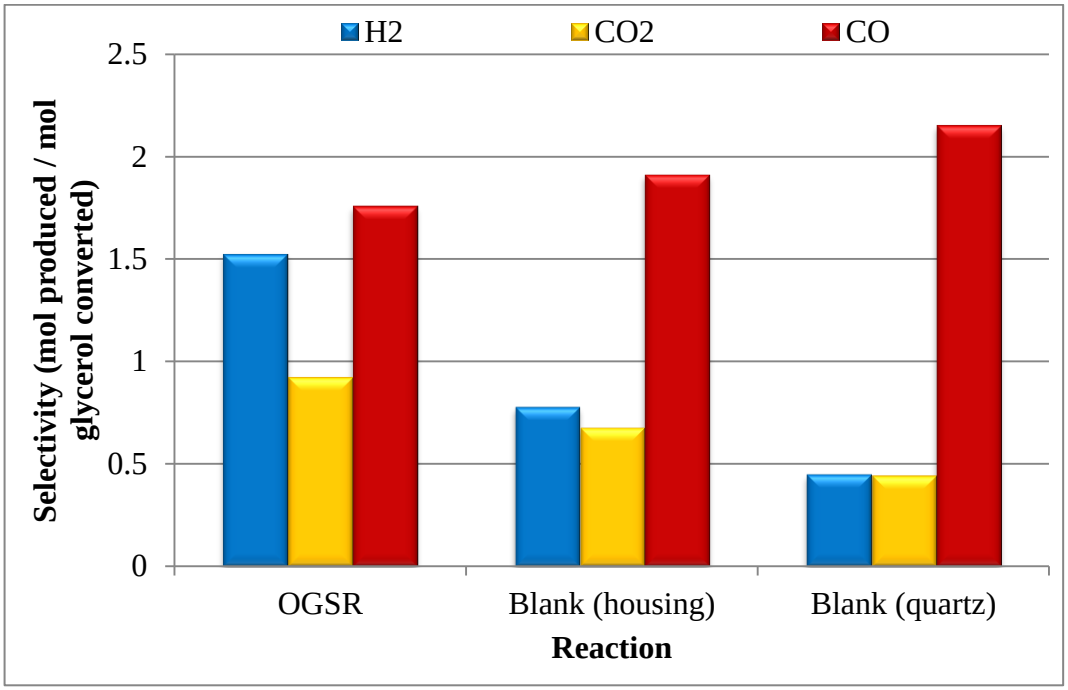

Figure 4.45. H_2, CO_2 and CO Selectivities vs Temperature for OGSR and Blank Tests (T = 600 °C, S/C = 5, C/O = 1.125, Total flow = 96 NmL min^{-1}).

H_2, CO, and CO_2 selectivities for the reactions OGSR, blank with housing and plate and blank with only quartz wool are given in Figure 4.45. H_2 selectivity is a clear sign of catalyst activity, and based on Figure 4.45, the selectivity decreases as 1.52, 0.78 and 0.45 corresponding to catalytic OGSR, blank with housing and blank with quartz wool. Moreover, H_2 yield is given in Table 4.4 and varies as 1.094, 0.591 and 0.357 based on catalytic OGSR, blank with housing and blank with quartz wool, respectively. CO selectivity is decreasing while the CO_2 selectivity is increasing according to blank test activity. WGS reaction occurs over catalytic surface, and that is why less amount of CO appears in catalytic OGSR compared to blank tests. The difference between two blank tests can be explained by the presence of Ni in the construction of housing. Activity appearing for blank tests with quartz is attributed to partial oxidation of glycerol to produce hydrogen and conversion increase indicates thermal decomposition of glycerol.

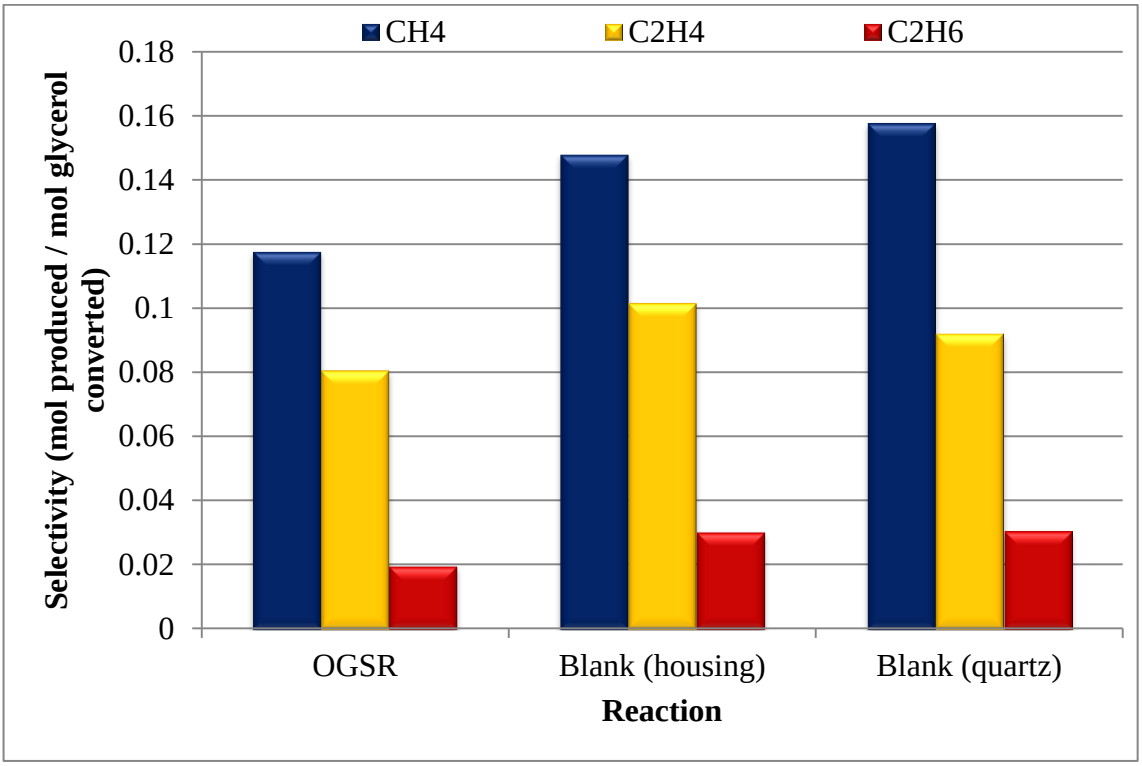

Figure 4.46. CH_4, C_2H_4, and C_2H_6 Selectivities vs Temperature for OGSR and Blank Tests (T = 600 °C, S/C = 5, C/O = 1.125, Total flow = 96 NmL min^{-1}).

Selectivity of produced hydrocarbons is given in Figure 4.46 according to catalytic OGSR, blank with housing and blank with quartz wool. From the figure, it is seen that catalytic activity leads to reduction in hydrocarbon selectivity. Yields of these hydrocarbons are given in Table 4.4, and yields are decreasing according to catalytic activity.

Table 4.4. Gaseous product yields in OGSR and blank tests (T = 600 °C, S/C = 5, C/O = 1.125, Total flow = 96 NmL min^{-1}).

	Product Yields (mol product/mol glycerol fed)					
Reactions	**H_2**	**CH_4**	**CO**	**CO_2**	**C_2H_4**	**C_2H_6**
OGSR	1.094	0.084	1.261	0.661	0.058	0.014
Blank (Housing)	0.591	0.112	1.450	0.513	0.077	0.023
Blank (Quartz)	0.357	0.125	1.706	0.352	0.073	0.024

4.3. Catalyst Characterization

Catalyst characterizations of reduced and spent 5 wt.% Ni/Al_2O_3 and 10 wt.% Ni/Al_2O_3 catalysts are performed by scanning electron microscopy (SEM) and energy dispersive X-ray spectroscopy (EDX) analyses. Mappings of the active species are given to represent the dispersion over the support surface. In order to understand the effect of temperature and S/C ratio on formation of carbon over the surface, ten samples of catalysts are analyzed by SEM and EDX. Comparative study is made in the following tables and figures using the visual and quantitative results of SEM and EDX analysis.

When beams of electrons are sent to sample surface, larger atoms scatters more electrons and they seem as lighter spots. The smaller atoms scatter fewer electrons, and their colors are observed as darker. In this study, investigated active metal is Ni and its atomic diameter is not so large than Al or O, and that is why it is hard to obtain clear images of Ni particles, especially in 5 wt.% Ni/Al_2O_3 samples. For the case of carbon formation over the surface, the Ni particle becomes more visible. It is worth noting that alumina is not a suitable material for SEM imaging and therefore the images have low resolutions. Figure 4.47 gives mapping diagrams of Ni over reduced 5 wt.% Ni/Al_2O_3 and 10 wt.% Ni/Al_2O_3 catalysts. Both Ni maps indicate well dispersion of active metal over the surface.

5 wt.% Ni/Al_2O_3 (Reduced)

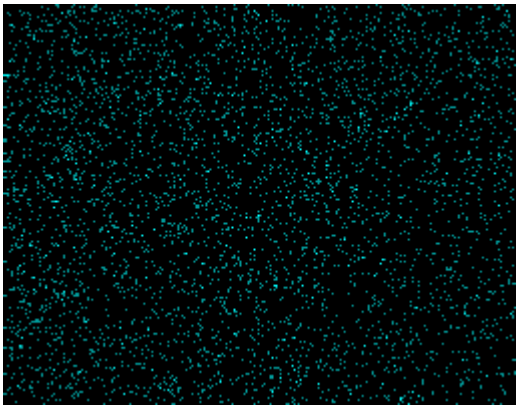

10 wt.% Ni/Al_2O_3 (Reduced)

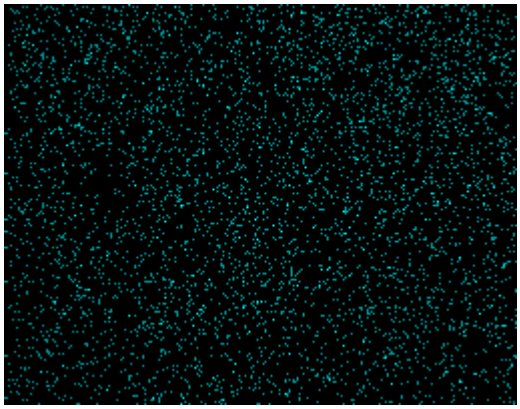

Figure 4.47. Mapping Diagrams of Reduced Catalysts.

Reduced 5 wt.% Ni/Al_2O_3 catalyst does not give clear SEM images, but in the presence of the coke, the Ni atoms become more visible. In order to represent homogenous

dispersion of Ni over 5 wt.% Ni/Al_2O_3 catalyst, SEM images of spent catalyst when S/C ratio of 4 are taken. Figure 4.48 gives SEM images at 50000 and 20000 magnitudes and well dispersion of active metal is observed.

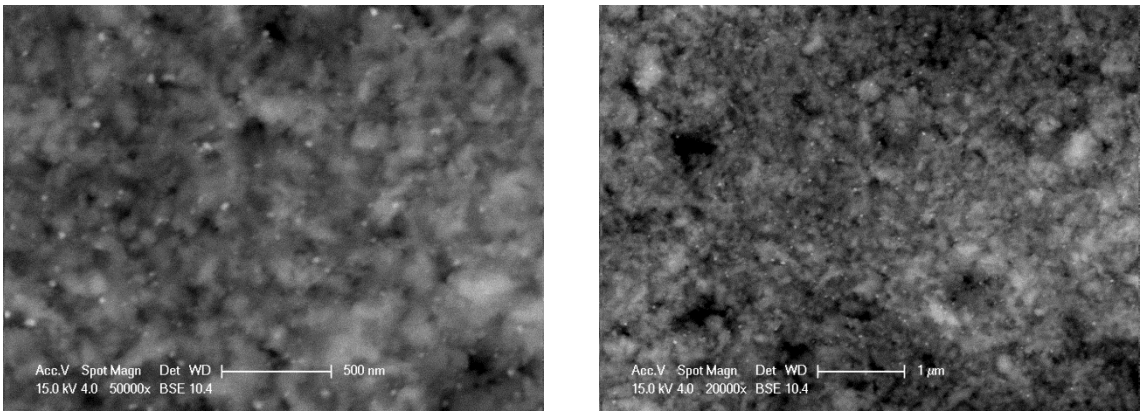

Figure 4.48. SEM Images of 5 wt.% Ni/Al_2O_3 Spent Catalysts at S/C Molar Ratio of 4 in Different Magnitudes.

Table 4.5 shows results of EDX analysis of reduced catalysts. EDX analysis is conducted to measure the amount (weight per cent) of Ni at Al_2O_3 surface. The targeted Ni weight percentages are 5 and 10 in this study. For reduced 5 wt.% Ni/Al_2O_3 catalyst, three random points are investigated and average mass percentages of Al, O, and Ni are determined. Average weight percentage for Ni is measured as 6.88% which is acceptable to represent the targeted weight percentage in the catalyst. Additionally, two random points of reduced 10 wt.% Ni/Al_2O_3 sample are analyzed for element percentages. Ni weight percentage is measured as 11.59% which is close to the targeted value.

Table 4.5. EDX analysis of reduced 5 wt.% Ni/Al_2O_3 and 10 wt.% Ni/Al_2O_3 catalysts.

	5 wt.% Ni/Al_2O_3 (Reduced)				10 wt.% Ni/Al_2O_3 (Reduced)		
wt.%	Point 1	Point 2	Point 3	Average	Point 1	Point 2	Average
O	27.50	32.35	31.72	30.52	26.37	31.61	28.99
Al	65.62	60.43	61.73	62.59	62.01	56.63	59.32
Ni	6.88	7.22	6.55	**6.88**	11.62	11.56	**11.59**

In catalytic reactions for GSR, the S/C ratio is one of the investigated parameters, and it is seen that increase in steam content causing the active phase sintering. The SEM images for reduced 10 wt.% Ni/Al_2O_3 and spent 10 wt.% Ni/Al_2O_3 samples at S/C ratio of 5 and 6 are given in Figure 4.49. Based on the SEM images, at S/C molar ratio of 6, the active metals are agglomerating and this leads to decrease in active metal sites. The decrease in active metal sites results in lower conversions of glycerol (Figure 4.10).

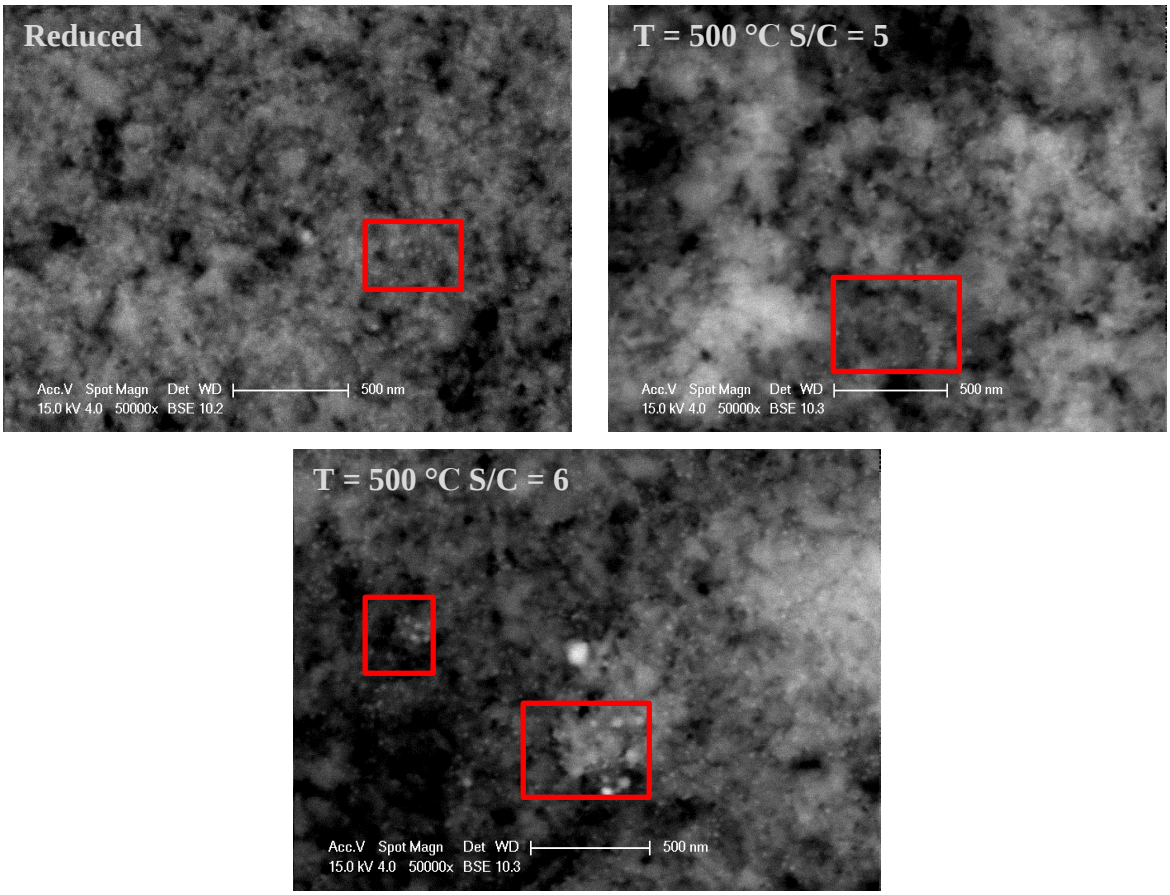

Figure 4.49. SEM Images of 10 wt.% Ni/Al_2O_3 Spent Catalysts with respect to S/C Ratio.

Mapping diagrams of active metal Ni for reduced 5 wt.% Ni/Al_2O_3 and spent 5 wt.% Ni/Al_2O_3 samples at S/C ratio of 4 and 6 are given in Figure 4.50. It can be observed that the particle density gets smaller in the case of spent catalyst at S/C ratio of 6. There are more blank empty spaces for spent catalyst sample at S/C molar ratio of 6. This is also an indication of active metal agglomeration, which is responsible for conversion decrease in GSR tests (Figure 4.10).

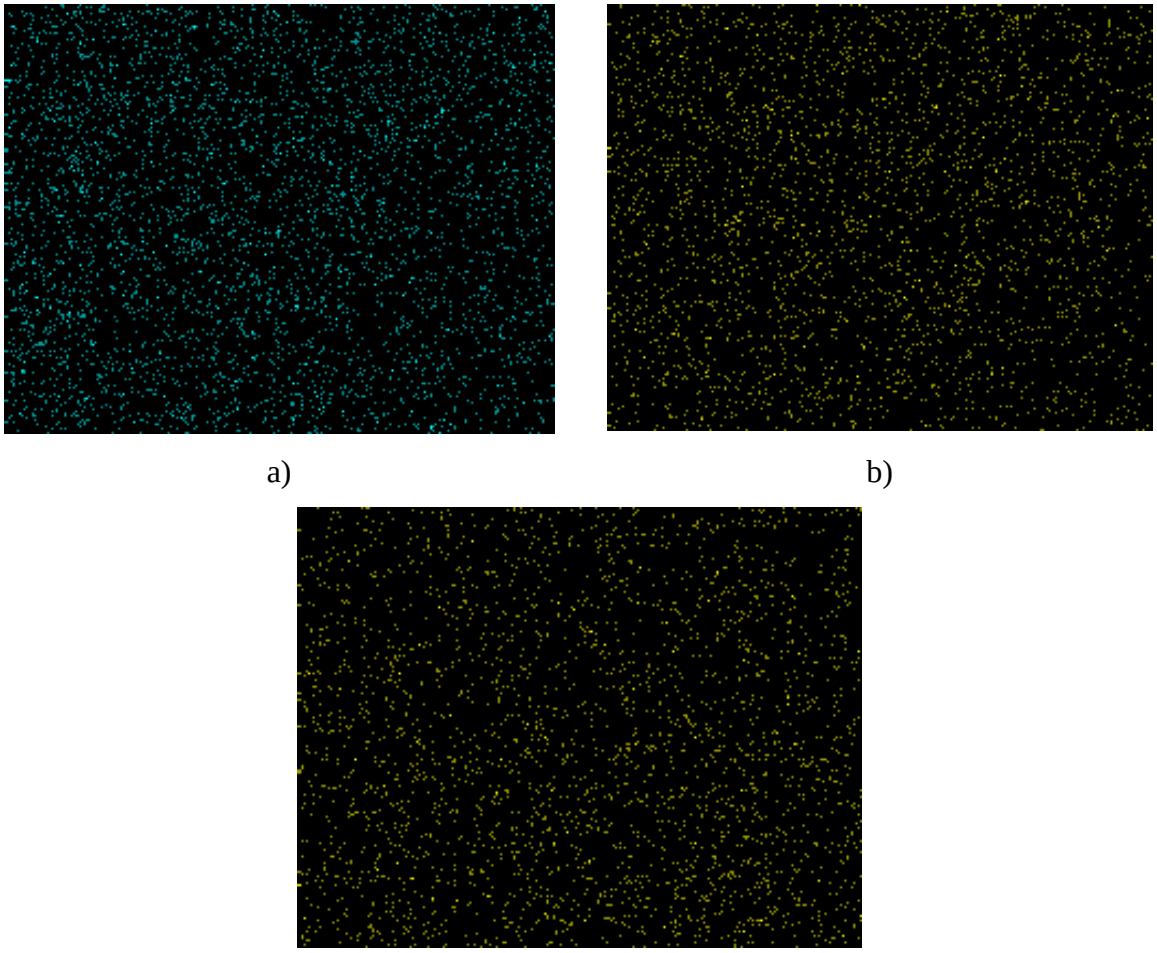

a) b)

c)

Figure 4.50. Mapping Diagrams of 5 wt.% Ni/Al_2O_3 Catalyst a) Reduced 5 wt.% Ni/Al_2O_3 Catalyst b) Spent Catalyst at S/C = 4 c) Spent Catalyst at S/C = 6.

The effect of temperature over the surface structure is also investigated over spent 5 wt.% Ni/Al_2O_3 catalyst. Figure 4.51 gives two SEM images of spent catalyst 475 °C and 550 °C. Images are given at 20000 magnitude, and it is seen that temperature increase leads to sintering of catalyst. Sizes of Ni particles are larger at 550 °C compared to sizes at 475 °C.

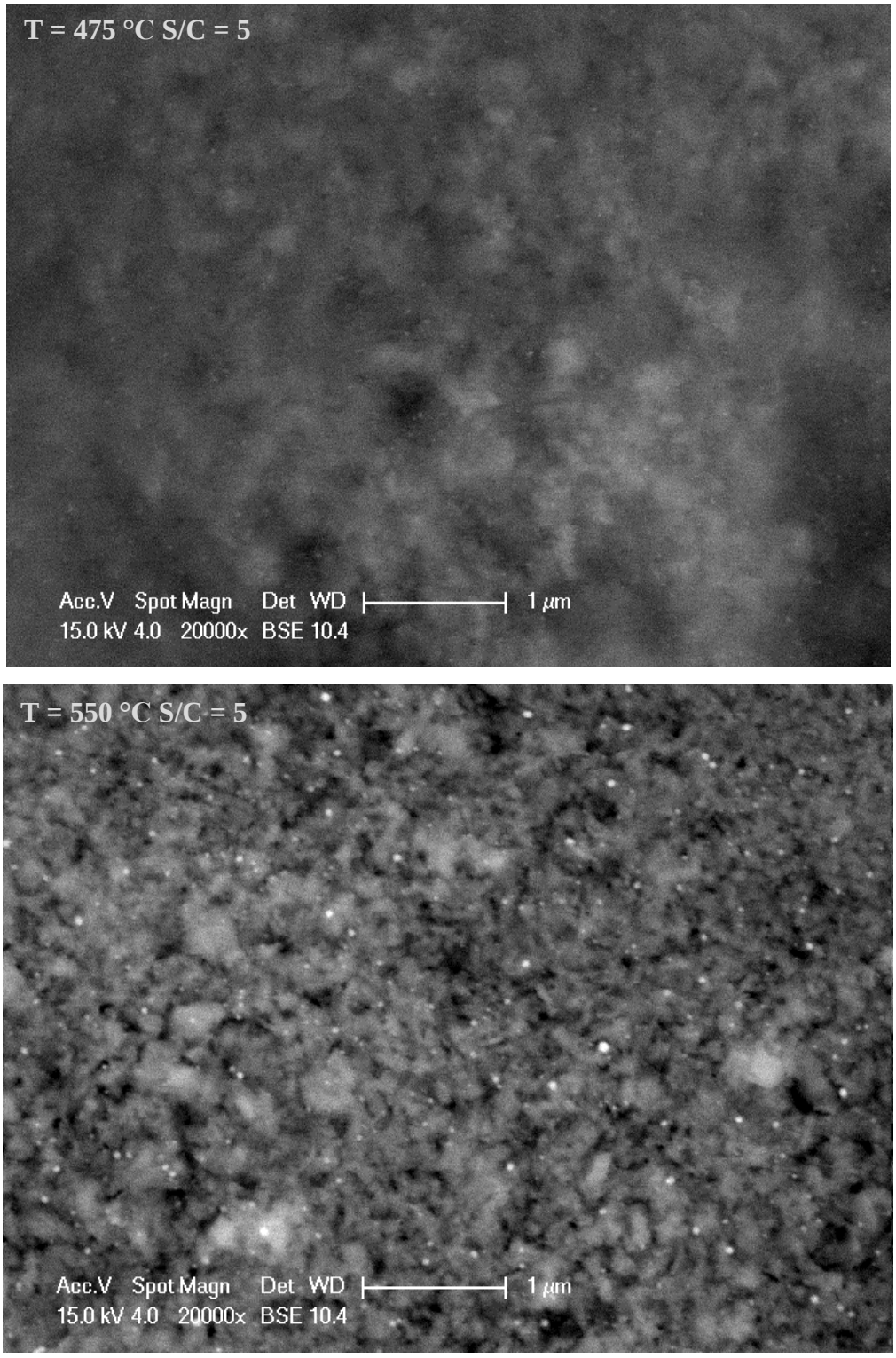

Figure 4.51. SEM Images of Spent 5 wt.% Ni/Al_2O_3 Catalyst at 475 °C and 550 °C.

Coke formation is an inevitable result of GSR and OGSR tests for all parameters investigated. However, carbon deposition over the surface is not uniform as given in Figure 4.52. More carbon deposition is observed at the entry region of the plate and then

the amount of observable carbon deposition over catalyst surface decreases while moving the plate towards the end. Thermal decomposition of glycerol is taking place inside the quartz tube, and the produced carbon first collects at the entrance of plate.

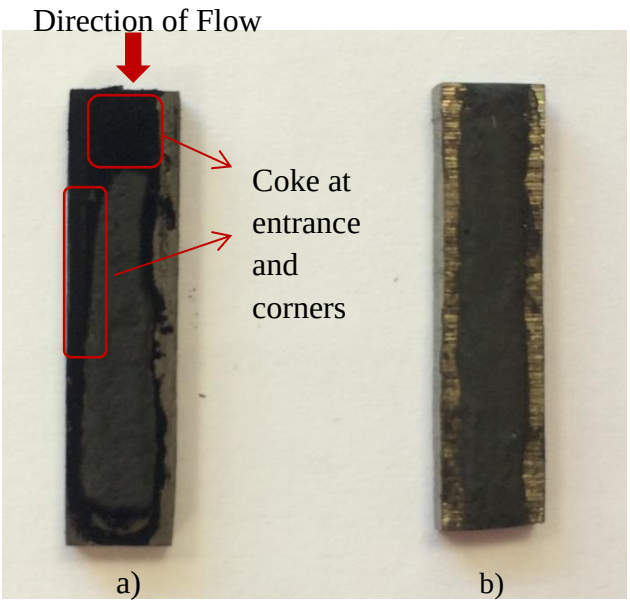

Figure 4.52. Catalyst-Coated Microchannel Plates with 10 wt.% Ni/Al_2O_3 catalysts a. Typical Spent Ni Catalyst (T = 550 °C, S/C = 5) b. Reduced Ni Catalyst.

SEM image in the Figure 4.53 is taken in lowest possible magnitude in order to show carbon layer over the catalyst surface. In the SEM image, it is decided that formed carbon over the surface cracks and leads to deformation of the coated surface.

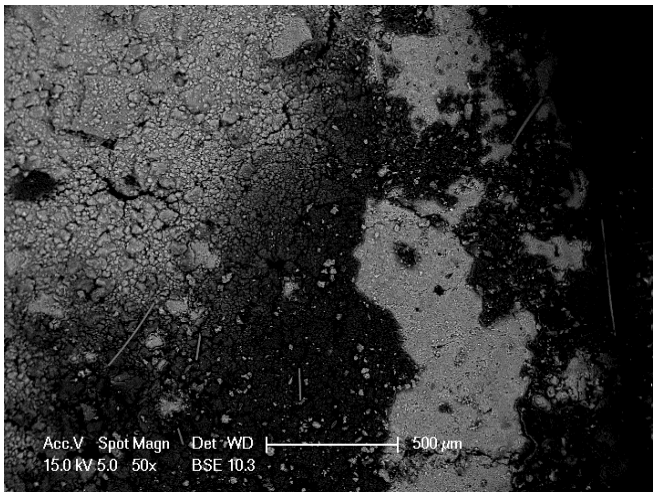

Figure 4.53. Carbon Formation over Spent 5 wt.% Ni/Al_2O_3 (T = 550 °C, S/C = 5).

EDX analyses of catalysts are made to determine the carbon formation over the surface. Table 4.6 gives EDX and SEM analysis of the spent 5 wt.% Ni/Al_2O_3 catalysts at 475 °C and 550 °C. Darker grays represent the coke over the surface. The results indicate that carbon formation increases as temperature increases.

Table 4.6. Coke formation over spent 5 wt.% Ni/Al_2O_3 catalyst with temperature.

wt.%	**EDX**	**SEM Image**
C	23.48	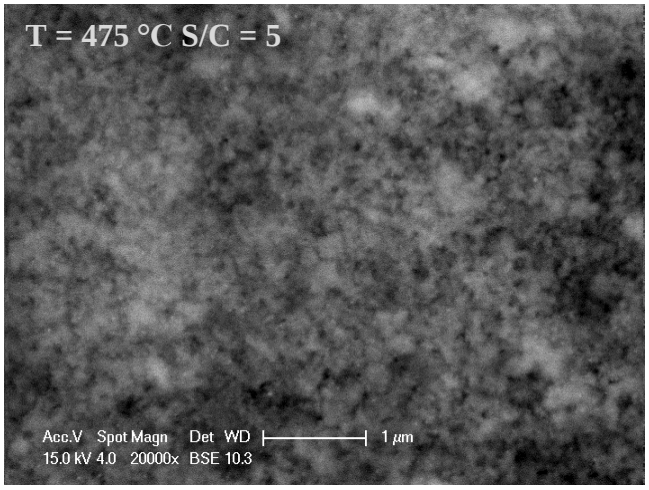
O	21.34	
Al	50.07	
Ni	5.11	
wt.%	**EDX**	
C	55.00	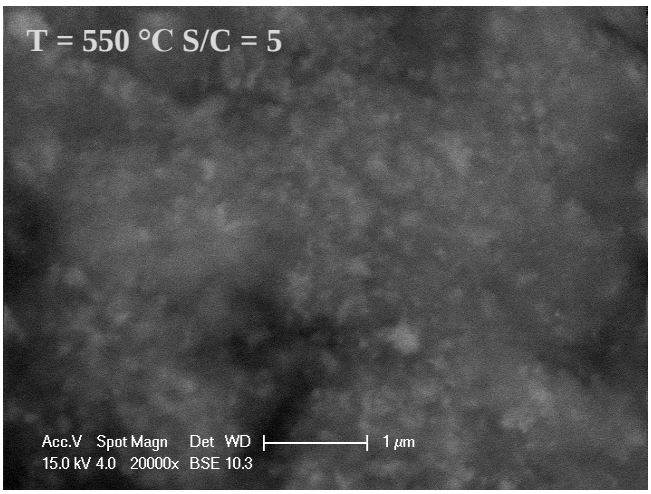
O	3.87	
Al	36.34	
Ni	4.78	

Effect of steam on carbon formation is given in Table 4.7 for spent 10 wt.% Ni/Al_2O_3 catalyst at S/C ratios of 5 and 6. It is seen that the coke formation is decreasing as steam increases in the system.

Table 4.7. Coke formation over spent 10 wt.% Ni/Al_2O_3 catalyst with S/C Molar Ratio.

wt.%	**EDX**	**SEM Image**
C	7.07	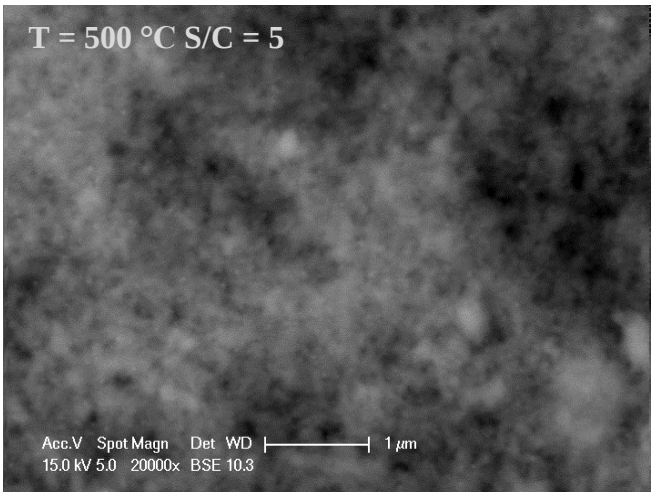
O	29.79	
Al	53.94	
Ni	9.19	
wt.%	**EDX**	
C	2.58	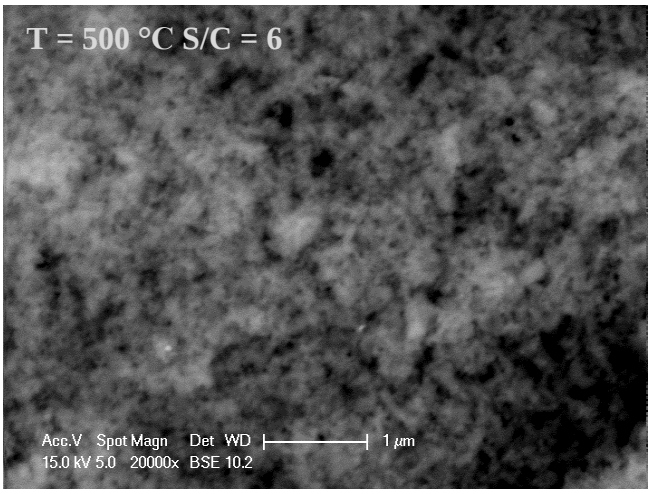
O	29.59	
Al	57.30	
Ni	10.53	

5. CONCLUSIONS AND RECOMMENDATIONS

In this study, two reactions - glycerol steam reforming and oxidative glycerol steam reforming – are studied separately. Responses of these reactions against changes in a number of operating conditions are investigated. The main conclusions from these reactions are given below.

5.1. Conclusions from Glycerol Steam Reforming

Glycerol steam reforming is studied over 5 wt.% Ni/Al_2O_3 and 10 wt.% Ni/Al_2O_3 catalysts. The investigated parameters in this study are active metal loading, temperature, S/C molar ratio, total feed flow rate, and the reactor configuration. Temperature effect is studied at 6 different temperature levels between 425 °C and 600 °C. S/C molar ratio is changed as 3, 4, 5, and 6. Four different total flow rates (64, 96, 128, and 160 Nml/min) and two reactor configurations (packed or coated microchannel) are the other parameters that are investigated. Glycerol conversion, product selectivity and yield are the calculated parameters. Major conclusions those are drawn from these investigations are given as follows:

- Blank tests show activity for glycerol steam reforming, and it is determined that stainless steel housing and FeCrAlY plate are not inert to reactants and responsible for the catalytic activity. This is probably stemmed from the Ni content present in reactor components.
- Metal loading (5 wt.% Ni or 10 wt.% Ni) does not have a considerable effect on glycerol conversion and on product distributions.
- Temperature is a key parameter for glycerol steam reforming. Glycerol conversions are less than 2% at temperatures below 500 °C. It sharply increases over 500 °C reaching ca. 20% at 600 °C.
- 475 °C is a specific point for product selectivities. This temperature level implies local maximum or minimum for product selectivities. For instance, maximum H_2 selectivity and minimum CH_4 selectivity are obtained at 475 °C. Further increase in the temperature leads to decrease in H_2 selectivity for both catalysts. The decrease in

H_2 selectivity stems from increase in glycerol conversion. However, the H_2 yield continuously increases with temperature.

- CO selectivity over both catalyst increases with temperature, but it decreases in blank tests as temperature increases.
- Selectivities of hydrocarbons (CH_4, C_2H_4 and C_2H_6) increase sharply at high temperatures. Alumina is considered to boost side reactions such as dehydration, dehydrogenation and CO-removal due to its acidic character.
- Glycerol conversions at 500 °C increase as S/C ratio is changed from 3 to 5. Maximum conversion is obtained at S/C ratio of 5 for both catalysts. At higher S/C ratios, conversions decrease.
- Increase in S/C ratio leads to increase in H_2 selectivity at 500 °C and 600°C. The lowest CO selectivity at 500 °C is obtained at S/C ratio of 5.
- Steam helps in carbon removal from the surface. However, it also leads to active phase sintering. These are affecting product distributions.
- Decreasing flow rate means increasing the residence time. Lower flow rates favor higher glycerol conversions. Conversion increases exponentially as flow rate decreases. Conversion converges to a level as the flow rate is increased.
- H_2 selectivity and yield increased with respect to decrease in total flow rate. CO selectivity shows the similar trend.
- Coated microchannel configuration shows higher glycerol conversion compared to packed microchannel reactor configuration. This is most probably caused from better heat transfer rates that are expected to exist in coated microchannel.
- H_2 and CO_2 selectivities are higher in coated microchannel configuration, but CO selectivity is higher in packed microchannel configuration.
- After all experimental tests, the plates are examined and for all reaction tests as well as for blank tests, coke formation is inevitable. At higher temperatures, coke formation becomes more severe.

5.2. Conclusions from Oxidative Glycerol Steam Reforming

Oxidative steam reforming reactions are performed over 5 wt.% Ni/Al_2O_3 catalyst in coated microchannel configuration. Temperature and C/O molar ratio are investigated parameters while molar ratio of S/C and total flow rate are kept constant at 5 and 96

Nml/min, respectively. Blank tests are also conducted to state catalytic activity. Major conclusions drawn from these investigations are given as follow:

- There temperatures (500, 550, and 600 °C) are investigated. Glycerol conversion in OGSR increases with temperature. However, the differential increments are also increasing with temperature. A 4.5% increase in glycerol conversion is observed for the increase in temperature from 500 to 550 °C, whereas the increase is 8.8% when temperature is increased from 550 to 600 °C.
- Glycerol conversion in OGSR is higher than those observed in GSR at each temperature levels as a result of O_2 presence at the reaction medium.
- H_2 selectivity is higher in OGSR. However, the difference in the selectivities obtained from OGSR and GSR diminishes with temperature. Selectivity in OGSR is lower because conversions are high compared to GSR. H_2 yields in OGSR are approximately two times higher than the yields of GSR tests at each temperature.
- At lower temperatures (500 and 550 °C), CO_2 selectivity is lower in OGSR. However, at 600 °C, CO_2 selectivity is higher in OGSR compared with those observed in GSR.
- At each temperature, CO selectivity is higher in OGSR, but the difference between selectivities decreases as temperature increases.
- Temperature increase leads to increase in hydrocarbon (CH_4, C_2H_4, and C_2H_6) selectivity which is the result of decomposition and oxidation of glycerol is higher at high temperatures.
- Selectivity calculation includes conversion at the denominator which affects the comparison between OGSR and GSR, and that is why the product yields are introduced. According to product yields, all product yields increase as oxygen is introduced to system. The biggest increase is observed in CO yield. H_2 yield is twice higher in OGSR than GSR.
- The effect of C/O molar ratio (0.75, 1.125 and 2.25) is the other investigated parameter while S/C ratio and total flow rate are kept constant at 5 and 96 Nml/min, respectively. Higher O_2 feeding to the system leads to higher glycerol conversions.
- Decrease in C/O molar ratio leads to decrease in H_2 and CO selectivities and increase in CO_2 selectivity. Increase in O_2 content favors the total oxidation rather than partial oxidation.

- Selectivity of hydrocarbons (CH_4, C_2H_4 and C_2H_6) decreases as C/O molar ratio decreases. This is the result of total oxidation reaction which is favored at high O_2 concentrations.
- H_2 yield decreases as C/O molar ratio decreases, whereas CO_2 yield considerably increases as O_2 flow rate increases.
- Blank tests for OGSR shows higher glycerol conversions than catalytic reactions for OGSR. H_2 selectivity in catalytic reactions is approximately twice higher than selectivity in blank tests. This is a clear indication of catalytic activity which leads to consumption of CO and production of CO_2 via water gas shift reaction. The amounts of hydrocarbons decrease as a result of the catalytic activity. Higher amount of hydrocarbons in blank tests are mainly result of glycerol decomposition and responsible for higher conversions.
- Coke formation is inevitable and observed for oxidative steam reforming tests over Ni-based catalyst. Moreover, coke is also formed in blank tests of OGSR. However, coking is found to be less severe than those observed in the GSR tests.

5.3. Conclusions from Catalyst Characterization

Catalyst characterization is performed via EDX and SEM analysis to observe the dispersion of active metal, elemental content in the catalyst and the carbon formation over the carbon surface. Mappings of active metal (Ni) are also given to have a visual representation of active metal dispersion. Main conclusions from these analyses are given as follows:

- SEM images and mappings show well and homogenous dispersion of Ni over the catalyst support.
- EDX analyses on reduced catalyst reveal that targeted Ni weight percentages are obtained. For 5 wt.% Ni/Al_2O_3 catalyst, the EDX analysis gives 6.88 weight percentage and for 10 wt.% Ni/Al_2O_3 catalyst, it gives 11.59 weight percentage.
- SEM images indicate that increase in steam content leads to active metal agglomeration. However, it is also seen that steam helps for the removal of carbon over the surface.
- Temperature increase from 475 °C to 550 °C leads to sintering of catalyst based on SEM images. Moreover, EDX and SEM images at the same point for two S/C ratio

are given in Table 4.7 which indicate that increase in steam removes carbon over the surface.

- In general, carbon formation over the plate is higher at the entrance and decreases as moving along the axial direction of the plate. This is explained as the formed carbon resulting from thermal decomposition of glycerol collects at the entrance.

5.4. Recommendations

There are some recommendations based on the results of the present study in order to improve some features of this study in the future works and these are given as follows:

- Liquid products and unreacted glycerol collected in cold traps can be analyzed using a GC/MS.
- Even if at oxidative steam reforming reactions, coke formation is inevitable over Ni-based catalyst, and to eliminate coke, catalysts of precious metals such as Rh can be introduced to reaction system.
- Higher S/C ratios for OGSR tests can be investigated to see its effect on coke elimination.
- Blank experiments in OGSR experiments show high conversions because thermal decomposition of glycerol. The OGSR reactions can be performed at lower temperature to see the catalytic activity caused from thermal decomposition of glycerol.
- Alumina is known as a support that causes side reactions, so another support that is thermally stable, has a decent surface area and easy to apply on microplates can be tried instead of alumina.

APPENDIX A: CALIBRATION OF MASS FLOW CONTROLLERS

Calibration curves of the Bronkhorst mass flow controllers used in the experiments are given below.

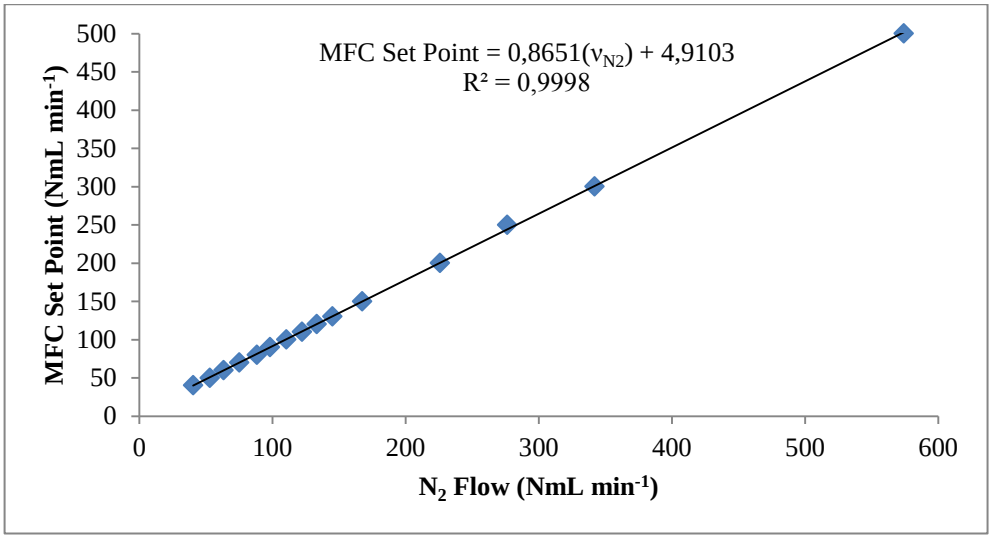

Figure A.1. Calibration Curve of the N_2 Mass Flow Controller.

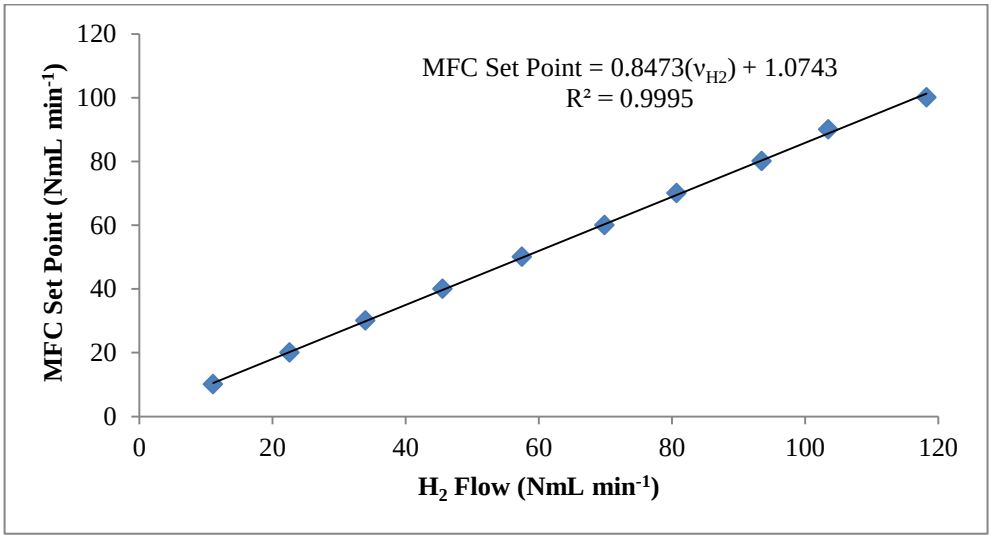

Figure A.2. Calibration Curve of the H_2 Mass Flow Controller.

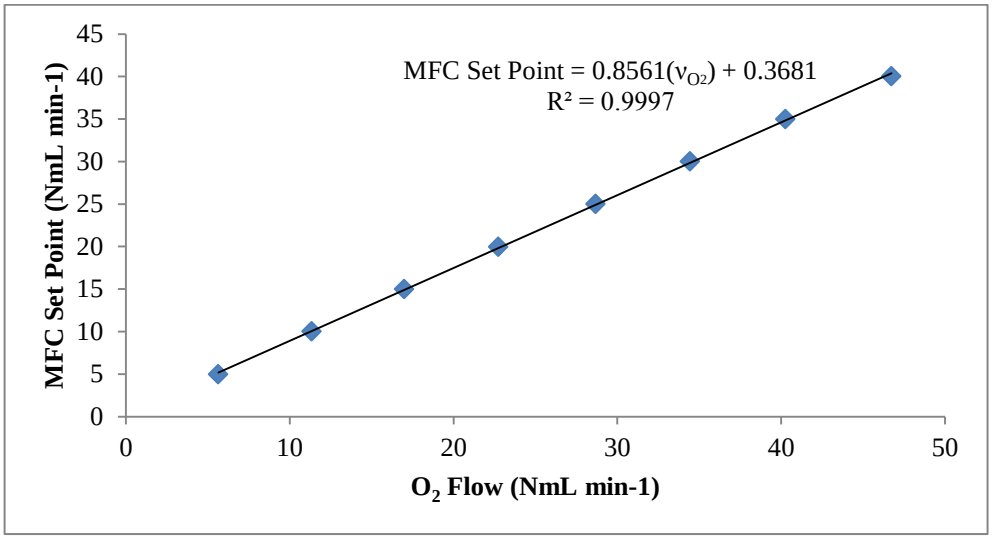

Figure A.3. Calibration Curve of the O_2 Mass Flow Controller.

APPENDIX B: CALIBRATION OF THE GAS CHROMATOGRAPHS

Calibration curves of gases analyzed at Shimadzu GC-2014 gas chromatograph equipped with Molecular Sieve 5A are given below.

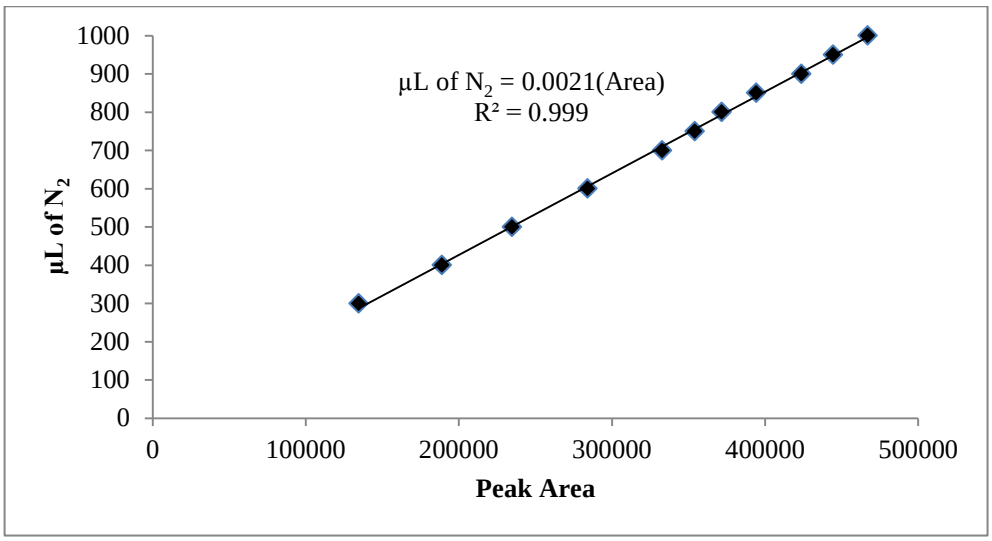

Figure B.1. Calibration Curve for N_2.

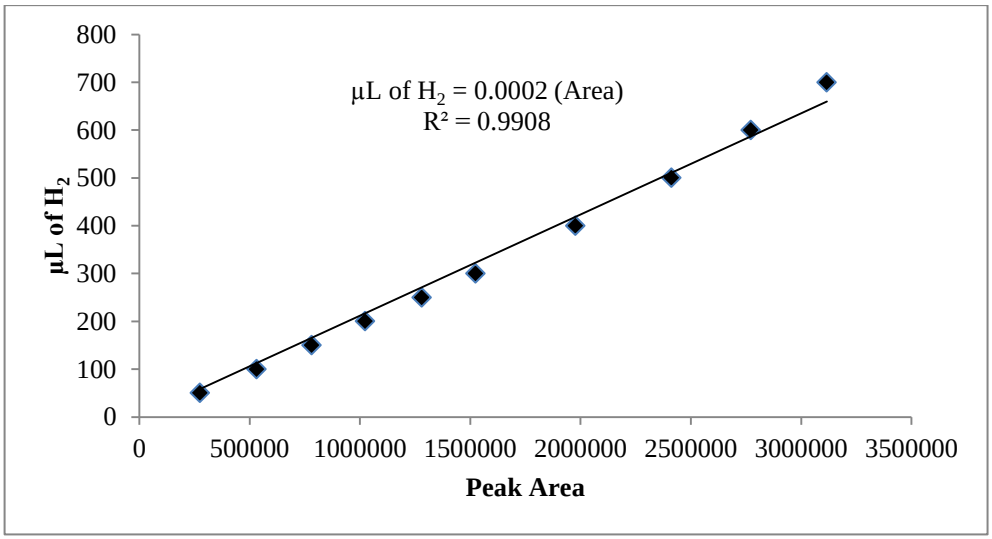

Figure B.2. Calibration Curve for H_2.

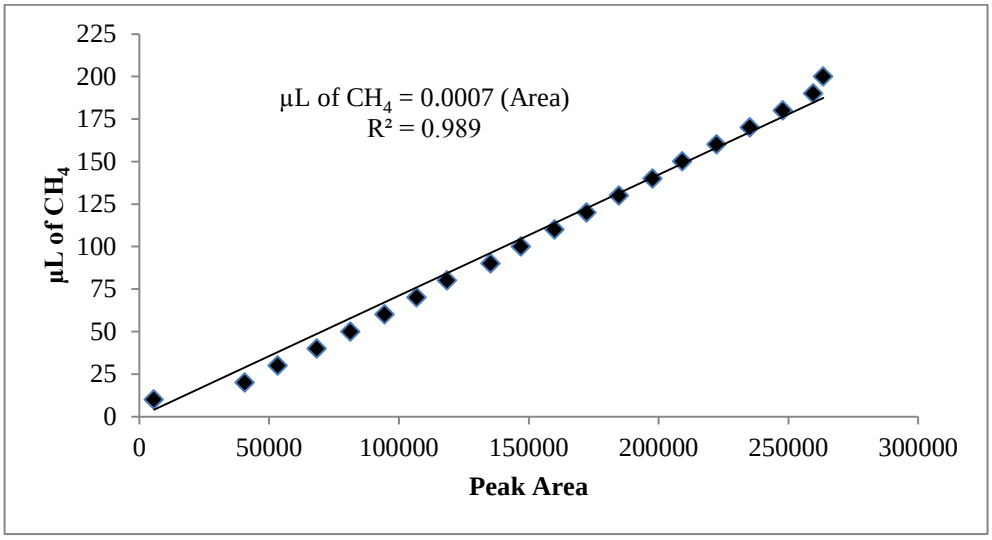

Figure B.3. Calibration Curve for CH_4.

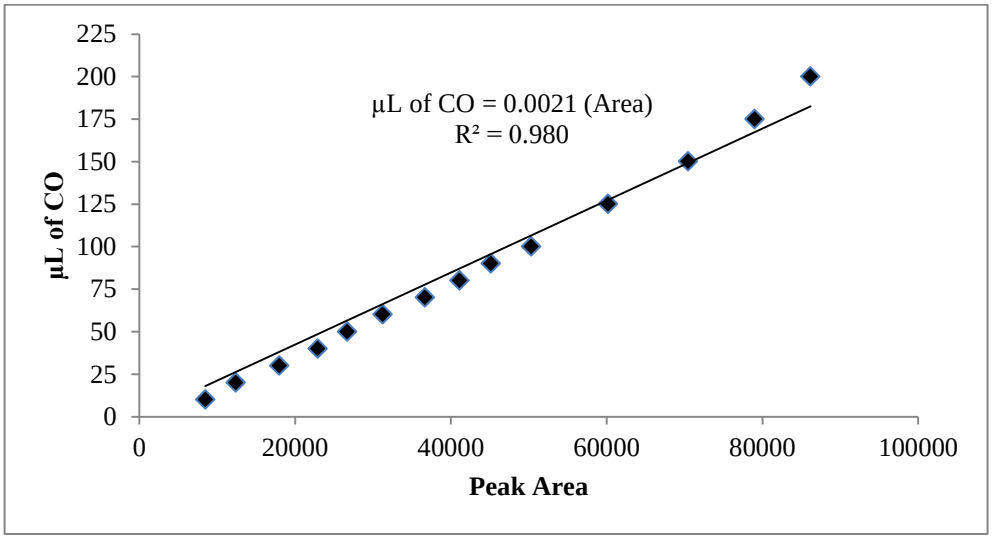

Figure B.4. Calibration Curve for CO.

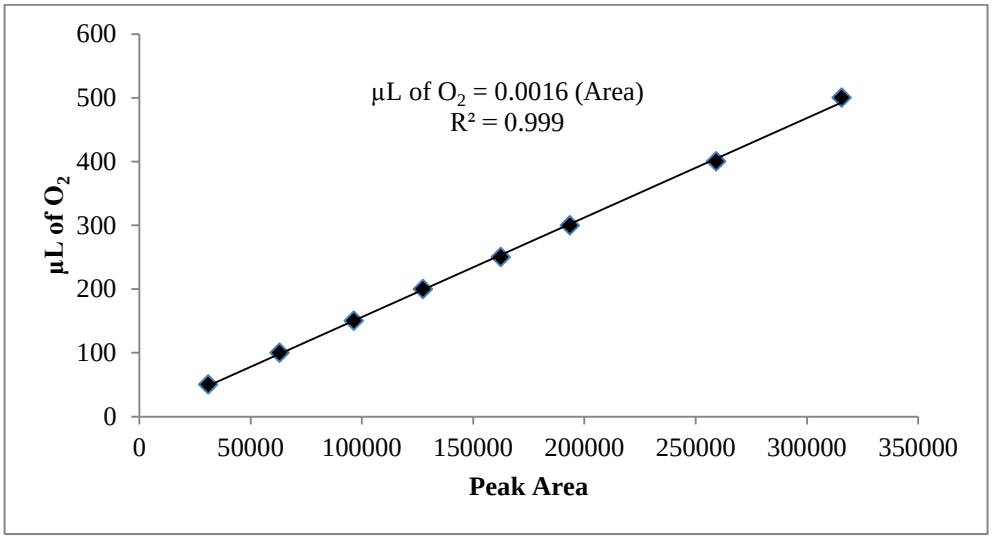

Figure B.5. Calibration Curve for O_2.

Calibration curves of gases analyzed at Shimadzu GC-8A gas chromatograph equipped with Porapak Q are given below.

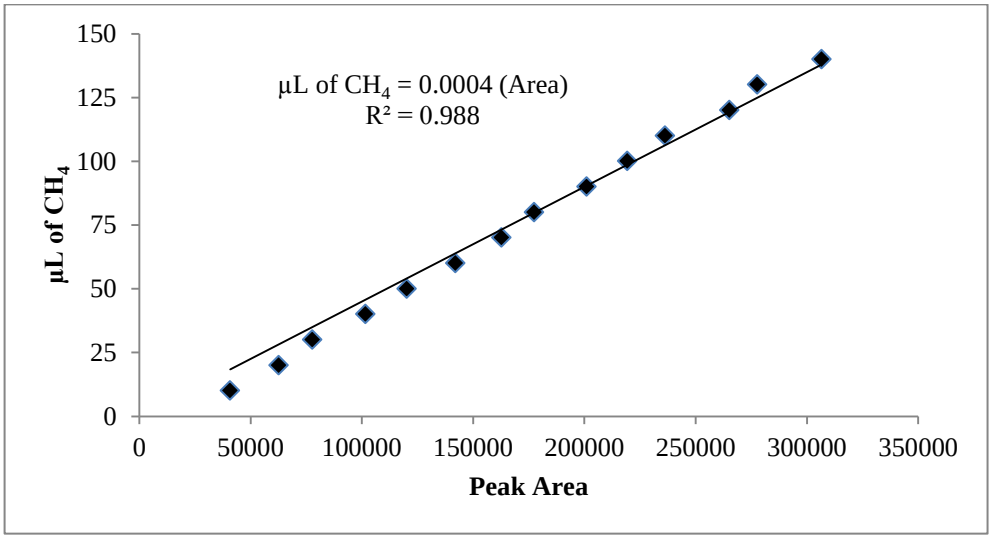

Figure B.6. Calibration Curve for CH_4.

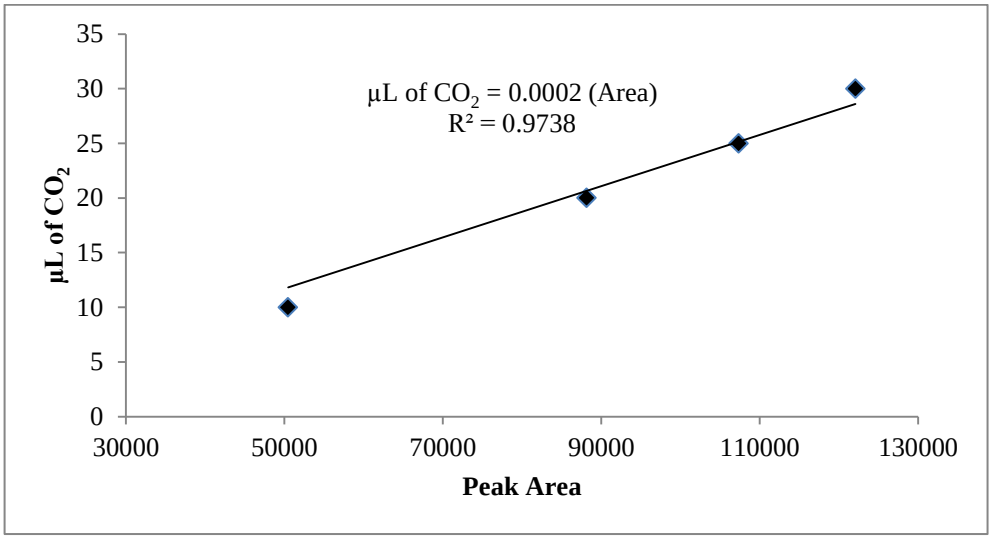

Figure B.7. Calibration Curve for CO_2.

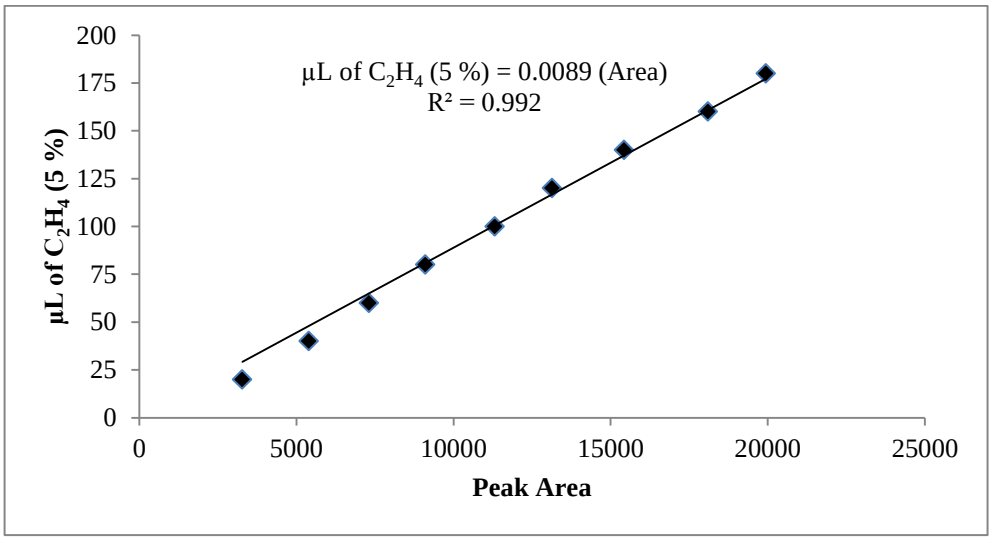

Figure B.8. Calibration Curve for C_2H_4.

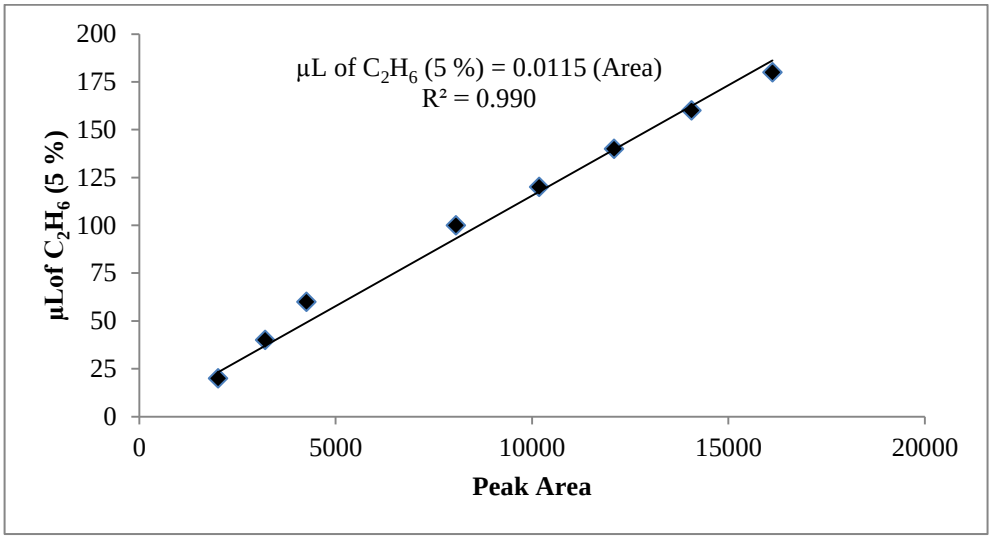

Figure B.9. Calibration Curve for C_2H_6.

REFERENCES

Adhikari, S., S. D. Fernando, S. D. Filip To, R. Mark Bricka, P. H. Steele, Agus Haryanto, 2008, "Conversion of Glycerol to Hydrogen via a Steam Reforming Process over Nickel Catalysts", *Energy & Fuels*, Vol. 22, pp. 1220-1226.

Avasthi, K. S., R. N. Reddy, S. Patel, 2013, "Challenges in the Production of Hydrogen from Glycerol-a Biodiesel Byproduct via Steam Reforming Process", *Procedia Engineering*, Vol. 51, pp. 423-429.

Avci, A. K., D. L. Trimm, A. E. Aksoylu and Z. I. Onsan, 2004, "Hydrogen Production by Steam Reforming of n-Butane over Supported Ni and Pt-Ni Catalysts", *Applied Catalysis A: General* , Vol. 258, No. 2, pp. 235-240.

Chang, C-Y., K-H. Lin, A. C-C. Chang, W-H. Lin, S-H. Chen, H-F. Chang, 2013, "Autothermal Steam Reforming of Glycerol for Hydrogen Production over Packed-Bed and Pd/Ag Alloy Membrane Reactors", *International Journal of Hydrogen Energy*, Vol. 38, No. 29, pp. 12946-12952.

Chiodo ,V., S. Freni, A. Galvagno, N. Mondello, F. Frusteri, 2010, "Catalytic Features of Rh and Ni Supported Catalysts in the Steam Reforming of Glycerol to Produce Hydrogen", *Applied Catalyst A*, Vol. 381, No. 1-2, pp. 1-7.

Commenge J. M., L. Falk, J. P. Corriou, and M. Matlosz, 2004, "Optimal Design for Flow Uniformity in Microchannel Reactors", *AlChE Journal*, Wiley, Vol. 48, No. 2, pp. 345-358.

Czernik, S., R. French, C. Feik, E. Chornet, 2002, "Hydrogen by Catalytic Steam Reforming of Liquid Byproducts from Biomass Thermoconversion Processes", *Industrial & Engineering Chemistry Research*, Vol. 41, pp. 4209-4215.

Dieuzeide M. L., M. Jobbagy, N. Amadeo, 2013, "Glycerol Steam Reforming over Ni/γ-Al_2O_3 Catalysts, Modified with Mg(II), Effect of Mg(II) Content", *Catalysis Today*, Vol. 213, pp. 50-57.

Doesburg, E. B. M., K. P. de Jong and J. H. C. van Hoff, 1999, *Catalysis: An Integrated Approach*, Elsevier, Amsterdam, Netherlands.

Ehrfeld, W., V. Hessel and V. Haverkamp, 2001, "Microreactors: New Technology for Modern Chemistry", Wiley-VCH.

Fichtner, M., J. Mayer, D. Wolf and K. Schubert, 2001, "Microstructured Rhodium Catalysts for the Partial Oxidation of Methane to Syngas under Pressure", *Industrial & Engineering Chemistry Research*, Vol. 40, pp. 3475-3483.

Hasebe, S., 2004, "Design and Operation of Micro-Chemical Plants: Bridging the Gap between Nano, Micro and Macro Technologies", *Computers & Chemical Engineering*, Vol. 29, No. 1, pp. 57-64.

He, L., J. M. S. Parra, E. A. Blekkan, D.Chen, 2010, "Towards Efficient Hydrogen Production from Glycerol by Sorption Enhanced Steam Reforming", *Energy Environmental Science*, Vol. 3, pp. 1046–1056.

Hessel, V. and G. Kolb, 2004, "Microstructured Reactors for Gas Phase Reactions" *Chemical Engineering Journal*, Vol. 98, No. 1-2, pp. 1-38.

Holger Löwe, H., V. Hessel, and A. Mueller, 2002, "Microreactors. Prospects already Achieved and Possible Misuse", *Pure & Applied Chemistry*, Vol. 74, No. 12, pp. 2271–2276.

Iriondo, A., V. L. Barrio, J. F. Cambra, P. L. Arias, M. B. Guemez, M. C. Sanchez-Sanchez, 2010, "Glycerol Steam Reforming over Ni Catalysts Supported on Ceria and Ceria-Promoted Alumina", *International Journal of Hydrogen Energy*, Vol. 35, No. 20, pp. 11622-11633.

Karakaya, M., A. K. Avcı, S. Keskin, 2012, "Parametric Study of Methane Steam Reforming to Syngas in a Catalytic Microchannel Reactor", *Applied Catalysis A: General*, Vol. 411-412, pp. 114-122

Kiwi-Minsker, L., and A. Renken, 2005, "Microstructured Reactors for Catalytic Reactions", *Catalysis Today*, Vol. 110, No. 1-2, pp. 2-14.

Kamonsuangkasem K., S. Therdthianwong, A. Therdthianwong, 2013, "Hydrogen Production from Yellow Glycerol via Catalytic Oxidative Steam Reforming", *Fuel Processing Technology*, Vol. 106, pp. 695-703.

Lin, Yu-Chuan., 2013, "Catalytic Valorization of Glycerol to Hydrogen and Syngas", *International Journal of Hydrogen Energy*, Vol. 38, No. 6, pp. 2678-2700.

Liu, Yu-Chuan., S. K. Liu., 2014, "Generation of Syngas through Autothermal Partial Oxidation of Glycerol over LaMnO3- and LaNiO3-coated Monoliths", *Catalysis Today*, Vol. 237, pp. 62-70.

Liu, Y., R. Farrauto, A. Lawal, 2013, "Autothermal Reforming of Glycerol in a Dual Layer Monolith Catalyst", *Chemical Engineering Science*, Vol. 89, pp. 31-39.

Ma, L., 1995, *Hydrogen Production from Steam Reforming of Light Hydrocarbons in an Autothermic System*, Ph.D. Thesis, University of New South Wales.

Manfro R. L., Nielsen F.P. Ribeiro, Mariana M. V. M. Souza, 2013, "Production of Hydrogen from Steam Reforming of Glycerol using Nickel Catalysts supported on Al_2O_3, CeO_2, and ZrO_2", *Catalysis for Sustainable Energy*, DOI. 10.2478/cse-2013-0001, pp. 60-70.

Montini, T., R. Singh, P. Das, B. Lorenzut, N. Bertero, P. Riello, 2010, "Renewable H_2 from Glycerol Steam Reforming: Effect of La_2O_3 and CeO_2 addition to Pt/Al_2O_3 Catalysts", *ChemSusChem*, Vol. 3, No. 5, pp. 619-628.

Nichele, V., M. Signoretto, F. Menegazzo, A. Gallo, V. Dal Santo, G. Cruciani, G. Cerrato, 2012, "Glycerol Steam Reforming for Hydrogen Production: Design of Ni Supported Catalysts", *Applied Catalyst B: Environmental*, Vol. 111-112, pp. 225-232.

Pompeo, F., G. Santori, NN. Nichio, 2010, "Hydrogen and/or Syngas from Steam Reforming of Glycerol, Study of Platinum Catalysts", *International Journal of Hydrogen Energy*, Vol. 35, No. 17, pp. 8912-8920.

Rennard, D. C., J. S. Kruger, L. D. Schmidt, 2009, "Autothermal Catalytic Partial Oxidation of Glycerol to Syngas and to Non-equilibrium Products", *ChemSusChem*, Vol. 2, No. 1, pp. 89-98

Sandmeyer Steel Company, 2014, *Specification Sheet: Alloy 310*, http://www.sandmeyersteel.com/310-310S.html, [Accessed December 2014].

Schmidt, L. D., D. C. Rennard, J. S. Kruger and B. C. Micheal, 2010, "Longtime Behavior of the Catalytic Partial Oxidation of Glycerol in an Autothermal Reactor", *Industrial & Engineering Chemistry Research*, Vol. 49, No. 18, pp. 8424-8432.

Simsek, E., M. Karakaya, A. K. Avci and Z. I. Onsan, 2013, "Oxidative Steam Reforming of Methane to Synthesis Gas in Microchannel Reactors", *International Journal of Hydrogen Energy*, Vol. 38, No. 2, pp. 870-878.

Slinn, M., K. Kendall, C. Mallon and J. Andrews, 2008, "Steam Reforming of Biodiesel By-product to Make Renewable Hydrogen", *Bioresource Technology*, Vol. 99, No. 13, pp. 5851-5858.

Soares, RR., D. A. Simonetti, J. A. Dumesic, 2006, "Glycerol as a Source for Fuels and Chemicals by Low-temperature Catalytic Processing", *Angewandte Chemie International Edition*, Vol. 45, No. 24, pp. 3982-3985.

Suzuki, T., T. Hirai, T. Miyake, N-O. Ikenaga, 2005, "Production of Hydrogen by Steam Reforming of Glycerin on Ruthenium Catalyst", *Energy Fuels*, Vol. 19, pp. 1761-1762.

Therdthianwong, S., K. Kamonsuangkasem, A. Therdthianwong, 2011, "Hydrogen Production via Oxidative Steam Reforming of Biodiesel by-products over Ni/CeO_2-ZrO_2/Al_2O_3 Catalyst", International Conference on Chemistry and Chemical Process, Vol. 10.

Thessen, V. V., T. A. Maia, Elisabete M. Assaf, 2013, "Ni Supported on La_2O_3-SiO_2 used to Catalyze Glycerol Steam Reforming", *Fuel*, Vol. 105, pp. 358-363.

Turn, S. Q., A. M. D. Douette, W. Wang, V. I. Keffer, 2007, "Experimental Investigation of Hydrogen Production from Glycerin Reforming", *Energy Fuels*, Vol. 21, No. 6, pp. 3499-3504.

US Department of Energy, 2013, "Clean Cities Alternative fuel price report", Energy Efficiency and Renewable Energy.

Vaidya, P. D., Alirio E. Rodrigues, 2009, "Glycerol Reforming for Hydrogen Production: A Review", *Chemical Engineering & Technology*, Vol.32, No. 10, pp. 1463-1469.

Wang, C., B. Dou, H. Chen, Y. Song, Y. Xu, X. Du, T. Luo, C. Tan, 2013, "Hydrogen Production from Steam Reforming of Glycerol by Ni-Mg-Al Based Catalysts in a Fixed-Bed Reactor", *Chemical Engineering Journal*, Vol. 220, pp. 133-142.

Wang, X., M. Li, S. Li, H. Wang, S. Wang, X. Ma, 2010, "Hydrogen Production by Glycerol Steam Reforming with/without Calcium Oxide Sorbent: A Comparative Study of Thermodynamic and Experimental Work", *Fuel Processing Technology*, Vol. 91, No. 12, pp. 1812–1818.

Watts, P. and C. Wiles, 2006, "Recent Advances in Synthetic Micro Reaction Technology", *Chemical Communications*, Vol. 5, pp. 443-467.

Zhang, B., X. Tang, Y. Li, Y. Xu, W. Shen, 2007, "Hydrogen Production from Steam Reforming of Ethanol and Glycerol over Ceria Supported Metal Catalysts", *International Journal of Hydrogen Energy*, Vol. 32, No. 13, pp. 2367- 2373.